Estimating flood peaks and hydrographs for small catchments:

R9 – Depth-duration-frequency analysis for short-duration rainfall events

FCERM Research & Development Programme

Research Report

Date: March 2024

Version: SC090031/R9

We are the Environment Agency. We protect and improve the environment.

We help people and wildlife adapt to climate change and reduce its impacts, including flooding, drought, sea level rise and coastal erosion.

We improve the quality of our water, land and air by tackling pollution. We work with businesses to help them comply with environmental regulations. A healthy and diverse environment enhances people's lives and contributes to economic growth.

We can't do this alone. We work as part of the Defra group (Department for Environment, Food & Rural Affairs), with the rest of government, local councils, businesses, civil society groups and local communities to create a better place for people and wildlife.

Contents

Acknowledgements

Particular thanks are due to the Environment Agency's Project Board, members of which were responsible for developing the vision and scope of this research. The board has continued to advise and support the project team, providing valuable feedback, practical suggestions and lively discussions. The project team is also grateful to staff from the Environment Agency, Natural Resources Wales, the Scottish Environment Agency (SEPA) and the Rivers Agency for supplying data and advice on data quality, and to those who have acted as external reviewers.

Executive summary

Small catchments and plot-scale areas often have short response times, making them potentially vulnerable to short, intense bursts of rainfall. The aim of this study was to investigate the depth–duration–frequency (DDF) characteristics of short-duration rainfall data and to assess the reliability of current national models in estimating rainfall frequency for durations shorter than the basic intervals that were used in developing them.

The study makes the following recommendations to users of short-duration DDF models:

- the FEH and FSR DDF models appear to provide reasonable estimates for frequencies of sub-hourly rainfall events down to a duration of 15 minutes, at least for the short return periods at which local data can be expected to provide suitable empirical evidence

- the FEH appears to give less biased results than the FSR and seems to be more suitable for extension to allow the model to estimate frequency curves for sub-hourly rainfall durations - however, due to the relatively small number of gauges used in the study reported here, these results should only be extrapolated to the national scale with caution

- larger uncertainties are associated with very short durations (one-minute to 15-minute durations) - the FSR and FEH were not fully calibrated on such short durations and larger errors are to be expected in the measured data, especially in the early years of the records

Nineteen sites with relatively long periods of high-resolution rainfall records were initially selected to provide good coverage of England and Wales. Data of the highest temporal resolution came from tipping bucket rain gauges where the rainfall data were recorded as tip times. These records were processed to represent depths of rainfall over one-minute intervals. However, some of the rainfall records available to the study were instead stored as 15-minute rainfall accumulations. The final data set consisted of nine gauges with basic data at one-minute intervals and 10 gauges with data at 15-minute intervals. Fifteen of these gauges had more than 20 years of data and the longest record was 46 years.

Several key rainfall durations were selected for the analysis, and annual and seasonal maxima were extracted accordingly. An initial exploration of the data was carried out to inform the building of the statistical model. A modified version of the generalised extreme value (GEV) distribution was used to model the annual and seasonal maxima at each station for a range of durations in order to provide rainfall depth estimates that are consistent across durations (that is, rainfall frequency curves for different durations that do not cross). The so-called unified GEV distribution builds on standard extreme value theory, and ensures consistency between estimated frequency curves by fixing some basic relationships between the model parameters and assuming a common lower bound for all event durations. The proposed unified GEV requires the estimation of six parameters: a relatively simple model for such a complex problem.

The unified GEV model was fitted to the data series at all stations. The fitting of the frequency curves is a compromise between the goodness-of-fit at each duration and the consistency of curves across durations.

A comparison between the rainfall frequency curves estimated in the present study and those obtained from previously developed DDF models (FSR, FEH and FEH13) has been carried out. No structural differences were identified between the rainfall frequency curves estimated with the unified GEV and the previously existing DDF models. Given that the unified GEV is fitted to the series at each station separately, the length and quality of the data at each station have a major impact on the precision of the estimated curves. Therefore, it is not clear if the lack of consistent differences across the methods is a result of the differing record length and data quality at each individual rain gauge site. A much more extensive high-quality data set would be needed to study this effectively.

The existing standard DDF models did not appear to give unreasonable rainfall depth estimates for very short durations when compared with the higher resolution estimates derived in the present study. Considering that the standard DDF models were developed using little or no rain gauge data for durations shorter than one hour and are designed to be used for a range of event durations, it is reassuring to see that the results obtained when extrapolating to such short durations appear to be reasonable.

It should be noted that short-duration FEH13 and FEH22 estimates, as delivered through the FEH Web Service, apply the FSR relationships between x-minute and 60-minute rainfall depths (where $5 \leq x < 60$) to the FEH13 or FEH22 60-minute rainfall depth, as appropriate.

Important Note:

Work on Project SC090031 'Estimating flood peaks and hydrographs in small catchments (Phase 2)' began in December 2013. Tasks carried out in the early stages of the project have already been documented in several project notes and reports, so it is possible that there may be inconsistencies, particularly in the various data sets and methods that have been applied at different points in time. This report provides a summary of the research carried out throughout the project, and we have detailed the data sets and methods used in each of the stages and tasks.

1. Introduction

1.1 Scope

Project SC090031 – 'Estimating flood peaks and hydrographs for small catchments (Phase 2)' aims to develop techniques for estimating flow and hydrographs for small UK catchments. Small catchments (for example, smaller than 25 km^2) and plot-sized areas are expected to be particularly vulnerable to short, intense cloudbursts due to their short response times. As Faulkner and others (2012) emphasise reliable estimates of sub-hourly design rainfalls are therefore needed to build credible flow and hydrograph estimates for the smallest catchments using rainfall–runoff techniques. These are needed for flood risk management as well as for development control and the design of sustainable urban drainage systems (SuDS). Current methods for estimating design rainfalls (see NERC 1975, Faulkner 1999, Stewart and others, 2013) were largely developed using data at hourly and daily resolution. For the Flood Estimation Handbook (FEH), and particularly for the Flood Studies Report (FSR), the hourly data records were relatively short and were sparse in some regions of the UK. Therefore, it is to be expected that existing methods may have some shortcomings when used to estimate the rainfall depths associated with short (for example, shorter than one hour) and very short (for example, smaller than 15-minute), intense storm events.

This report presents the details of a pilot depth–duration–frequency (DDF) study of short-duration rainfall extremes at several locations in England and Wales. In total, 19 stations with long records of sub-hourly rainfall data, representing different climatological regimes in England and Wales, were selected. In particular, a number of tipping bucket stations providing time of tip data were identified, from which information on very short durations (for example, one minute) could be extracted. For areas in which no long time of tip records could be identified, data at 15-minute resolution were used.

Annual and seasonal maxima were extracted for a representative subset of the identified stations in order to provide good geographical coverage of England and Wales. A new single-site DDF model was applied to the extracted maxima series at each station. Unlike many of the DDF models used in practice, the single-site model presented in this work does not use information from nearby stations.

1.2 Current depth–duration–frequency models used in practice

DDF models serve two purposes. The first is to estimate the rainfall depth of a hypothetical event, specifying a duration and rarity (or return period) for use in rainfall–runoff methods of design hydrograph analysis such as the revitalised flood hydrograph (ReFH) model (Kjeldsen 2007) or the FSR/FEH rainfall–runoff method (Houghton-Carr 1999). The second purpose is to assess the rarity of an observed storm event with a known rainfall depth and duration. DDF models are generally intended to apply over entire regions or

countries. However, the data used to build and parameterise these models is primarily or entirely collected from rain gauges – sources which are points in physical space and which monitor only a small fraction of the region. In order to allow DDF models to make predictions in between these points, it is necessary to build a model which can borrow information from the gauges surrounding the location of interest. Furthermore, systematic records of rainfall totals generally started relatively recently, with digital records mostly starting in the 1960s for England and Wales. The pooling of data from surrounding stations also allows rainfall of long return periods to be estimated with higher confidence.

In England and Wales, the most widely used DDF model is the one described in Volume 2 of the FEH (Faulkner 1999). This has been calibrated for rainfall of durations from one to 192 hours using data from a large number of hourly rain gauge records throughout the UK. However, no data at higher temporal resolution were available and therefore extrapolation to durations below 30 minutes is strongly discouraged.

The FEH DDF model was developed to replace the model presented in Volume II of the FSR (NERC 1975), which was developed using annual and seasonal maxima from about 200 autographic rain gauges, about half of which had records of 20 years or more. Some data were also available for sub-hourly durations from the limited period experiments at Cardington and Winchcombe, and the Jardi rate of rainfall data at several other locations. Therefore, although the FEH analysis used many more hourly rain gauge records than the FSR throughout the UK, the FSR model remains in use in the context of urban drainage studies for very short design durations and relatively short return periods (up to 30 years).

This report aims to investigate how a model for short-duration rainfall events could be developed at a national scale, and how the methods currently used perform when extended to short-duration events, in particular when shorter return periods are of interest.

A new modelling framework is presented and fitted to a set of annual maxima with durations from one to 120 minutes for 19 stations across England and Wales. It is not intended to replace any existing DDF model entirely, as it is not intended to be calibrated to events over 120 minutes in duration or (in its current state) to provide estimates for return periods above 100 years. The suggested model is only fitted to a limited number of observed series and would need to be fitted to a larger data set to be suitable for national coverage and longer return periods.

1.3 Structure of the report

Section 2 gives some background on the use of the DDF models previously developed for the UK.

Section 3 focuses on the selection and quality assurance of rainfall records for calibrating the model and extracting annual and seasonal sliding window maxima for several short durations.

Section 4 investigates the possible statistical distributions to which the block maxima of the rainfall data discussed in Section 3 can be fitted.

Section 5 shows the performance of the statistical model described in Section 4 when fitted to the subset of rainfall data at time of tip stations, for which block maxima series of duration as short as one minute are available.

Section 6 shows the performance of the statistical model for all stations included in the study, for event durations of 15 to 120 minutes.

Section 7 gives some indication of how the estimated DDF relationships presented in Sections 5 and 6 compare with the DDF relationships estimated by the other current methods (FSR, FEH and FEH13).

Some final remarks and lessons learned are presented in Section 8.

It is assumed that the reader has a detailed understanding of FEH methods, hydrological terminology, and catchment descriptors.

2. Current depth–duration–frequency models

This section outlines DDF models that have been developed for use as national standards in the UK. Other nations use different methods; a range of these are summarised and briefly described by Svensson and Jones (2010).

2.1 Flood Studies Report

The Flood Studies Report (FSR) was published in 1975 (NERC, 1975) and the model presented in Volume II provided the first generalised method of estimating rainfall frequency applicable to the whole of the UK. While the FSR methods have been largely superseded by the Flood Estimation Handbook (FEH) in practice, there are some applications which continue to rely on the FSR DDF model, notably the procedures currently recommended for reservoir flood risk assessment (ICE 1996, Defra 2004) for which rainfall estimates of very low frequency up to probable maximum precipitation (PMP) are required. Also, the FSR rainfall analysis made some limited use of very short-duration rainfall data from the Jardi rate of rainfall stations and, therefore, its use is still widespread in urban drainage design practice.

The FSR rainfall analysis adopted an index-flood method based on analysis of annual rainfall maxima. The FSR index value is the 5-year return period rainfall, M5. For short durations (down to a minute), this is derived based on various quantities that have been mapped across the UK, including the depth of the 2-day, 5-year return period rainfall. For the regional growth curves, the UK is divided into two regions: England and Wales, and Scotland and Northern Ireland. However, within each region, there are different growth curves depending on the magnitude of the index variable. The growth curves were initially fitted graphically using the results of quartile analysis – the ordered annual maxima are divided into quarters or 'quartiles', and the geometric means of the quarters can be shown to correspond to particular return periods. The FSR method has been criticised for not capturing local, within-region, variations well, and for the discontinuity in growth curves at the boundary between the two geographical regions.

Records from only about 200 autographic rain gauges were used for the FSR analysis, 101 of which had at least 20 years of record. Although it was found that short-duration rainfalls could be acceptably approximated to vary with the ratio of 60-minute M5 to 2-day M5 – which were derived from about 6,600 gauges – the FSR short-duration rainfall estimates need to be regarded with some caution because of the limited data availability.

2.2 Flood Estimation Handbook (FEH)

The current UK standard method of estimating rainfall frequency is presented in Volume 2 of the FEH (Faulkner 1999). The design rainfalls are derived using an 'index-flood' method

(for example, Stedinger and others, 1993), based on analysis of annual rainfall maxima. The distribution of rainfall (or floods) at different sites in a region is assumed to be the same except for a scaling factor, 'the index'. This reduces the problem to estimating the index at the target site, and a standardised regional growth curve (which expresses the ratio of an arbitrary T-year event to the index). The design rainfall estimate at a target site is simply obtained by multiplying the site's index value with the regional growth curve.

The FEH DDF model is based on the FORGEX method of estimating rainfall growth (Reed and others, 1999), which generates a regionally derived growth curve from standardised AMAX obtained from gauges within a circular region around the site of interest, while the rainfall frequency curve is obtained by multiplying the regionally derived growth curve with an index variable. Here, the index variable is the median annual maximum rainfall, RMED, which was mapped across the UK on a 1 km grid using georegression on topographical and other variables (Faulkner and Prudhomme, 1998). The regional growth curve is derived using data pooled from a hierarchy of expanding circular regions centred on the target site. Because regions defined this way vary only slightly for nearby target sites, the regional growth curves change relatively smoothly across the country. This avoids the boundary discontinuities of regionally based methods while still capturing local variations.

The output from FORGEX consists of frequency curves derived separately for each rainfall duration. So that the curves for the different durations do not cross (mainly a problem at long return periods because of uncertainties in the extrapolation), a 6-parameter DDF model was fitted to the FORGEX outputs. Rainfall depth, given a frequency and an event duration under 12 hours, is predicted by Equation 1 where c, d_1, e and f are constants whose values vary spatially, y is the Gumbel reduced variate, $-\ln(-\ln(1 - 1/T))$, R is rainfall depth in mm and D is event duration in hours:

Equation 1 – Rainfall depth given a frequency and event duration under 12 hours

$$\ln(R) = (cy + d_1)\ln(D) + ey + f$$

As noted in Section 1.2, the FEH method is not necessarily suitable to use on very small catchments where critical storm durations are very short. Because of its calibration range of one to 192 hours, the estimation of frequencies for shorter durations will require extrapolation.

2.3 Reservoir Safety (FEH13)

The FEH13 model was developed within the Joint Defra/Environment Agency project FD2613 WS194/2/39 'Reservoir Safety – Long return period rainfall' (Stewart and others, 2013) and was further developed during subsequent research funded by CEH. The need for a new model arose because of concerns that extreme rainfall events were not actually as common as the FEH predicted. The FEH13 method was developed for return periods from two to 100,000 years superseding both the FEH and the legacy uses of the FSR. The FEH13 DDF model was developed to fit the output from a new version of FORGEX, based on rainfall data at many sites in the UK. A very flexible DDF model was needed to reflect

the variable patterns in the relationship between rainfall depth, duration and frequency that were observed at the calibration sites. A 11-parameter rainfall distribution function, comprised of two different gamma distribution functions, was proposed (Equation 2) where $G(x; \alpha(D), \beta(D))$ is the cumulative distribution function of the gamma distribution, with duration-dependent scale and shape parameters $\alpha(D)$ and $\beta(D)$. The site-specific constant p_1 controls the weighting of the two gamma distributions. V is a site-specific constant that extends the rainfall distribution function to allow distributions similar to the generalised extreme value (see Section 4.3 for a discussion of the GEV):

Equation 2 - A 11-parameter rainfall distribution function comprised of two different gamma distribution functions

$$F(x,D) = \left\{ p_1 G\left(x; \alpha_1(D), \beta_1(D)\right) + (1 - p_1) G\left(x; \alpha_2(D), \beta_2(D)\right) \right\}^V$$

Each of the two instances of $\alpha(D)$ and $\beta(D)$ is defined by site-specific constants, according to Equations 3 and 4:

Equation 3 – A duration-dependent function for the shape parameter (α) of the gamma distribution functions comprising the 11-parameter rainfall distribution function

$$\alpha(D) = v_0 + v_1 D$$

Equation 4 – A duration-dependent function for the rate parameter (β) of the gamma distribution functions comprising the 11-parameter rainfall distribution function

$$\beta(D) = \gamma_1 D + \gamma_2 \left\{ 1 - 1 / (1 + \gamma_3 D) \right\}$$

Further information on the development of the FEH13 model, including additional processing for better spatial coherence at locations between sites, can be found in Volume 1 of the report of the Defra study (Stewart and others, 2013). A "plain language" summary of the method is given by Vesuviano and Stewart (2021). The most recent FEH22 DDF model uses the same method as FEH13, with one very minor bug fix and a greatly extended data set (Vesuviano, 2022). FEH22 was not available at the time of study.

It is important to note that a direct comparison with the new model presented in this study will not be valid for long return periods, as the number of station-years available for the 19 sites considered in this study is not enough to allow the new model to be fitted to extreme rainfall events. However, the new model and FEH13 model can be compared for events that may be of interest at plot scale (for example, a 20-year event).

3. The data

Acquiring long records from about 10 to 12 short-duration rainfall stations to ensure a reasonable coverage of the different climatological regimes in England and Wales proved to be a complex task. Some regions appeared to have more time of tip records from tipping bucket stations with long periods of record than others, and, in some cases, only data at a fixed 15-minute resolution were available. Section 3.1 provides a more exhaustive discussion of the issues related to agreeing the final set of stations used in this study.

After some discussion with the regional representatives of the Environment Agency, and the collaboration of the central Hydrometry and Telemetry (H&T) team, the CEH team acquired data from about 70 stations.

Two different types of data were used in this study: time of tip data and 15-minute rainfall totals in millimetres. For a few stations, a mixture of the two data formats was available, with time of tip information typically available for the more recent years. In these cases, the time of tip data were transformed into regular 15-minute series and the station was treated as a purely 15-minute station. Only stations with at least 10 years of complete data were processed: if the data were in the form of tip times, one-minute series were extracted; otherwise, 15-minute series were constructed.

At 15-minute stations, the rainfall information is available at specific predefined intervals of 15 minutes (at 0, 15, 30 and 45 minutes past each hour), whereas time of tip data provides a record of the clock time at which the bucket of a tipping bucket rain gauge tips (that is, empties its contents). A tip is triggered whenever the bucket is filled by a nominally fixed volume of water, which relates to a convenient equivalent depth of rainfall (normally 0.1, 0.2, 0.5 or 1.0 mm). This volume is a property of the tipping bucket station, which might change slightly in time (for example, due to sediment collecting in the bucket) or, more significantly, over time (for example, if the specific instrument used at a station is replaced by a different model). From the time of tip information, one-minute series can be produced (in addition to a series of virtually any higher or even lower resolution), although the level of precision that the station can reach is highly related to the tip volume: in many stations used in this study, the highest resolution (one-minute, 2-minute) annual maxima at several stations have the same values due to the level of precision of the tipping bucket. This is more pronounced in the earlier years of the records, when buckets with larger tip volumes were installed.

Besides giving a biased representation of the actual maximum values recorded in certain years, the repeated values of short-duration annual maxima in many years might also give numerical issues in estimating the DDF model. Indeed, tipping buckets are known to give systematically biased estimates of the rainfall intensities, with lower intensities being overestimated and higher intensities being underestimated. Molini and others (2005) provide further discussion on this topic. Furthermore, although standards of practice regarding operating rain gauges exist in the UK (BSI 2012), the actual measurements recorded at the different tipping bucket stations are also affected by the way in which the

bucket has been installed throughout the years. Molini and others (2005) and Pavlyukov (2007) provide a more detailed discussion of the issues connected with rainfall measurements using tipping bucket rain gauges, and the effect of installation practices on the final estimates.

Once all the one-minute and 15-minute series had been compiled, monthly maxima of the 15-, 30-, 45-, 60-, 90- and 120-minute accumulations were extracted from the one-minute and 15-minute series for all complete months. The one-, 2-, 5- and 10-minute monthly maxima were also extracted from the one-minute series generated from time of tip records. A month was considered complete if at least 75% of the data in the month were non-missing. Finally, the annual and seasonal maxima series were constructed from the monthly maxima series. A year or season was considered complete if no more than one monthly record within that year or season was incomplete. Annual maxima were extracted as the maximum single value recorded in each calendar year. Summer maxima were extracted as the maximum value recorded at each station from May to October (inclusive). Winter maxima were extracted as the maximum value recorded at each station from November to April (inclusive).

Although the Environment Agency had regularly quality checked the available data, some basic quality controls on extremely high or suspiciously low points (for example, seasonal maxima being equal to 0) were also carried out. Many of the very high values turned out to correspond to accumulations larger than the nominal ones; some of the very low values resulted from missing data being noted by a non-standard method that was not identified by the automated data processing routines in place. These issues were relatively easy to identify but required additional checks after the automatic reading of the data.

Figure 1 shows maps of all the stations processed by CEH (left panel) and the final selected subset used in the study (right panel). The light grey lines indicate the Environment Agency Water Management regions (as in 2012). In both panels, stations with time of tip data are indicated in red and 15-minute stations in blue. In the left panel, the solid dots indicate the stations that were selected in the final subset; the selection process considered the length of the record and the overall spatial coverage of England and Wales. Most of the short-duration records processed are in Wales and the Midlands area. Overall, most of the stations included in the study are in the southern half of England and Wales.

The right panel of Figure 1 shows the locations of the 19 stations included in the final selected subset with the additional information of the record length for the annual maxima series. Fifteen of the stations have more than 20 years of data and the record length exceeds 35 years at three of them. The shortest record in the final subset of stations is 15 years. Section 3.1 examines some of the issues and problems in selecting these stations. Tables 1 and 2 provide some basic information about the stations.

3.1 Issues in selecting stations for the study

It was hoped that the metadata available from the Environment Agency could be used to choose a suitable set of stations to be used in the study. After an initial request for data, it became clear that the metadata did not clearly differentiate between the resolutions at which data were stored for each station. In some cases, stations in which the metadata suggested a record longer than 20 years were found to have only a few years of tipping bucket data at a high resolution (for example, time of tip). More precise metadata would allow stations with long records of high-resolution data to be quickly identified.

Direct contact with local representatives in the different Environment Agency regions allowed sets of time of tip stations and 15-minute stations across the country to be quickly identified. The experience of the local representatives should ensure that the selected stations are of the best quality available in the region.

An additional issue with some station data was that the format used to store the data can be inconsistent from station to station. Reading and compiling the non-standard data formats would require additional effort and time: this was pursued as part of this work.
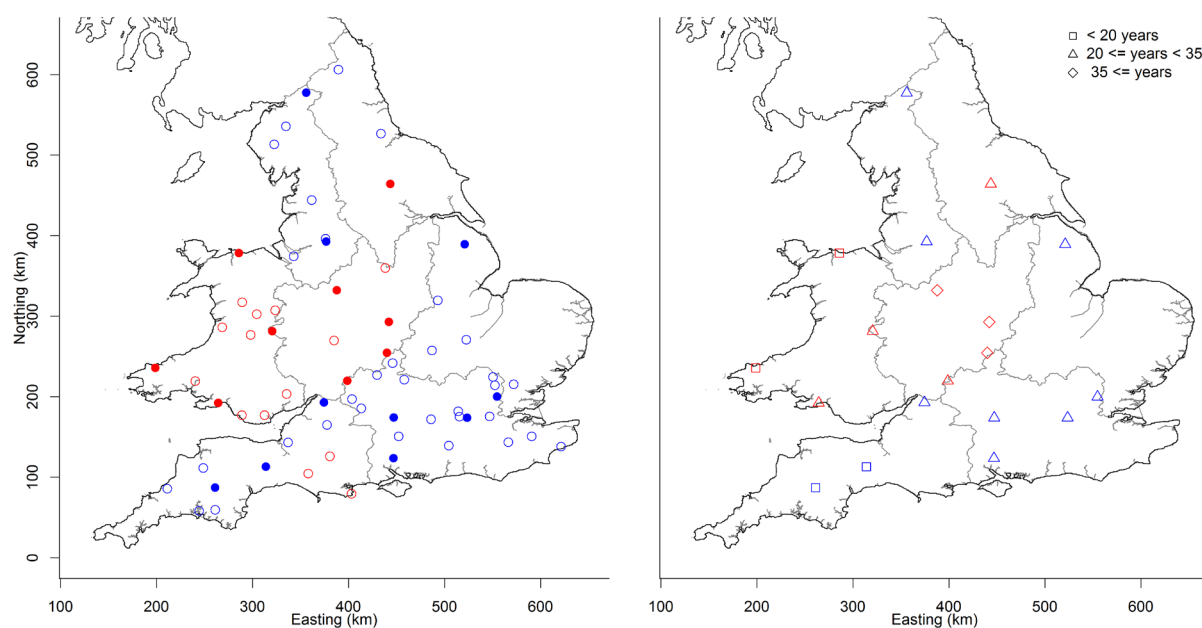
Figure 1 - Locations of all stations available to CEH (left panel) and the final selected subset (right panel). Red indicates time of tip stations and blue indicates 15-minute stations

The left panel in Figure 1 shows the location of all stations available to CEH in England and Wales. Red circles show time of tip stations, with blue circles representing 15-minute stations. The right panel shows the final selected subset. Red shapes denote time of tip stations and blue shapes represents 15-minute stations. The legend shows:

- Squares: < 20 years
- Triangles: 20 <= years < 35
- Diamonds: 35 <= years

Table 1 – Summary information of the time tip final subset stations used in the study

Station name	Easting (km)	Northing (km)	AMAX length (years)	RMED (mm)	*SAAR* (mm)
Bettws-y-Crwyn	320.360	281.360	28	34.7	1,000
Colwyn Bay	285.805	378.474	19	34.3	777
Dowdeswell	398.769	219.616	30	35.6	772
Hinckley	441.980	292.690	46	31.4	643
Knightcote	439.835	254.472	35	33.6	631
Llanychaer	198.551	235.552	19	46.6	1,263
Lower Dunsforth	443.496	464.307	26	33.2	632
Stone	387.760	332.060	46	29.8	740
Victoria Park	264.238	192.222	21	42.3	1,150

- Notes: AMAX = annual maxima, RMED = median annual maximum rainfall, SAAR = standard-period average annual rainfall

Table 2 – Summary information of the 15-minute final subset stations used in the study

Station name	Easting (km)	Northing (km)	AMAX length (years)	RMED (mm)	*SAAR* (mm)
Chieveley	446.952	173.862	22	33.2	699
Crew Fell	355.894	577.422	20	37.7	1,188
Hemyock	313.829	112.888	18	39.5	995
Kingswood	374.306	192.842	33	33.8	777
Ludford	520.820	389.330	23	31.7	700
Otterbourne	446.726	123.487	26	34.4	786
Putney Heath	523.480	173.770	25	33.3	614
Sale Carrington	376.614	392.651	23	32.4	836
Stanford Rivers	554.586	199.866	22	31.0	606
Taw Head	260.890	86.913	15	57.0	2,186

- Notes: AMAX = annual maxima, RMED = median annual maximum rainfall, SAAR = standard-period average annual rainfall

Figure 2 shows a map of the standardised average annual rainfall (SAAR; Spackman 1993) for the whole of the UK. The western part of the country is characterised by higher average annual rainfall, with the larger variability enhanced by the orographic characteristics of the different regions.
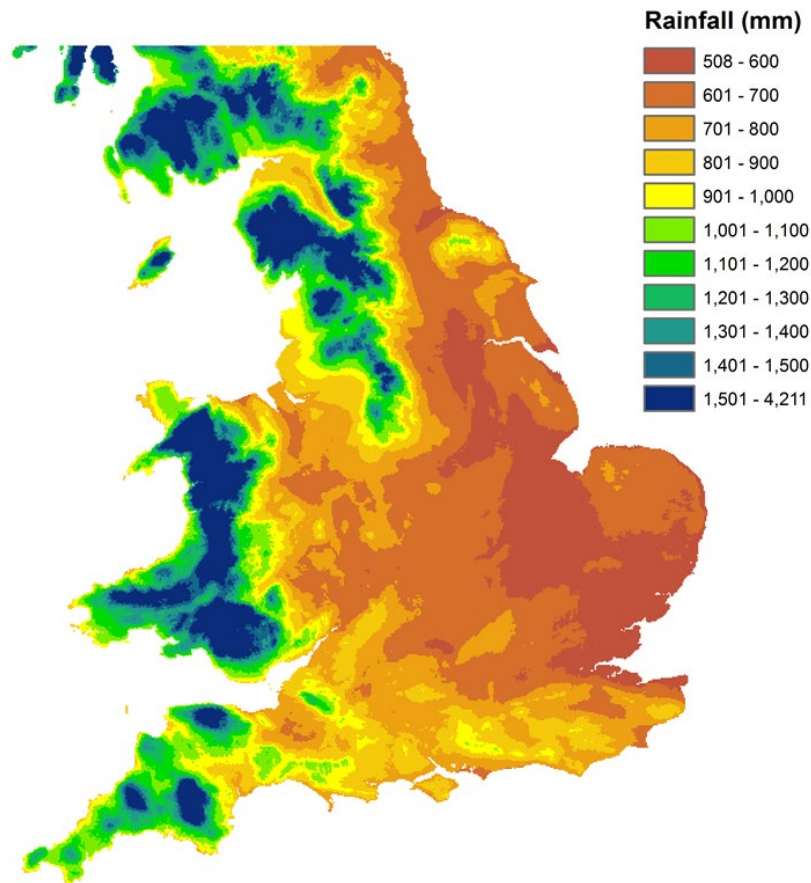
Figure 2 - Standard-period average annual rainfall (SAAR 1961 to 1990) values for the UK

3.2 Sliding window corrections

Due to the different nature of the records, the series of maxima extracted from the time of tip stations do not provide the same information as the series extracted from the 15-minute stations for series of maxima which are multiples of 15 minutes. The time of tip maxima are computed using a sliding window and, for example, the 15-minute annual maximum value corresponds to the actual largest amount of rainfall recorded in any 15-minute interval in the year; see Figure 3 for a schematic representation of the different time periods corresponding to the sliding window and fixed window. However, the maximum obtained from the 15-minute records instead corresponds to the maximum recorded in one predefined 15-minute interval and is likely to be lower than the actual maximum amount of rainfall, which could have been recorded in a 15-minute interval without a fixed start time. The true maximum rainfall is most likely to be under-recorded when its duration is the

same as the fixed-duration recording unit, as the rainfall event is very unlikely to align neatly with the station clock. However, when longer durations are considered, the alignment between the rainfall event and the station clock is less important, as the depths of rainfall at the tail ends of the storm, which are difficult to capture exactly, become less and less important to the storm depth.

In order to adjust the maxima extracted from the 15-minute stations so that they are closer to the higher values which would be attained using sliding windows, correction factors were introduced. This is in line with the methods used in Stewart and others (2013), in which discretisation correction factors were used to relate the data extracted from daily series to the 24-hour sliding window data. For each time of tip record, annual and seasonal maxima starting at 0, 15, 30 or 45 minutes past the hour were extracted for durations of 15, 30, 45, 60, 90 and 120 minutes. These series correspond to those which would be obtained if the data for the time of tip stations were stored as 15-minute series (fixed window) rather than time of tip series (sliding window). The average ratio between the sliding window maxima and the fixed window maxima at each duration is used as a sliding window correction factor for that duration. See Figure 8 for a diagram showing the different steps involved in building the correction factors.

In the rest of this work, the maxima extracted from the 15-minute series are multiplied by the appropriate correction factor in Table 3 to give estimates of the equivalent sliding window maxima. The aim of this correction is to obtain results which are more representative of the higher true rainfall values that could be recorded and are therefore more useful for practitioners. The drawback of fixed correction factors is that they might be too coarse to differentiate between the scaling required for a 15-minute annual maximum that falls evenly between two consecutive 15-minute periods and a 15-minute annual maximum that falls mostly in one 15-minute period. In an extreme example, a true 15-minute annual maximum, which happens to be distributed evenly between two consecutive time steps, may not be correctly registered as the annual maximum in a 15-minute accumulation record if the second largest 15-minute event falls mostly in a single time step. Furthermore, taking the same correction factors across all stations might be a simplistic solution, resulting in overcorrection at some stations. Given the coarse nature of the tipping bucket network, it might not be feasible to compute regional correction factors, or correction factors might be based on too few stations and therefore might not be robust.

Table 3 - The correction factor to be applied to the maxima obtained from the 15-minute series for different seasons and event durations

Season	15 minutes	30 minutes	45 minutes	60 minutes	90 minutes	120 minutes
Annual	1.15	1.05	1.03	1.02	1.02	1.01
Winter	1.14	1.05	1.04	1.03	1.02	1.02
Summer	1.15	1.06	1.03	1.02	1.02	1.01

The schematic in Figure 3 shows the different time periods corresponding to the sliding window (time of tip stations – shown in green) and fixed window (15-minute stations – shown in blue).
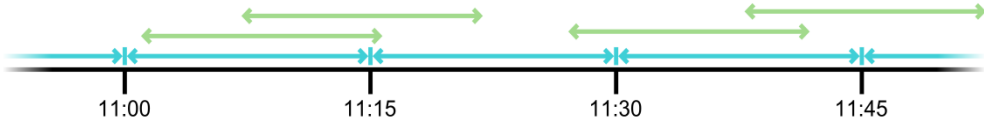
Figure 3 - Schematic representation of fixed (blue) and sliding (green) durations of 15 minutes

The flow chart in Figure 4 shows the procedure used to calculate sliding window correction factors.

For each time of tip station, the sliding window annual and seasonal maxima are extracted:

$$S_{(Station, Year)}$$

At the same station, the fixed window annual and seasonal maxima are extracted:

$$F_{(Station, Year)}$$

For each year at each station, the ratio between the sliding window maximum and the fixed window maximum is computed:

$$R_{(Station, Year)} = S_{(Station, Year)} / F_{(Station, Year)}$$

Compute the sliding window correction as:

$$W_{Corr} = average(R_{(Station, Year)})$$

Figure 4 - Illustration of the procedure used to calculate sliding window correction factors

4. Building the depth–duration–frequency model

The aim of a DDF model is to model the relationship between some properties of the depth and the duration of rainfall event maxima, and to use the modelled relationship to obtain estimates of frequency (or return period) which are consistent across event durations. The data set from which the relationship is modelled is typically composed of the annual or seasonal maxima over several years, which should be representative of the potentially large events that might occur in the location under study. When analysing block maxima, extreme value theory considerations come into play: these methods generally aim at modelling the 'long tail' of the data distribution and are particularly suitable for capturing the high skewness of block maxima data. Different approaches could be taken when constructing the data set used in building the DDF model: see Section 4.1 for a brief discussion of the challenges connected to compiling the data sets used to build the DDF model.

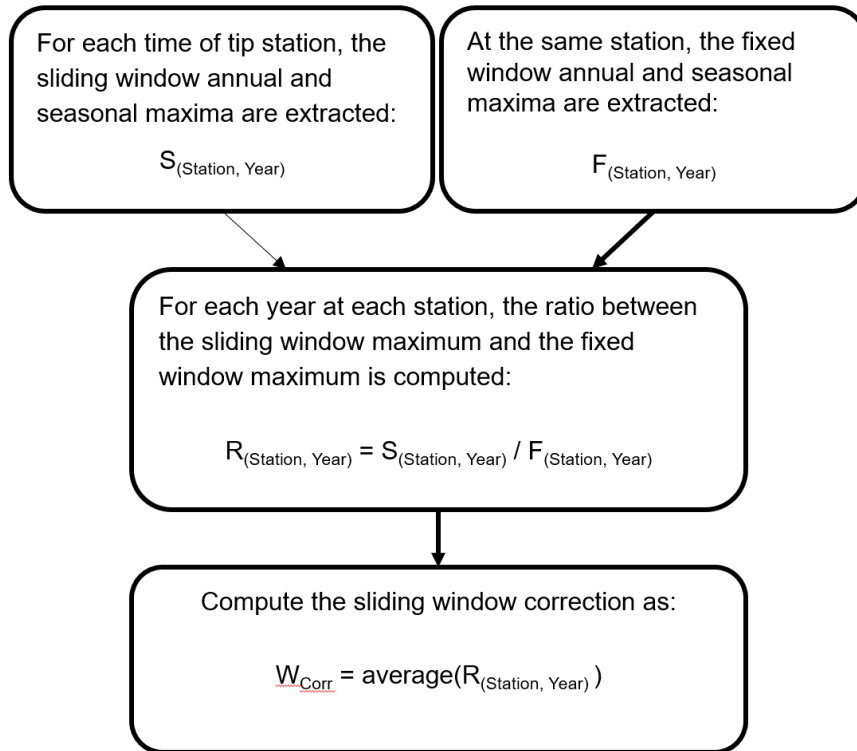In the FEH13 DDF model (Stewart and others, 2013), a combination of two gamma distributions was assumed to describe the distribution of the rainfall data (Equation 2). Indeed, a standard gamma distribution, which is often chosen as the assumed distribution for rainfall data, is sometimes unable to effectively describe the high skewness often observed in rainfall block maxima and might therefore underestimate the return periods of very rare events. The modified double gamma distribution of the FEH13 model allows each of the two gamma components to model different types of events, allowing for a high flexibility and many different possible shapes of frequency curves through the calibration of 14 separate parameters. The richness of the FORGEX outputs used in the FEH13 model makes it feasible to estimate such a high number of parameters. In a study based on the single-site approach (like the one presented in this work), very few stations would have long enough data records to allow the FEH13 model to be fitted. The two longest station records in this study contain 46 years of data each, while the median record is only 23 years long; records of these lengths would not allow for a model with as many parameters as FEH13 to be fitted to the data. Given the exploratory scope of this work, a simpler model was tested, which builds on classical extreme value theory (Coles 2001). In particular, the models presented in this study are based on an at-site analysis, which does not include information from nearby stations. Furthermore, the analysis is performed on recorded data, rather than model outputs. This implies that all caveats regarding data quality and the potential for measurement errors are in place.

Finally, given the nature of the records, two different sets of analysis are carried out: one for the nine stations at which block maxima of durations under 15 minutes are available and one for all 19 stations, on block maxima of 15 minutes and longer.

4.1 The challenge of building a peak-over-threshold data set

In addition to block (for example, annual or seasonal) maxima, so-called peak-over-threshold (POT) data are also commonly used when estimating extreme value models. Although the two methods can be shown to be equivalent asymptotically (i.e. for infinitely long records), the level curves which are estimated using relatively small sample values can be different and can be affected by a number of factors which come into play when compiling POT data sets. The idea of using POT data is that all values which can be considered large are used to estimate the return periods of rare and large events. This contrasts with block maxima data, which considers only the single maximum value in each block, regardless of whether it is typical of large events at that location. Typically, the final POT data set is composed of all events which exceed a certain threshold; therefore, more than one event may be present in some years, while no events at all may be present in other years. The advantages of compiling a POT data set (over a block maxima data set) for the analysis are that potentially more events can enter the data set and that all events in the data set are informative about extremal behaviour. The disadvantages are that a threshold value for large events must be decided and that rules to identify independent events need to be defined, as all events in a POT data set should be independent. Defining these rules can be complex, as they need to generalise the many different rainfall patterns which may be observed at one station. Moreover, in a DDF study, the set of rules which define independent peaks, and the choice of the threshold above which events should be retained, should also be dependent on the duration of the events, as they have an important impact in the final selected data set.

Using a POT approach to DDF modelling would therefore require some additional work in terms of initial choices and data processing. It is not clear if the advantage in terms of sample size and representativeness of the sample would justify the effort.

4.2 Preliminary investigations

The aim in building this model was to find a single structure that could be fitted separately at each station (that is, representing each station by the same model form, but using the data record at each station to obtain estimates of return period). Unlike some commonly used models, no information from nearby stations or from the characteristics of the station is used in model fitting. The final proposed model uses relatively few parameters, but is flexible enough to be able to estimate consistent curves for all the stations in the study.

An initial exploration of the relationship between some properties of the data distribution and the event duration was carried out. Figure 5 shows, for all stations, the relationship between event duration and the distribution's location, scale and skewness parameters. The points shown in the plot correspond to the sample L-moment values (Hosking and Wallis, 1997), estimated separately for annual maxima of each considered duration at the different stations, which are connected by lines. The left panel of Figure 5 shows the estimated sample L-moments for the first moment of the distribution, which gives

information on the centre of the distribution of the data. The centre panel of Figure 5 shows the estimated sample L-moments for the second moment of the distribution, which gives information on the spread of the distribution of the data. Finally, the right panel of Figure 5 shows the estimated sample third-order L-moment ratios (that is, the third-order L-moment divided by the second-order L-moment), which gives information on the skewness (for example, asymmetry) of the data distribution. Figures 6 and 7 show similar information for the winter and summer maxima series respectively.

For the annual and seasonal series, a predominant feature is the non-linear relationship between the event duration and the location parameter, with a similar relationship also observed between event duration and scale. The value of the first moment for all stations and all seasons increases non-linearly for increasing durations; the increase seems to be steeper for lower durations slowing down towards an asymptote (i.e. straight line on the plot) for longer durations. A similar behaviour is seen in the sample estimate of the second-order L-moment, although more variability can be seen across the different stations, in particular for longer durations.

Figure 5 - Sample L-moments for the first-order L-moment (left panel), second-order L-moment (central panel) and third-order L-moment ratio (right panel) for each duration at all stations (annual maxima series)

Figure 5 shows the annual maxima series sample L-moments for the first-order L-moment (left panel), second-order L-moment (central panel) and third-order L-moment ratio (right panel) for each duration (0-120 minutes) at all stations (Bettws-y-Crwyn, Chieveley, Colwyn Bay, Crew Fell, Dowdeswell, Hemyock, Hinckley, Kingswood, Knightcote, Llanychaer, Lower Dunsforth, Ludford, Otterbourne, Putney Heath, Sale Carrington, Stanford Rivers, Stone, Taw Head, Victoria Park). The x-axis on all panels shows the duration (0-120 minutes). The y-axis plots the L-moment location (0-20) on the left panel, the L-moment scale (0-8) on the central panel and the L-moment shape (0.0-0.8) on the right panel.
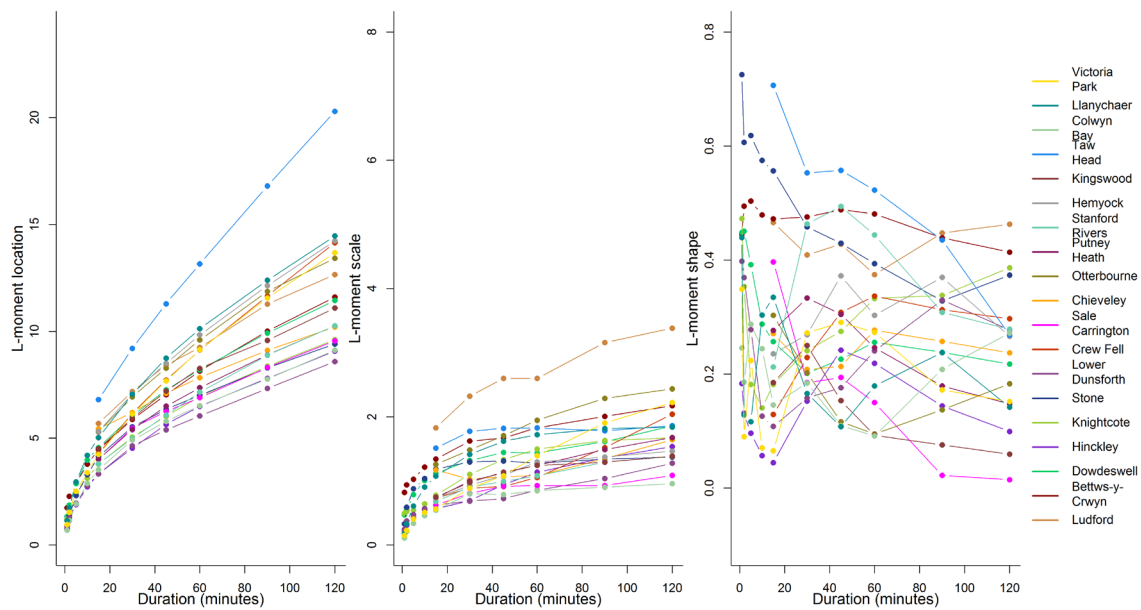
Figure 6 - Sample L-moments for the first-order L-moment (left panel), second-order L-moment (central panel) and third-order L-moment ratio (right panel) for each duration at all stations (winter maxima series)
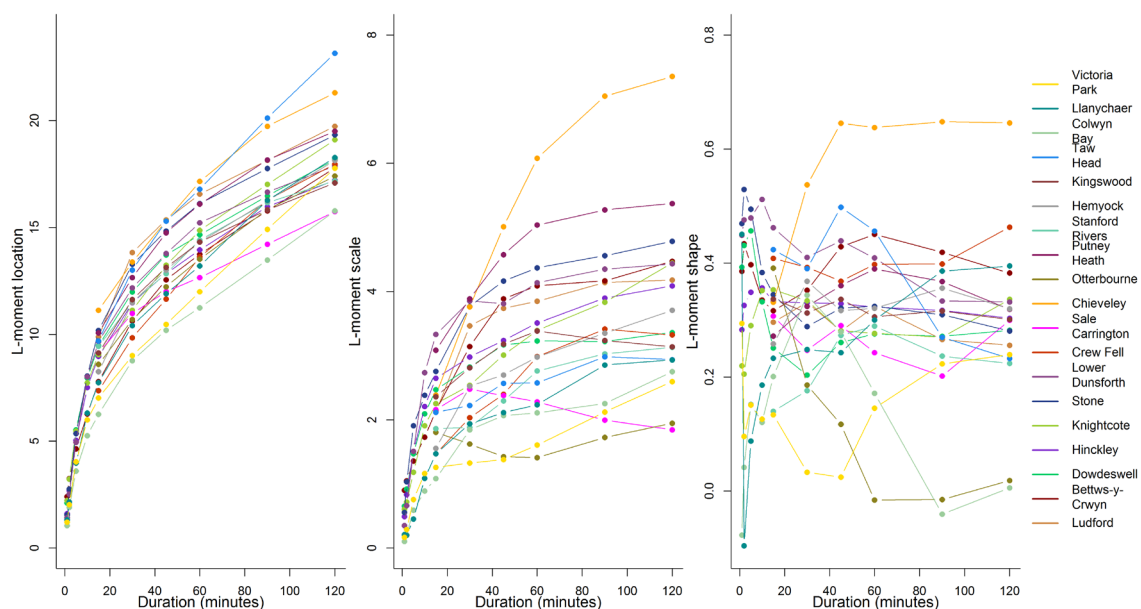
Figure 6 shows the winter maxima series sample L-moments for the first-order L-moment (left panel), second-order L-moment (central panel) and third-order L-moment ratio (right panel) for each duration (0-120 minutes) at all stations (Bettws-y-Crwyn, Chieveley, Colwyn Bay, Crew Fell, Dowdeswell, Hemyock, Hinckley, Kingswood, Knightcote, Llanychaer, Lower Dunsforth, Ludford, Otterbourne, Putney Heath, Sale Carrington, Stanford Rivers, Stone, Taw Head, Victoria Park). The y-axis plots the L-moment location (0-20) on the left panel, the L-moment scale (0-8) on the central panel and the L-moment shape (0.0-0.8) on the right panel.
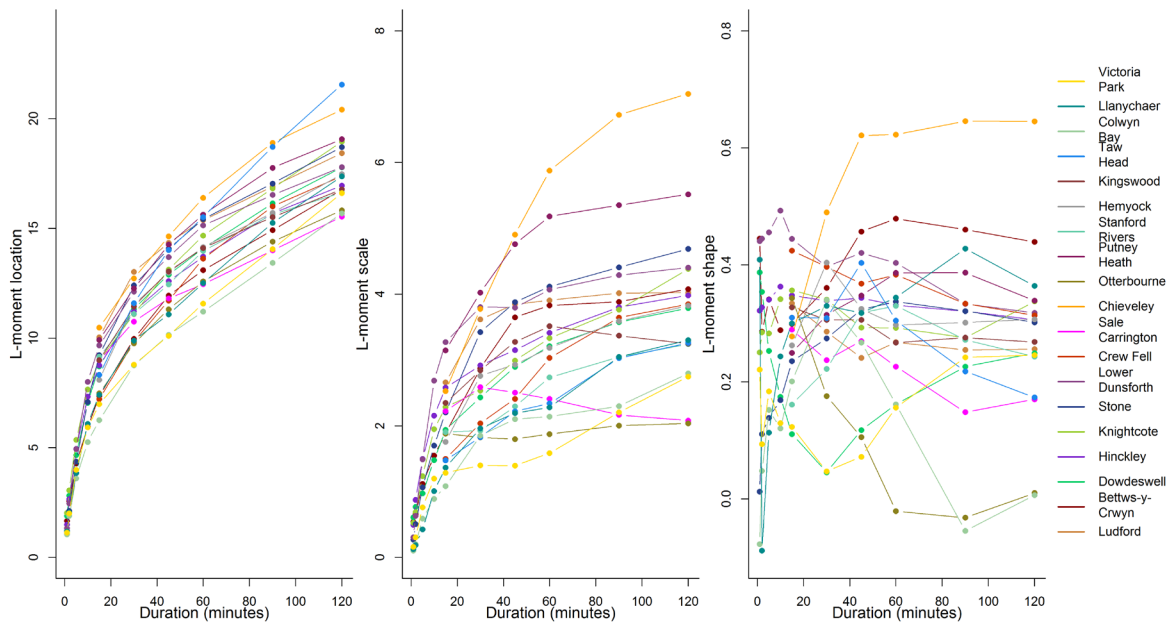
Figure 7 - Sample L-moments for the first-order L-moment (left panel), second- order L-moment (central panel) and third-order L-moment ratio (right panel) for each duration at all stations (summer maxima series)

Figure 7 shows the summer maxima series sample L-moments for the first-order L-moment (left panel), second-order L-moment (central panel) and third-order L-moment ratio (right panel) for each duration (0-120 minutes) at all stations (Bettws-y-Crwyn, Chieveley, Colwyn Bay, Crew Fell, Dowdeswell, Hemyock, Hinckley, Kingswood, Knightcote, Llanychaer, Lower Dunsforth, Ludford, Otterbourne, Putney Heath, Sale Carrington, Stanford Rivers, Stone, Taw Head, Victoria Park). The y-axis plots the L-moment location (0-20) on the left panel, the L-moment scale (0-8) on the central panel and the L-moment shape (0.0-0.8) on the right panel.

The plot in Figure 8 indicates that a linear relationship between the location and scale parameters could exist. On the other hand, the relationship between event duration and the third-order ratio seems to be less consistent across the different stations and shows an erratic pattern. Estimating the third-order moment is a difficult task and can be heavily influenced by a few extreme points in the data set, especially when only small sample sizes are available.
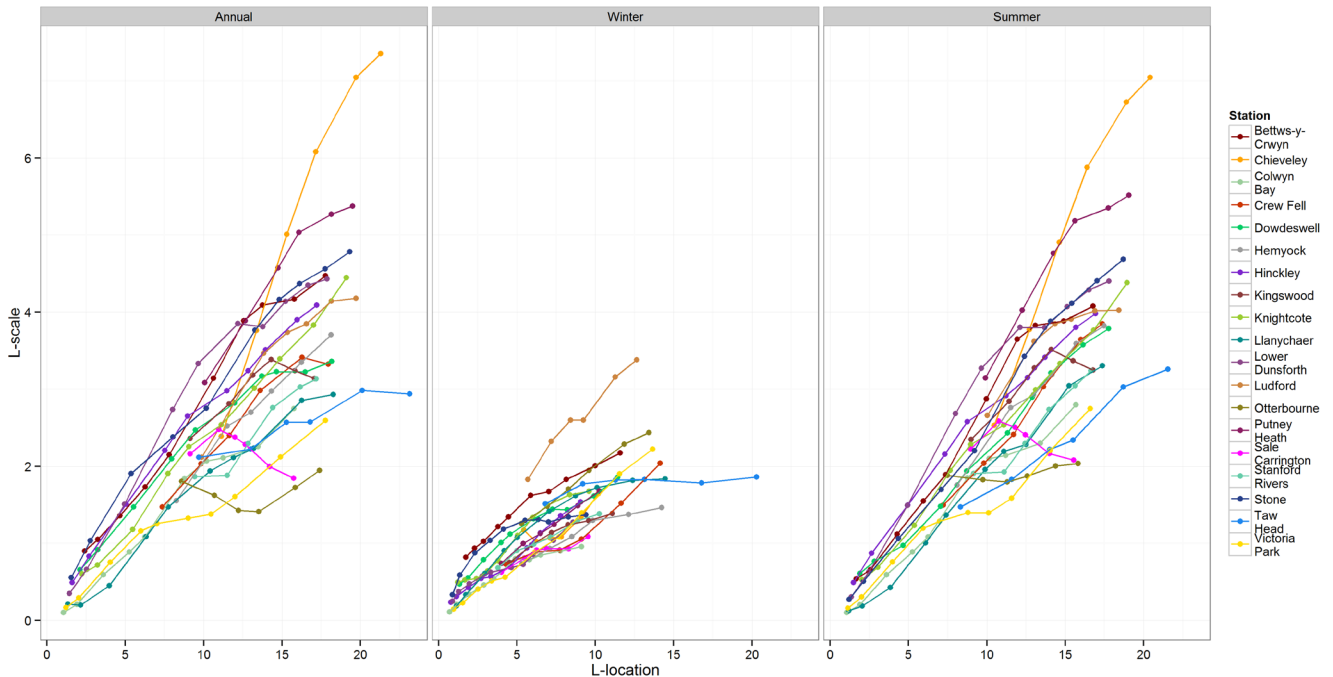
Figure 8 - Sample L-moments for the first-order L-moment and second- order L-moment for the annual series (left panel), the winter series (central panel) and the summer series (right panel)

Figure 8 shows the sample L-moments for the first-order L-moment and second-order L-moment for the annual series (left panel), the winter series (central panel) and summer series (right panel) at all stations (Bettws-y-Crwyn, Chieveley, Colwyn Bay, Crew Fell, Dowdeswell, Hemyock, Hinckley, Kingswood, Knightcote, Llanychaer, Lower Dunsforth, Ludford, Otterbourne, Putney Heath, Sale Carrington, Stanford Rivers, Stone, Taw Head, Victoria Park. The x-axis shows the L-location (0-20) and the y-axis plots the L-scale (0-6).

The sample parameters estimated for the summer maxima series seem to behave in a similar way to the sample parameters estimated for the annual maxima series. This is not surprising since approximately 86% of the annual maxima are recorded during the summer months. The two series are therefore likely to be similar, although, due to the requirement for 'completeness', some years that are missing too much data to be included in the annual series contribute a valid value to the summer series (and vice versa). For the winter series, the observed relationship between the location parameter and event duration seems to be less curved and less steep than in the annual and summer series. Also, the location and scale parameters tend to have much lower values in the winter

series, which is an indication that larger events are, on average, more likely to happen in summer.

A modelling method which could exploit the fact that L-moment location and scale vary similarly, relative to duration, was pursued. In a DDF model, frequency curves for different durations should not cross, meaning that the depth of the T-year event should always increase with increasing event duration. The relatively small sample size of some stations also had to be considered, and so a simple model with only a small number of fitted parameters was pursued. Initially, a gamma distribution with a changing scale parameter was investigated, but it soon became clear that the high skewness observed in the maxima series could not be accommodated by a simple 2-parameter distribution. Therefore, the unified generalised extreme value (GEV) distribution described in the next section was proposed.

4.3 A unified generalised extreme value distribution

The GEV distribution is widely used when analysing block maxima, both for its theoretical justification and its practicality. For block maxima, the GEV distribution allows different tail behaviours to be modelled with one functional form: the skewness parameter value, κ, defines whether the distribution has a finite upper bound (when κ > 0) or a finite lower bound (when κ < 0). For values of κ = 0, the GEV distribution coincides with the Gumbel distribution and has non-finite lower and upper bounds. Apart from the skewness parameter, κ, the GEV distribution is characterised by the location parameter, ξ, which gives an indication of the central tendency of the distribution, and the scale parameter, α (with α > 0), which gives an indication of the variability of the distribution. By *X~GEV(ξ, α, κ)* one denotes that a random variable *X* is assumed to follow a GEV distribution. As already mentioned, the skewness parameter governs the boundary of the distribution support (that is, the possible set of values that the variable can take) as shown in Equation 5:

Equation 5 – Lower and upper bounds of the generalised extreme value (GEV) distribution as related to GEV skewness parameter (κ)

$$
\begin{cases}
-\infty < x \leq \xi + \dfrac{\alpha}{\kappa} & \text{if } \kappa > 0 \\
-\infty < x < \infty & \text{if } \kappa = 0 \\
\xi + \dfrac{\alpha}{\kappa} < x < \infty & \text{if } \kappa < 0
\end{cases}
$$

The lower and upper bound values for the cases in which $\kappa \neq 0$ are a linear combination of the location of the GEV distribution and the scale parameter weighted by the skewness parameter. This property is used in this work to build consistent frequency curves. The quantile function for the GEV distribution is shown in Equation 6:

Equation 6 – The quantile function for the GEV distribution

$$x(F) = \begin{cases} \xi + \dfrac{\alpha}{\kappa}[1 - (-\ln F)^{\kappa}] & \text{if } \kappa \neq 0 \\ \xi - \alpha \ln(-\ln F) & \text{if } \kappa = 0 \end{cases}$$

In Equation 6, F is the non-exceedance probability, corresponding to F = (1 − 1/T) for a T-year event. The desired property of a DDF model is that the quantile functions for increasing durations of rainfall accumulation, D, do not cross. When analysing rainfall maxima, the skewness parameter is expected to be negative, meaning that no upper bound can be determined. The development of the model which follows is therefore focused on the case of $\kappa < 0$ although similar ideas would apply for $\kappa > 0$.

The lower bound of the distribution, ℓ, is assumed to be the same across all durations. The location and scale parameters of the distributions are taken to be functions of the duration: $\xi(D)$ and $\alpha(D)$. Based on the mixed results in Figures 5, 6 and 7 (right panels) the skewness parameter κ is taken to be the same across all durations. This translates into the following relationship shown in Equation 7:

Equation 7 – Lower bound of GEV distribution with time-independent skewness (κ)

$$l = \xi(D) + \frac{\alpha(D)}{\kappa} \leq \xi(D)$$

Equation 7 can be rewritten as shown in Equation 8:

Equation 8 – Re-arrangement of Equation 7

$$\alpha(D) = (l - \xi(D))\kappa$$

Taking the location and shape parameters as functions of the event duration, the quantile function of Equation 6 can be rewritten for $x_D(F)$, the rainfall value at different durations (shown in Equation 9):

Equation 9 – Quantile function of GEV distribution in terms of location parameter (ξ) and lower bound (Equation 8)

$$x_D(F) = \xi(D) + \frac{\alpha(D)}{\kappa}[1 - (-\ln F)^{\kappa}] = \xi(D) + (l - \xi(D))[1 - (-\ln F)^{\kappa}]$$

$x_D(F)$ is an increasing function of D, provided that $\xi(D)$ is increasing. The similar shapes seen in the relationship between the location and scale L-moments for the different durations support the assumption that the scale functions could be described as linear combinations of the location functions. The assumption that a unique common lower bound exists also seems to be reasonable from a physical point of view. Figures 5, 6 and 7 indicate that the relationship between the event duration and the first order parameter could be described by an exponential function, which allows for a steeper increase for short durations and then tends to an asymptote (straight line) for longer durations. Inspired by the models used in FEH13, the following relationship (shown in Equation 10) is therefore suggested to model the location function:

Equation 10 – Modelling the location function

$$\xi(D) = a + bD + c(1 - \exp\{\text{-}gD\})$$

This is an increasing function of D provided that $b + cg\exp\{-gD\} > 0$

Once the lower bound and the skewness parameter are also determined, the scale function can be determined from the relationship in Equation 8. Therefore, the model has a total of six parameters, five fewer than the FEH13 model. The maximum likelihood (ML) estimation procedure is used, with $\xi(D)$ enforced as an increasing function of D in the estimation procedure. To make the estimation more stable, the duration D (ranging from one to 120 minutes) is standardised so that the actual values used in the estimation procedure correspond to D/480.

A model similar to the unified GEV presented here could be proposed, in which the scale is directly modelled as a function of duration, together with a lower bound and the skewness parameter. The location function would then be estimated via the same linear relationship as used in this work. This modelling strategy has not been attempted.

It was initially hoped that the skewness parameter could be estimated before the maximum likelihood estimation, by taking some form of the average of the L-moment estimates of the skewness across the different durations. This proved to be problematic as the skewness parameter at some stations happened to be estimated as positive for some durations and the sample averages could be positive or very close to zero. This mostly happened at stations with short records (which are therefore less likely to have information on very large events). Although some forms of weighting could have been used to overcome this issue, it was decided to estimate the skewness parameter via the maximum likelihood procedure as well.

Maximum likelihood methods are well established in extreme value models and enjoy some desirable asymptotic properties (for example, unbiasedness and efficiency). Nevertheless, in the context of this study, the sample size available is often not very large and this might undermine the estimation procedure. Indeed, the estimation procedure has been found to be somewhat sensitive to starting values and the optimisation of the likelihood function has sometimes proved to be difficult: it is suspected that local maxima might exist in the likelihood function. If the methods presented in this work were to be

generalised to a larger scale, it would be advisable to use more robust methods than likelihood or to limit the study to stations with very long series. If maximum likelihood were to be used, the sensitivity of the results to starting values should be assessed.

The estimation procedure is divided into two parts. In the first part, the model is fitted only to the series obtained from the time of tip stations, therefore spanning durations from one to 120 minutes. In the second part, the model is fitted to the series available from all 19 stations, spanning durations from 15 to 120 minutes. For both sets of analyses, the annual and seasonal maxima are processed separately.

5. Results of the depth–duration–frequency model: the time of tip stations

The unified GEV model presented in Section 4 was estimated for each series extracted from the stations for which time of tip data were available.

Results for the annual, winter and summer maxima at each time of tip station are shown in Figures 9 to 11 respectively. Lines on the left panel of each figure show the estimated location parameter function for increasing event duration for all time of tip stations. Lines on the right panel show the relationship between increasing event duration and the scale parameter value. The two functions have a similar shape as a result of the linear relationship assumed in the model; this assumption might not allow enough flexibility for some stations. Together with the estimated functions, dots on both panels show the GEV parameter values obtained via the L-moment estimation method, for each duration separately. The advantage of using the DDF model over the separate L-moment estimates lies in the fact that frequency curves produced by the DDF model cannot cross. However, the fact that the estimated location and scale functions are close to the L-moment estimates lends additional confidence to the DDF model.

As already shown in Figures 5, 6 and 7, the location parameters estimated for the winter series here are well below those estimated for the annual and summer series, especially at longer durations. Furthermore, the estimated location functions of the winter series less steep than those estimated for the summer series.

Tables 4 to 6 show the estimated values of the six model parameters, including the lower bound (ℓ) and skewness parameter (κ), for the annual, winter and summer series respectively. Overall, the skewness estimated for the winter series is smaller than the skewness estimated for the annual and summer series; frequency curves for the winter months will be less steep and a tiny probability will be assigned to very large events. This is evident in the plots from Figures 18 to 26, which show the frequency curves estimated by the unified GEV model for the different durations considered (note that the figures are ordered by easting value, so that the most westerly stations appear first).

As desired, the frequency curves are consistent and do not cross. The curves are superimposed on the observed data points for each event duration, which are located according to Gringorten plotting positions. The x-axis is transformed to the Gumbel reduced variate, $-\ln(-\ln(1 - 1/T))$, which increases with increasing return periods: vertical bars indicate the x-axis locations of the 1.2-, 2-, 5-, 10-, 50-, 100- and 200-year event. In each of Figures 18 to 26, the left panel shows the results for the annual series, the central panel shows the results for the winter series and the right panel shows the results for the summer series. The overall fit of the estimated frequency curves against the observed frequency curves seems to be satisfactory, with some unavoidable lack of fit at some stations for some durations. Setting a constant skewness value across the different durations ensures that the frequency curves for different durations do not cross but may apparently overestimate the skewness of the frequency curves for some event durations

(see, for example, the left panel of Figure 20). On the other hand, especially in short records, it may be that the maxima extracted for a specific station do not contain a record of all possible types of events which a station might register for each duration. Sharing information across the different durations might help in obtaining lower return periods for events which are not represented in the sample simply because of chance (and not because they are unrealistically large). Furthermore, the strict relationship between the location and scale function forces the scale function to increase with increasing event duration: this implies that curves for longer durations will become steeper and steeper, therefore the 'fanning out' effect seen in Figures 18 to 26. This increase in the steepness of the frequency curves might be unrealistic if one were to extrapolate to durations longer than those considered.
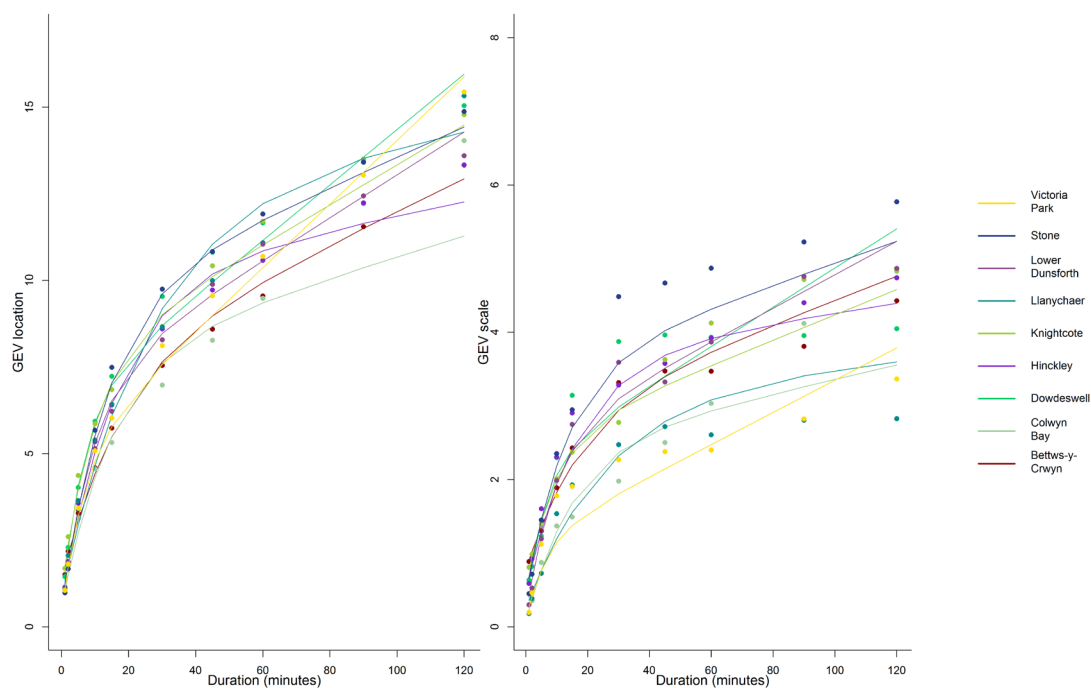
Figure 9 - Estimated location and scale parameter values for the unified GEV model for each station as a function of duration - annual series

Figure 9 shows the estimated location values (left panel) and scale parameter values (right panel) for the unified GEV model as a function of duration (0-120 minutes) for each station (Bettws-y-Crwyn, Colwyn Bay, Dowdeswell, Hinckley, Knightcote, Llanychaer, Lower Dunsforth, Stone, Victoria Park) as a function of duration (0-120 minutes) - annual series. The x-axis shows the duration (0-120 minutes). The y-axis plots the GEV location (0-15) on the left panel, and the GEV scale (0-8) on the right panel. Dots indicate L-moment estimates obtained when treating each duration separately

Table 4 - Parameter estimates for the unified GEV model based on one-minute data – annual series

| Station name	*a*	*b*	*c*	*g*	ℓ	κ
Bettws-y-Crwyn	1.35	22.44	5.97	27.32	-0.88	-0.34
Colwyn Bay	0.53	14.36	7.16	31.88	0.33	-0.32
Dowdeswell	0.59	38.37	5.77	73.14	-0.24	-0.33
Hinckley	0.68	9.26	9.27	28.57	-0.67	-0.34
Knightcote	1.04	27.60	6.54	49.46	-0.82	-0.30
Llanychaer	0.87	7.76	11.60	17.96	-0.12	-0.25
Lower Dunsforth	0.39	29.71	6.46	52.33	0.03	-0.37
Stone	0.41	20.77	8.82	36.22	-0.86	-0.34
Victoria Park	0.35	44.04	4.51	72.60	0.00	-0.24
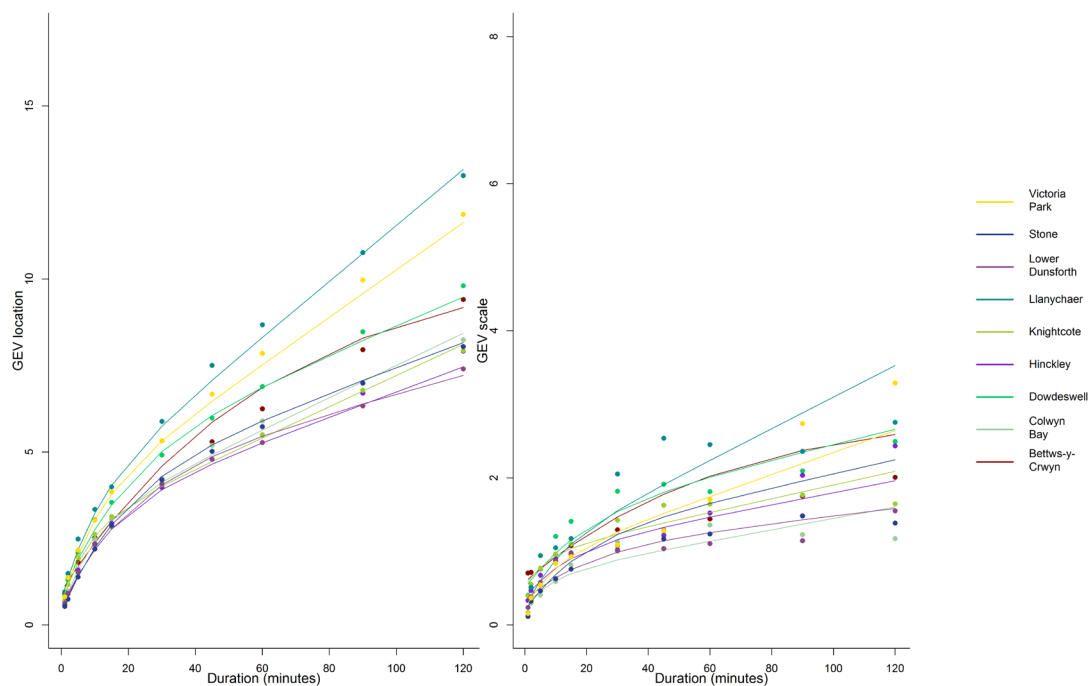
Figure 10 - Estimated location and scale parameter values for the unified GEV model for each station as a function of duration – winter series.

Figure 10 shows the winter series estimated location values (left panel) and scale parameter values (right panel) for the unified GEV model as a function of duration (0-120 minutes) for each station (Bettws-y-Crwyn, Colwyn Bay, Dowdeswell, Hinckley, Knightcote, Llanychaer, Lower Dunsforth, Stone, Victoria Park) as a function of duration (0-120 minutes). The x-axis on both panels shows the duration (0-120 minutes). The y-axis plots the GEV location (0-15) on the left panel, and the GEV scale (0-8) on the right panel. The dots indicate the L-moment estimates obtained when treating each duration separately.

Table 5 - Parameter estimates for the unified GEV model based on one-minute data – winter series

| Station name	a	b	c	g	ℓ	κ
Bettws-y-Crwyn	0.97	-0.72	10.00	7.29	-1.41	-0.24
Colwyn Bay	0.36	22.35	2.48	49.25	-1.15	-0.17
Dowdeswell	0.84	19.55	3.76	24.60	-1.16	-0.25
Hinckley	0.38	17.36	2.73	35.78	-1.23	-0.23
Knightcote	0.57	21.62	2.13	61.14	-1.95	-0.21
Llanychaer	0.70	38.80	2.76	46.67	-0.10	-0.27
Lower Dunsforth	0.52	12.74	3.51	24.02	-1.26	-0.19
Stone	0.34	17.17	3.52	27.07	-0.39	-0.26
Victoria Park	0.56	32.80	2.86	47.01	-0.46	-0.22
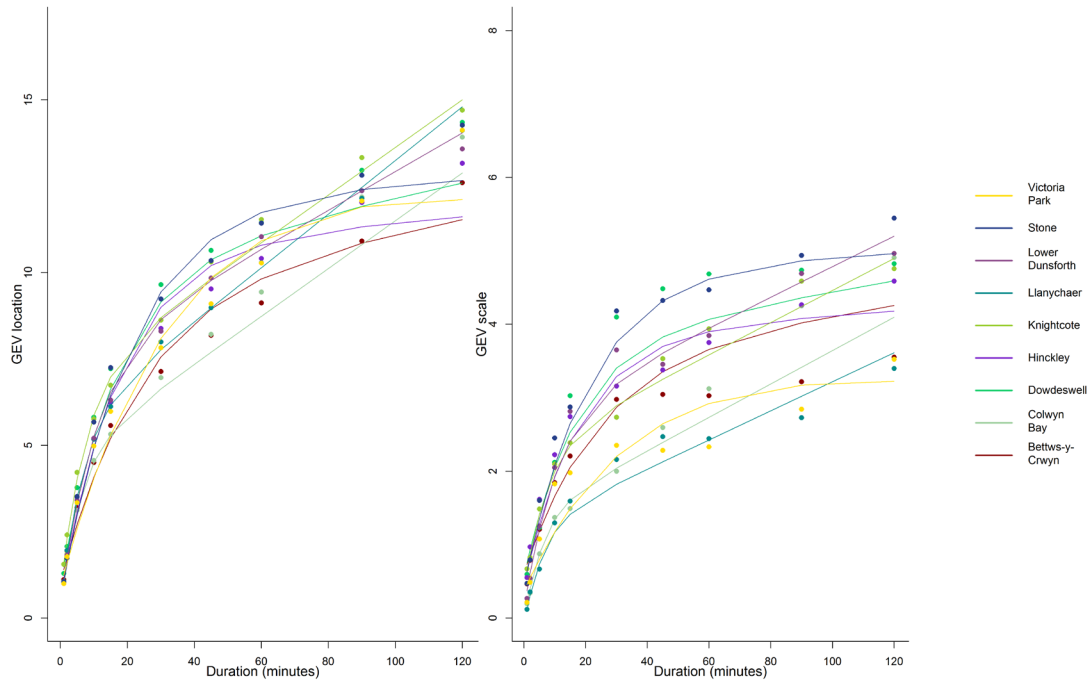
Figure 11 - Estimated location and scale parameter values for the unified GEV model for each station as a function of duration – summer series.

Figure 11 shows the summer series estimated location values (left panel) and scale parameter values (right panel) for the unified GEV model as a function of duration (0-120 minutes) for each station (Bettws-y-Crwyn, Colwyn Bay, Dowdeswell, Hinckley, Knightcote, Llanychaer, Lower Dunsforth, Stone, Victoria Park) as a function of duration (0-120 minutes). The x-axis on both panels shows the duration (0-120 minutes). The y-axis plots the GEV location (0-15) on the left panel, and the GEV scale (0-8) on the right panel. The dots indicate the L-moment estimates obtained when treating each duration separately.

Table 6 - Parameter estimates for the unified GEV model based on one-minute data – summer series

Station name	a	b	c	g	ℓ	κ
Bettws-y-Crwyn	1.04	8.67	8.38	19.95	-0.69	-0.35
Colwyn Bay	0.17	33.17	4.41	84.01	0.43	-0.33
Dowdeswell	0.93	10.18	9.12	28.49	-0.69	-0.35
Hinckley	0.58	3.74	10.12	26.48	-0.70	-0.34
Knightcote	0.74	33.07	5.98	64.69	-0.41	-0.32
Llanychaer	0.20	37.28	5.28	77.10	0.63	-0.25
Lower Dunsforth	0.39	26.77	6.96	46.32	0.09	-0.37
Stone	0.51	2.13	11.67	22.41	-0.66	-0.37
Victoria Park	0.88	-5.62	13.04	13.89	-0.55	-0.25

Finally, in Figures 18 to 26 in Appendix A.1, the same (or very similar) rainfall depths are often recorded across some shorter durations in several years. In addition, in some years and at some stations, the recorded maximum has the same value for multiple durations (therefore, the fact that some data points seem to not exist; they are covered by points of a different colour with the same value).

6. Results of the depth–duration–frequency model: longer durations

The unified GEV model presented in Section 4 is estimated for each series of duration 15 minutes or longer, extracted from both the 15-minute and the time of tip stations. The series extracted from the 15-minute stations are multiplied by the sliding window coefficients shown in Table 3.

Results for the annual, winter and summer maxima are shown in Figures 12 to 14 (similar to Figures 9 to 11 respectively). The location functions estimated here increase in a more linear shape than those estimated in Section 5. Again, it is reassuring to see the relative similarity between the location and scale functions estimated for each event duration separately, via L-moments, and the unified GEV parameter function. The estimated curves shown in Figures 12 to 14, for durations of 15 minutes or greater, are less steep than those estimated when lower durations are also included (shown in Figures 9 to 11). It is possible that a less complex model could have been used for DDF modelling of longer durations, but it was decided to use the same model for both subsets of stations in this work. The difference in shape needed to represent the location functions in Figure 9 and Figure 12 exemplifies the difficulties of extrapolating results for durations outside the calibration range: it might not be realistic for the function to behave in a similar way across much longer or shorter durations.

Estimated parameter values for the annual, winter and summer series are shown in Tables 7 to 9 respectively. It should be noted that the estimated value of the skewness parameter κ is very close to zero for a number of sites in each table. This is mostly driven by the fact that, for some durations, no very large event is recorded across the years in the record. For these durations, the estimated skewness values are very close to zero or positive. Therefore, the skewness parameter of the unified GEV is somewhat pulled towards zero at these sites, and therefore the frequency curves become fairly straight. This effect is visible in the estimated frequency curves at, for example, Otterbourne (Figure 41) and Victoria Park (Figure 29).

Figures 27 to 45 (Appendix A.2) show the estimated unified GEV frequency curves, for all series of annual and seasonal maxima, for all events of at least 15-minutes duration, at all 19 stations included in the study. The stations are again ordered from the most western to the most eastern.
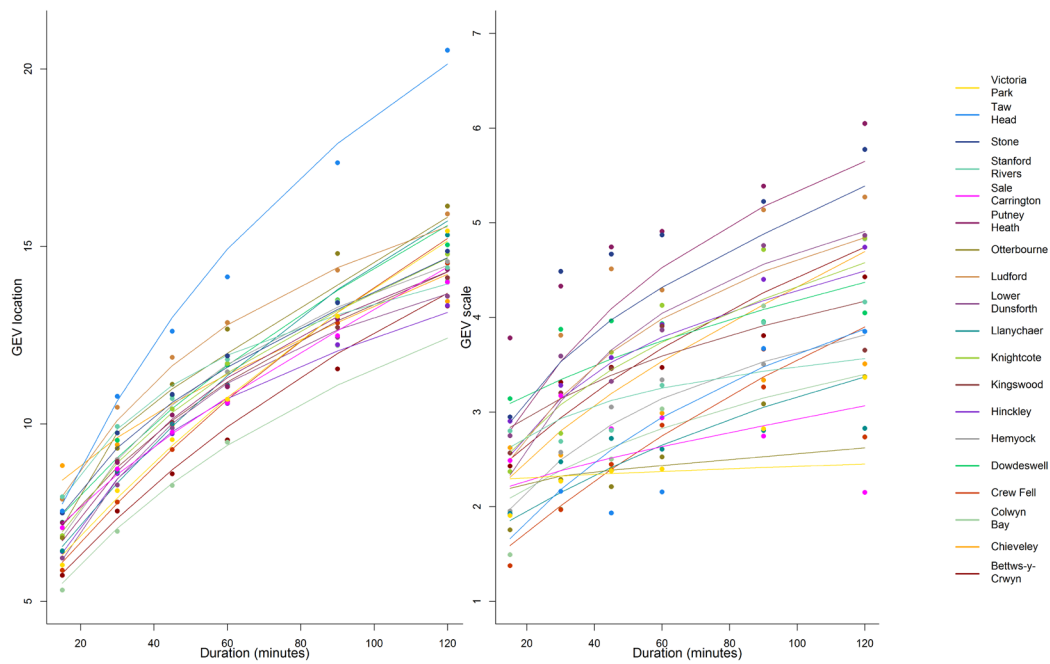
Figure 12 - Estimated location and scale parameter values for the unified GEV model for each station as a function of duration – annual series.

Figure 12 shows the annual series estimated location values (left panel) and scale parameter values (right panel) for the unified GEV model as a function of duration (0-120 minutes) for each station (Bettws-y-Crwyn, Chieveley, Colwyn Bay, Crew Fell, Dowdeswell, Hemyock, Hinckley, Kingswood, Knightcote, Llanychaer, Lower Dunsforth, Ludford, Otterbourne, Putney Heath, Sale Carrington, Stanford Rivers, Stone, Taw Head, Victoria Park). The x-axis on both panels shows the duration (0-120 minutes). The y-axis plots the GEV location (0-20) on the left panel, and the GEV scale (0-7) on the right panel. Dots indicate L-moment estimates obtained when treating each duration separately.

Table 7 - Parameter estimates for the unified GEV model based on 15-minute data – annual series

| Station name	a	b	c	g	ℓ	κ
Bettws-y-Crwyn	4.03	12.72	8.68	5.48	-3.01	-0.28
Chieveley	6.80	21.00	2.19	18.64	2.81	-0.41
Colwyn Bay	3.61	13.01	6.26	8.74	-5.54	-0.19
Crew Fell	4.29	5.25	17.77	3.12	-0.17	-0.25
Dowdeswell	5.56	23.44	4.64	9.18	-12.21	-0.16
Hemyock	3.69	13.81	7.53	14.19	-1.36	-0.24
Hinckley	2.81	15.92	6.39	20.83	-2.47	-0.29
Kingswood	5.04	16.40	5.50	10.87	-8.04	-0.19
Knightcote	4.15	21.19	5.30	16.64	-2.92	-0.26
Llanychaer	4.57	-6.73	23.88	3.08	-4.66	-0.17
Lower Dunsforth	2.82	10.62	8.42	14.19	-0.61	-0.34
Ludford	4.91	13.03	7.65	13.59	-0.10	-0.31
Otterbourne	-4.08	30.59	12.26	57.43	-37.70	-0.05
Putney Heath	4.08	13.52	7.22	11.60	-0.77	-0.38
Sale Carrington	5.37	28.14	2.02	20.14	-11.65	-0.12
Stanford Rivers	4.61	11.91	6.40	19.39	-9.10	-0.15
Stone	4.47	22.55	4.60	22.19	-0.88	-0.35
Taw Head	4.11	19.79	12.41	8.91	-1.54	-0.18
Victoria Park	4.55	3.20	18.77	2.96	-124.57	-0.02
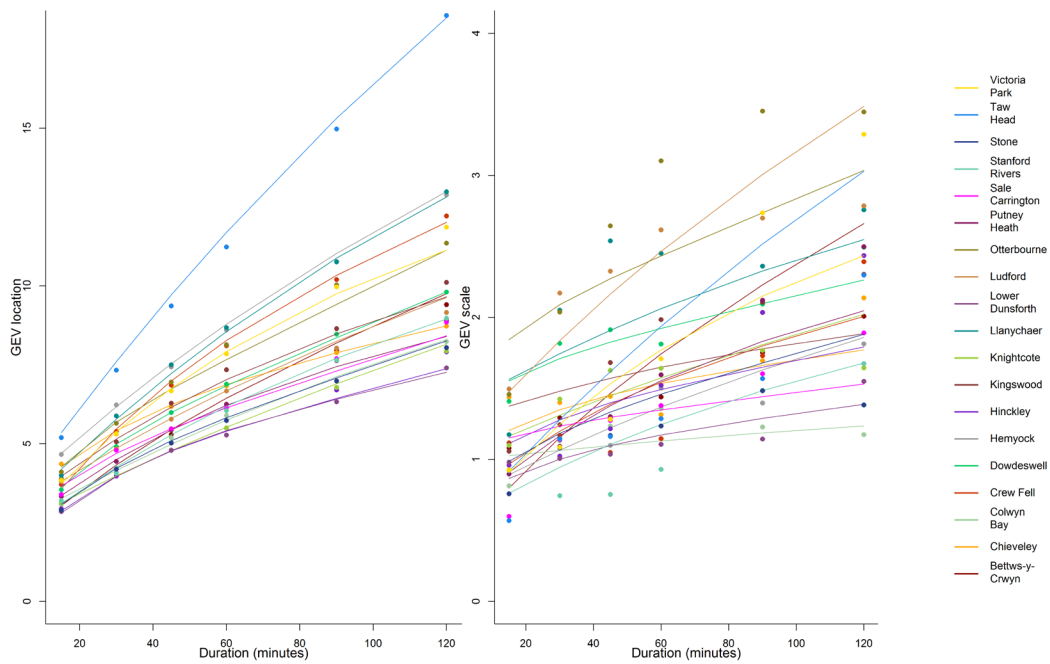
Figure 13 – Estimated location and scale parameter values for the unified GEV model for each station as a function of duration – winter series.

Figure 13 shows the winter series estimated location values (left panel) and scale parameter values (right panel) for the unified GEV model as a function of duration (0-120 minutes) for each station (Bettws-y-Crwyn, Chieveley, Colwyn Bay, Crew Fell, Dowdeswell, Hemyock, Hinckley, Kingswood, Knightcote, Llanychaer, Lower Dunsforth, Ludford, Otterbourne, Putney Heath, Sale Carrington, Stanford Rivers, Stone, Taw Head, Victoria Park). The x-axis on both panels shows the duration (0-120 minutes). The y-axis plots the GEV location (0-15) on the left panel, and the GEV scale (0-4) on the right panel. Dots indicate L-moment estimates obtained when treating each duration separately.

Table 8 – Parameter estimates for the unified GEV model based on 15-minute data – winter series

| Station name	*a*	*b*	*c*	*g*	*ℓ*	*κ*
Bettws-y-Crwyn	1.52	21.44	3.12	10.21	0.17	-0.28
Chieveley	2.57	12.38	3.11	17.49	-5.23	-0.13
Colwyn Bay	2.30	-9.27	23.71	1.73	-21.42	-0.04
Crew Fell	1.18	20.77	6.05	10.88	-4.28	-0.12
Dowdeswell	1.48	22.90	2.61	25.44	-9.89	-0.11
Hemyock	3.07	18.07	7.93	4.57	-2.97	-0.12
Hinckley	1.16	14.45	2.61	20.97	-4.52	-0.15
Kingswood	2.58	11.46	4.98	7.44	-11.33	-0.09
Knightcote	2.19	16.32	2.38	6.29	-3.72	-0.17
Llanychaer	2.48	-14.33	34.15	2.09	-9.49	-0.11
Lower Dunsforth	1.07	12.51	3.10	18.20	-4.58	-0.12
Ludford	2.66	15.76	3.96	5.83	-0.47	-0.35
Otterbourne	1.83	27.48	2.44	33.30	-6.38	-0.17
Putney Heath	1.94	8.92	4.77	8.65	-0.67	-0.23
Sale Carrington	2.06	17.56	1.97	24.17	-10.78	-0.08
Stanford Rivers	1.75	9.64	6.25	5.80	-1.78	-0.16
Stone	1.42	18.22	2.30	20.60	-2.63	-0.17
Taw Head	2.94	2.11	36.86	2.09	-0.37	-0.16
Victoria Park	1.73	9.51	8.42	7.20	-0.67	-0.21
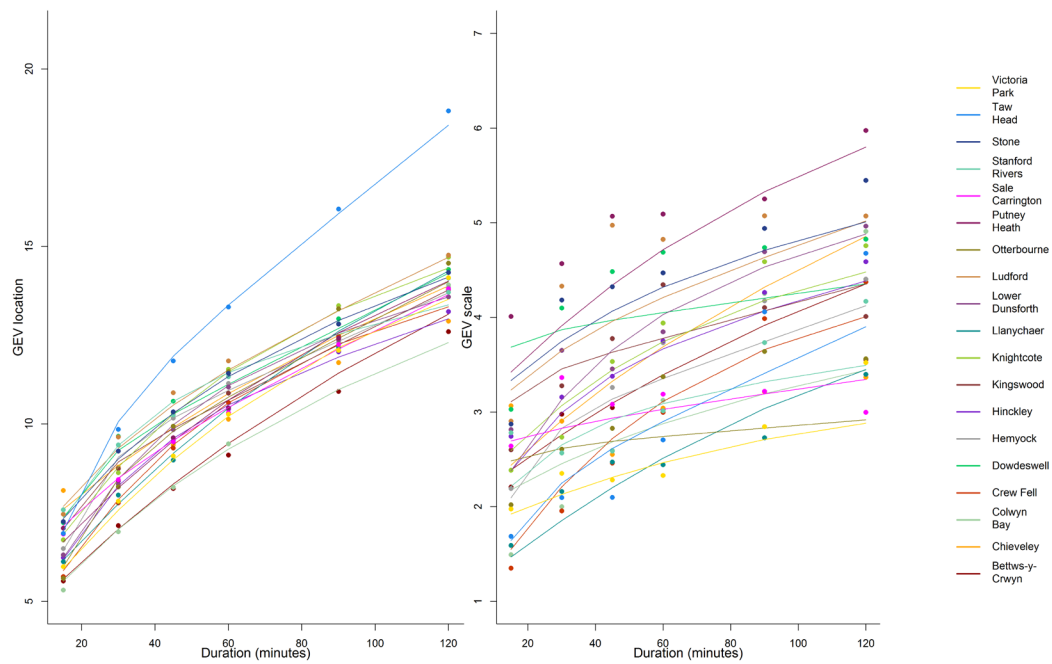
Figure 14 - Estimated location and scale parameter values for the unified GEV model for each station as a function of duration – summer series.

Figure 14 shows the summer series estimated location values (left panel) and scale parameter values (right panel) for the unified GEV model as a function of duration (0-120 minutes) for each station (Bettws-y-Crwyn, Chieveley, Colwyn Bay, Crew Fell, Dowdeswell, Hemyock, Hinckley, Kingswood, Knightcote, Llanychaer, Lower Dunsforth, Ludford, Otterbourne, Putney Heath, Sale Carrington, Stanford Rivers, Stone, Taw Head, Victoria Park). The x-axis on both panels shows the duration (0-120 minutes). The y-axis plots the GEV location (0-20) on the left panel, and the GEV scale (0-7) on the right panel. Dots indicate L-moment estimates obtained when treating each duration separately.

Table 9 - Parameter estimates for the unified GEV model based on 15-minute data – summer series

Station name	a	b	c	g	ℓ	κ
Bettws-y-Crwyn	4.05	11.48	8.96	4.67	-3.45	-0.26
Chieveley	6.17	15.70	4.48	7.48	1.25	-0.38
Colwyn Bay	3.81	12.39	6.24	7.95	-6.03	-0.19
Crew Fell	3.24	4.35	9.98	9.18	1.19	-0.33
Dowdeswell	1.70	24.90	6.32	47.47	-30.57	-0.10
Hemyock	-3.14	21.78	11.39	48.72	-1.03	-0.28
Hinckley	2.75	15.58	6.36	19.98	-1.85	-0.30
Kingswood	-0.78	24.78	8.36	59.34	-9.76	-0.18
Knightcote	4.46	7.39	9.07	8.87	-3.42	-0.25
Llanychaer	4.41	-20.92	34.45	2.31	0.12	-0.24
Lower Dunsforth	2.93	11.30	8.03	14.60	-0.77	-0.34
Ludford	5.26	23.12	3.68	19.68	-5.05	-0.25
Otterbourne	-0.13	25.35	7.79	36.60	-40.12	-0.05
Putney Heath	4.93	2.30	12.45	4.61	-3.90	-0.32
Sale Carrington	5.29	23.86	2.40	19.24	-19.90	-0.10
Stanford Rivers	3.65	11.71	6.81	21.29	-3.10	-0.21
Stone	5.10	14.54	5.68	12.01	-6.20	-0.25
Taw Head	0.15	39.73	8.33	35.55	-1.33	-0.20
Victoria Park	4.03	-15.58	22.93	3.50	-9.2138	-0.13

7. Comparison of the unified generalised extreme value model with existing models

The three existing DDF models (FSR, FEH and FEH13) were run in order to allow comparison with the outputs of the unified GEV DDF model as presented in Sections 5 and 6. Rainfall depths were computed for a set of durations which includes and extends that for which observed data were extracted (1, 2, 5, 10, 15, 30, 45, 60, 90, 120, 240, 360 and 480 minutes) and for a set of return periods which also includes rarer events (1.2, 1.5, 2, 3.5, 5, 10, 20, 50, 100 and 200 years). Results are presented for durations up to 120 minutes and return periods up to 50 years, since it was felt that results of the unified GEV would not be fully reliable in the extended ranges. The three existing DDF models compared in this section were developed to be applied to different ranges of event durations and rarities. None, however, was specifically aimed at estimating rainfall associated with short return periods and very short event durations. Therefore, although existing models can provide estimates for these types of events, they should be treated with caution. Similarly, the unified GEV was fitted to observed records which are in some cases quite short and therefore can hardly provide reliable estimates for long return periods. Indeed, the unified GEV model is the only model compared in this section that is built purely on single-site analysis rather than on pooled data from an entire region, and that is not yet developed to be valid across the whole country.

7.1 Methods

The parameters needed to estimate rainfall via the FSR model were extracted from a 1 km gridded digitisation of the data used to generate the paper maps that formed Volume 5 of the published FSR, at the four grid points enclosing each of the 19 stations of interest. Linear interpolation was then used to obtain the final parameter values at the exact locations of the rainfall gauging stations, to the nearest metre. The growth curve for each station was then calculated according to the procedure described in Volume 2 of the FSR (Faulkner, 1999). Linear interpolation was used when parameter values that were not tabulated in Tables 3.10 and 2.6 in Volume 2 of the FSR were needed.

For the original FEH model, the values of the four constants c, d_1, e and f were extracted from the 1 × 1 km grids at the four grid points enclosing each station of interest. Linear interpolation was used to estimate the point values of c, d_1, e and f at the exact locations of the rainfall gauging stations, to the nearest metre. The FEH rainfall model for durations up to 12 hours (Equation 1) was applied at each station, considering all combinations of duration and y (corresponding to return period).

For the FEH13 model, the 14 parameter values (see Equations 3 and 4) defining the DDF model for a given site have been obtained for the nearest point on the 1 × 1 km grid over which the full results were originally derived, but no spatial interpolation has been applied.

A modified version of the original project's program was then used to allow accurate evaluation of the results for durations shorter than one hour. This allows rainfall depths to be estimated for the required ranges of durations and return periods.

7.2 Comparison – time of tip stations

Figures 46 to 54 (Appendix A.3) show the frequency curves estimated by the unified GEV method when fitted to the series of the nine time of tip stations and compare them to the corresponding frequency curves estimated by the FEH13, FEH and FSR methods. All the models tend to span similar ranges of rainfall depths, with some of the largest differences across models being visible at very short durations, for which results from the current DDF models should be treated with caution. For many of the return periods below 10 years, the frequency curves estimated for the medium durations (typically 10 to 30 minutes) using the unified GEV model and the current DDF models, especially the FSR model, tend to give comparable results.

On the $-\ln(-\ln(1 - 1/T))$ scale used for the x-axis, all frequency curves estimated by the unified GEV method become steeper as the measure of the return period, $-\ln(-\ln(1 - 1/T))$, increases. Due to the fixed relationship between the location and scale functions, the increase in steepness is sharper in the frequency curves for longer durations (that is, the curves for different durations 'fan out' as T is increased). Indeed, the depth of the 8-hour, 100-year rainfall (not shown in the plots) predicted by this method is greater than the depth of the 8-hour, 200-year rainfall predicted by the FEH13, FEH and FSR methods at eight of the nine sites, being lower at Llanychaer only, a site with one of the highest estimated values of skewness parameter (and therefore one of the flattest scale functions) in the whole data set.

The left panels of Figures 46 to 54 (Appendix A.3) compare the frequency curves estimated by the unified GEV method with those estimated by the FEH13 method. FEH13 frequency curves are generally flatter than unified GEV frequency curves for more common events, before sharply increasing in steepness at return periods of five to 10 years, with low dependence on event duration (that is, they do not 'fan out' as much as unified GEV frequency curves). The fact that unified GEV frequency curves depend on event duration, whereas FEH13 frequency curves, relatively speaking, do not, means that, for shorter events of one to five minutes, the FEH13 frequency curves become steeper than the equivalent unified GEV frequency curves as T increases. For events of 10 to 30 minutes, both methods generate curves of similar steepness across the range of return periods considered, and there is often some agreement between the depths of rainfall predicted by both methods. For events of 45 to 120 minutes, the unified GEV frequency curves become steeper than the FEH13 frequency curves at a value of T that generally reduces as event duration increases. It is worth noting that, at all sites, the depth of the one-minute, 1.2-year storm predicted by the FEH13 model is 0 mm, while at Lower Dunsforth, the depths of both the 2-minute, 1.5-year and 1-minute, 2-year storms predicted by the FEH13 model are also 0 mm. This suggests that the FEH13 model gives unrealistically low estimates of rainfall depth for shorter and more common events: the

model was not calibrated to extend to such short event durations, so it is not unexpected that its estimates are unrealistic. This issue is currently resolved in both the FEH13 and FEH22 models by applying the x-minute to 60-minute scaling factors from the FSR (where $5 \leq x < 60$) to the relevant 60-minute FEH13 or FEH22 estimate, as appropriate.

The central panels of Figures 46 to 54 (Appendix A.3) compare the frequency curves estimated by the unified GEV method with those estimated by the original 6-parameter FEH method. At the event durations considered here, FEH frequency curves of different durations at the same site are similar in shape and do not 'fan out' greatly as T increases. This means that the range of rainfall depths estimated by the FEH model generally sits inside the range of depths estimated by the unified GEV model, when all event durations are considered at all but the lowest return periods. Apart from Colwyn Bay, the closest match between the unified GEV and FEH models normally occurs for events of 10- or 15-minute duration. The general rule that FEH frequency curves do not fan out as much as unified GEV frequency curves is challenged at Victoria Park, where, from visual inspection, the FEH frequency curves appear to fan out approximately as much as the unified GEV frequency curves. Colwyn Bay and Victoria Park are unusual cases in that the rainfall depth estimated by the FEH method exceeds that estimated by the unified GEV method for all 80 combinations of event duration and return period considered here. At Llanychaer, the FEH estimates exceed the unified GEV estimates for most combinations of duration and return period, with slightly lower values only in the estimated short return period values for the 30- and 45-minute events. Given that Colwyn Bay, Victoria Park and Llanychaer are the most western stations in Wales and that all are coastal, it might be that some regional differences occur between the FEH and unified GEV approaches.

The right panels of Figures 46 to 54 compare the frequency curves estimated by the unified GEV method with those estimated by the FSR method. Though necessarily based only on the data available before it was published (1975), the FSR method is included here as the Flood Studies Report explicitly states that this method is suitable for estimating rainfall depths associated with very short-duration rainfall events. The frequency curves produced by the FSR method are, in all cases, very flat relative to those produced by the unified GEV method. Consequently, the FSR method generally predicts greater depths of rainfall than the unified GEV method for short return periods (more so for longer durations), and smaller depths of rainfall than the unified GEV method for longer return periods (again, more so for longer durations). The crossover point, at which the rainfall depths predicted by the unified GEV method exceed those predicted by the FSR method, often occurs for T in the range two to 10 years. The crossover points at Colwyn Bay and Llanychaer either occur at higher values of T or not at all, while at Victoria Park the FSR method predicts a greater depth of rainfall than the unified GEV method for all 80 combinations of event duration and return period, therefore no crossover is plotted at any event duration. Again, there appear to be structural differences in the frequency curves estimated by unified GEV and FSR models for the coastal Welsh stations.

The four different models behave differently across the different event durations and return periods, and no structural difference is easily detected across all stations, although some consistent features observed at the western, coastal Welsh time of tip stations indicate

that some regional differences may exist. It is unclear if such regional differences are the result of some climatological characterisation not taken into account by the models (for example, proximity to the Atlantic coast) or by the differences in data management practices between the different Environment Agency regions. It should be noted, however, that the FEH13 method does not produce such greatly different frequency curves from the unified GEV method at these sites.

7.3 Comparison – longer durations

In order to keep the presentation more readable, the frequency curves estimated by the unified GEV method for durations of 15 minutes or more are compared to the frequency curves estimated by the FEH13, FEH and FSR methods for the ten 15-minute stations only. Figures 55 to 64 (Appendix A.4) show these comparisons to the FEH13 method (left panel), FEH method (central panel) and FSR method (right panel). As already noted in Section 6, the frequency curve estimates from the unified GEV method for durations of at least 15 minutes are flatter and tend to have less of the 'fanning out' behaviour seen at time of tip stations. This may be related to the sliding window correction applied to the series extracted for the 15-minute stations, as these corrections might overcorrect shorter event rainfalls to a larger extent than longer event rainfalls. Nevertheless, the stations for which the flatter curves are estimated are characterised by a lack of very large events in the records at all durations: the flatness of a curve could be related more to the specific station being considered than to the estimation procedure itself.

The left panels of Figures 55 to 64 compare the frequency curves estimated by the unified GEV method with those estimated by the FEH13 method. At these sites, the FEH13 frequency curves are generally steeper than the unified GEV frequency curves for both short and longer return periods, the only exceptions being at Chieveley, Ludford and Putney Heath, for events that are both longer duration and rarer. In general, the FEH13 method estimates smaller depths of rainfall than the unified GEV method for the more common events; this discrepancy reduces as event duration increases. Due to the flatness of the unified GEV frequency curves, rainfall depths estimated by the FEH13 method mostly exceed those estimated by the unified GEV method for return periods greater than two to five years, even at Ludford. At Chieveley and Putney Heath, rainfall depths estimated by the unified GEV method are generally greater than those estimated by the FEH13 method, with very few exceptions. It should be noted that the frequency curves estimated by the unified GEV method at Chieveley, and Putney Heath are among the steepest estimated frequency curves, which accommodate some very extreme recorded rainfall maxima reasonably well (see Figures 42 and 44). As noted in Section 7.2, the FEH13 method appears to under-predict rainfall depths when extrapolating to shorter durations and more common events. As an example, the 4.6 mm depth of the predicted 15-minute, 2-year event at Taw Head is smaller than every 15-minute annual maximum at that site. However, the 23.4 mm depth predicted for the 120-minute, 2-year event at Taw Head is similar to the median of the ordered 120-minute annual maximum series (21 mm).

The central panels of Figures 55 to 64 (Appendix A.4) compare the frequency curves estimated by the unified GEV method with those estimated by the original 6-parameter FEH method. Apart from Otterbourne, there is good agreement between the two methods for the more common events. The frequency curves estimated by the unified GEV method at Otterbourne (Figure 60) are among the flattest of all the estimated frequency curves for the 15-minute stations; this is probably because no very high maximum is recorded for any duration in the relatively short record. At Kingswood (Figure 58), there is a very close agreement between the frequency curves estimated by the unified GEV and FEH methods, at all durations and all return periods up to 20 years. At the other sites, the difference between the rainfall depths predicted by the two methods increases with return period, more so for longer event durations (except at Crew Fell). However, neither method clearly and consistently predicts greater rainfall depths than the other. Therefore, neither method predicts consistently steeper frequency curves than the other and neither method fans out consistently more than the other. This suggests that there are no systematic differences between the methods.

The right panels of Figures 55 to 64 compare the frequency curves estimated by the unified GEV method with those estimated by the FSR method. No extrapolation of the FSR method is required to estimate frequency curves as it is calibrated to event durations of 15 minutes and shorter. In general, there is better agreement between the unified GEV and FSR methods for shorter-duration, more common events. For longer-duration, more common events, rainfall depths predicted by the FSR are greater than those predicted by the unified GEV, while for rarer events, the relative flatness of the FSR frequency curves results in predictions that are smaller than those of the unified GEV method. Some exceptions to this are at Otterbourne, Sale Carrington, Stanford Rivers and Taw Head, where the unified GEV frequency curves for some or all durations are flatter than the equivalent FSR frequency curves for some or all the considered range of return periods. At certain stations (for example, Crew Fell), the FSR rainfall depth estimates for a return period of 1.2 years are so much higher than the equivalent unified GEV estimates that even the greater steepness of the unified GEV frequency curves cannot cause the unified GEV and FSR frequency curves to cross for T < 50 years. This is more pronounced when longer-duration events are considered (for example, Hemyock, Kingswood).

Again, no structural differences between the models could be identified across stations and durations. Some relatively consistent patterns can be identified when comparing each of the currently used DDF models against the unified GEV estimates, although typically one or two stations defy the general rule. The unexpected behaviour of the GEV model at these stations can mostly be explained by specific characteristics found in the observed series, whose records are often not very long. Any maximum likelihood model based on few data points is bound to be non-robust to influential points, and therefore an advantage of pooling data from different stations and using more robust estimation procedures (as in the FEH and FEH13 methods).

7.4 Estimation performance in practice

At present, practitioners that need to assess the frequency curves of some short-duration events would most likely rely on an interpolation of the FEH method or on the FSR estimation procedure. Use of the FEH13 method for durations lower than one hour has not been tested. For this reason, detailed comparisons between the results of this study and the FEH13 model are not reported in the discussion below.

In order to assess the performance of the models for sub-hourly durations the estimated depth corresponding to pre-specified frequencies obtained with the FSR, the FEH and the unified GEV method are compared to the empirical estimates obtained from the recorded data series at each station. Due to the short records of some stations, only the 2-year, 5-year and 10-year events are considered in this comparison, as rarer events could not be estimated with confidence in short series. The empirical estimates are obtained as the median (50th percentile), the 80th percentile and the 90th percentile of the recorded data series. For gauges with less than 20 years of data, the total length of the sample would be less than 2T when estimating the 10-year event: this might result in less precision in the empirical estimate. In general, to estimate rarer events empirically from a sample, large sample sizes would be needed. The focus in this comparison is on the sub-hourly durations down to 15 minutes, as even in small catchments it is expected that this is a suitable lower limit for most applications. Furthermore, fewer data series are available for durations of less than 15 minutes and the uncertainty of the measured values is larger.

In Figure 15 the differences between the estimated 2-year rainfall event and empirical 2-year event are shown for each station. The average and standard deviations for the differences across all stations for all three methods are shown in Table 10. From both the figure and the table one can see that estimates from the unified GEV, which is fitted directly to the data series of each station, appear to have much less variability compared to the FEH and the FSR. For the 2-year return period, the FSR estimates appear to be consistently positively biased, with the bias increasing for longer durations. The FEH estimates instead appear to have a small bias across all durations, but the variability of estimates seems to increase for higher durations.

Figure 16 and Table 11 show information on the differences between the estimates obtained with the three different estimation procedures and the empirical 80th percentile of each data series. The performance of the three different methods appears to be more similar for longer return periods, although the FEH results would seem to be less biased.

Figure 17 and Table 12 show the summary of the differences between the estimates obtained with the three estimation methods for the 10-year return period event and the empirical 90th percentile of the recorded samples. Again, the unified GEV, which is fitted to the original data, seems to perform quite well, with less variability in the results. The FEH and the FSR perform similarly, with FSR still exhibiting some positive bias which increases for longer durations.

Overall, the FEH seems to give better results than the FSR for both the return periods examined here.

Tables with the empirical and estimated values for the *2*-year and *5*-year events for each station are shown in Appendix B.

More formal testing of the mean difference between estimates derived from the different methods across the different durations and return periods could be carried out, for example, by applying several ANOVA (analysis of variance) or MANOVA (multivariate analysis of variance) tests (e.g. Maxwell and others, 2017). Given the relatively small number of stations in this study, results for all stations are provided in the plots below, rather than overall summaries, to allow for a site-by-site comparison.
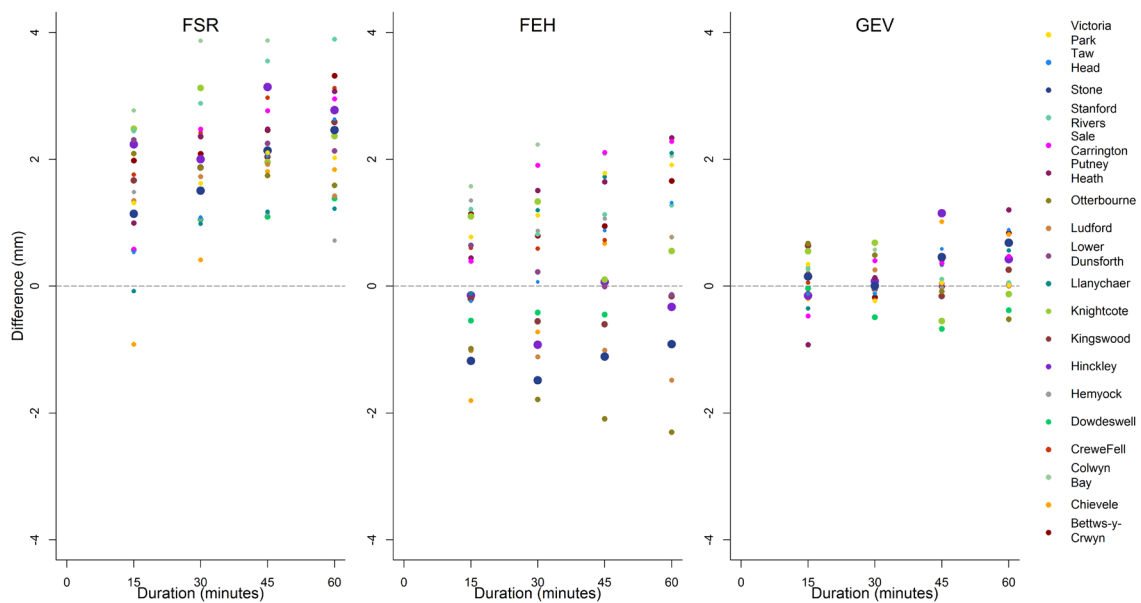

Figure 15 - Depth difference between the *2*-year rainfall depth estimated value and the 50th percentile recorded rainfall depth.

Figure 15 shows the differences between the estimated 2-year rainfall depth estimated value and the 50th percentile recorded rainfall depth as a function of duration (0-60 minutes) for the unified FSR (left panel), FEH (central panel) and GEV (right panel) for each station (Bettws-y-Crwyn, Chieveley, Colwyn Bay, Crew Fell, Dowdeswell, Hemyock, Hinckley, Kingswood, Knightcote, Llanychaer, Lower Dunsforth, Ludford, Otterbourne, Putney Heath, Sale Carrington, Stanford Rivers, Stone, Taw Head, Victoria Park). The x-axis on all panels shows the duration (0-60 minutes). The y-axis plots the difference (-4 to 4 mm). Larger dots correspond to stations with longer record length.

Table 10 - Summary statistics of 2-year rainfall found by each method, averaged across all stations

Mean difference and standard deviation (GEV, FEH, FSR)	15 mins	30 mins	45 mins	60 mins
GEV (mean difference, mm)	0.10	0.07	0.21	0.27
GEV (standard deviation, mm)	0.42	0.30	0.45	0.49
FEH (mean difference, mm)	0.16	0.30	0.51	0.64
FEH (standard deviation, mm)	0.96	1.17	1.18	1.33
FSR (mean difference, mm)	1.41	1.93	2.25	2.39
FSR (standard deviation, mm)	0.96	0.84	0.76	0.89

Note: Mean difference indicates depth difference (in mm) between 2-year rainfall depth estimate and 50th percentile recorded rainfall depth, averaged across all stations
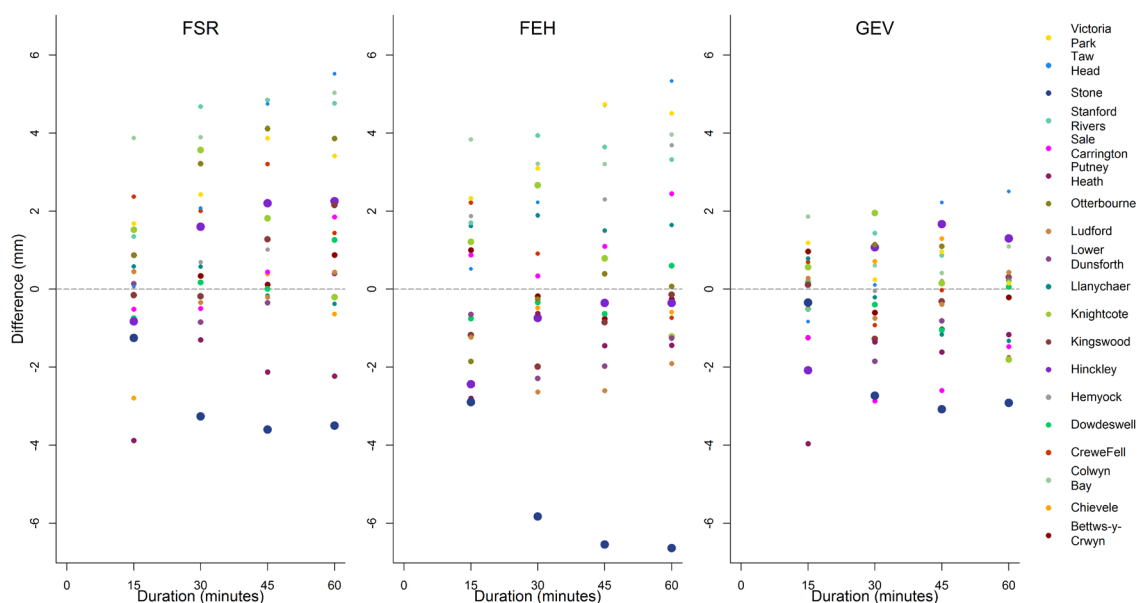

Figure 16 - Depth difference between the 5-year rainfall depth estimated value and the 80th percentile recorded rainfall depth.

Figure 16 shows the differences between the estimated 5-year rainfall depth estimated value and the 80th percentile recorded rainfall depth as a function of duration (0-60 minutes) for the unified FSR (left panel), FEH (central panel) and GEV (right panel) for each station (Bettws-y-Crwyn, Chieveley, Colwyn Bay, Crew Fell, Dowdeswell, Hemyock, Hinckley, Kingswood, Knightcote, Llanychaer, Lower Dunsforth, Ludford, Otterbourne, Putney Heath, Sale Carrington, Stanford

Rivers, Stone, Taw Head, Victoria Park). The x-axis on all panels shows the duration (0-60 minutes). The y-axis plots the difference (-6 to 6 mm). Larger dots correspond to stations with longer record length.

Table 11 - Summary statistics of 5-year rainfall found by each method, averaged across all stations

Mean difference and standard deviation (GEV, FEH, FSR)	15 mins	30 mins	45 mins	60 mins
GEV (mean difference, mm)	-0.24	-0.30	-0.17	-0.13
GEV (standard deviation, mm)	1.3	1.3	1.4	1.3
FEH (mean difference, mm)	0.05	0.25	0.48	0.58
FEH (standard deviation, mm)	2.0	2.4	2.7	2.8
FSR (mean difference, mm)	0.22	0.96	1.35	1.50
FSR (standard deviation, mm)	1.7	2.0	2.3	2.4

Note: Mean difference indicates depth difference (in mm) between 5-year rainfall depth estimate and 80th percentile recorded rainfall depth, averaged across all stations.
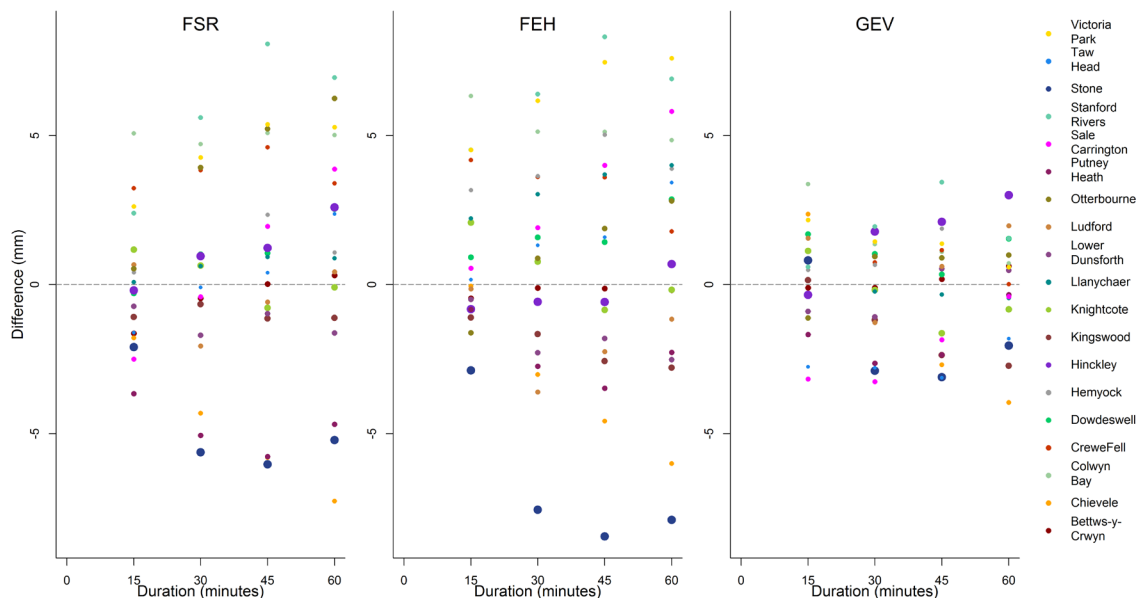

Figure 17 - Depth difference between the 10-year rainfall depth estimated value and the 90th percentile recorded rainfall depth.

Figure 17 shows the differences between the estimated 10-year rainfall depth estimated value and the 90th percentile recorded rainfall depth as a function of duration (0-60 minutes) for the unified FSR (left panel), FEH (central panel) and GEV (right panel) for each station (Bettws-y-Crwyn, Chieveley, Colwyn Bay, Crew Fell, Dowdeswell, Hemyock, Hinckley, Kingswood, Knightcote, Llanychaer, Lower Dunsforth, Ludford, Otterbourne, Putney Heath, Sale Carrington, Stanford Rivers, Stone, Taw Head, Victoria Park). The x-axis on all panels shows the duration (0-60 minutes). The y-axis plots the difference (-**5** to **5** mm). Larger dots correspond to stations with longer record length.

Table 12 - Summary statistics of 10-year rainfall found by each method, averaged across all stations

Mean difference and standard deviation (GEV, FEH, FSR)	15 mins	30 mins	45 mins	60 mins
GEV (mean difference, mm)	0.34	-0.36	-0.2	-0.03
GEV (standard deviation, mm)	1.07	0.68	0.92	1.14
FEH (mean difference, mm)	0.03	0.33	0.80	1.11
FEH (standard deviation, mm)	1.7	1.7	2.0	1.7
FSR (mean difference, mm)	2.5	3.6	4.3	4.2
FSR (standard deviation, mm)	2.2	3.2	3.9	3.9

Note: Mean difference indicates depth difference (in mm) between 10-year rainfall depth estimate and 90th percentile recorded rainfall depth, averaged across all stations.

7.5 Discussion

As discussed in Section 3, two different data sources have been used in this study: time of tip data, which can be used to construct very high-resolution data series, and 15-minute rainfall totals. The unified GEV model has been fitted to series of both types. In the initial stages of the SC090031 project, it was hoped that sufficient time of tip series would have been available for good spatial coverage of England and Wales. However, 15-minute stations were included in the study due to the poor geographical coverage of the available time of tip gauges. Indeed, practitioners are likely to be more interested in the results for very high-resolution data and it should be possible to fit a unique model spanning all durations. The differences seen in the estimated location and scale functions, in Sections 5 and 6, show the difficulty of designing models to span a large range of durations, especially when the series behaviour changes significantly with duration. If a model is desired to span a large range of durations, then a more complete description of the relationship between rainfall depth and duration may require a model with many more parameters than the unified GEV model; a single-site model like the unified GEV can only cope with estimating a limited number of parameters when relatively small sample sizes are available.

The unified GEV at-site analysis presented in this work, like the FEH and FSR models, build on the assumption that the observed series are representative of the stochastic (random) distribution of the rainfall extremes at each site. In particular, it is assumed that the stochastic distribution is constant at each site and does not change over time. Kendon and others (2014) predict an increase in hourly rainfall in part of the UK, due to climate change. The current methods presented in this work can be extended to model changes in the rainfall distributions but are presently not taking these potential changes into account.

As already mentioned, tipping buckets are affected by systematic bias and the same annual maxima are recorded in several years in the observed series. This is a consequence of the limited precision of the tip. Estimates of depth frequencies for short durations can be a useful tool for practitioners, but caution is required when using such estimates. In addition, the 15-minute totals are subject to uncertainties in the sliding window correction factors. It is therefore difficult to discern if one type of data series is better or more reliable than the other. The choice of which unified GEV model to use will depend on the required application.

8.   Conclusions and recommendations

An outline of the results presented in this report is given here. Some warnings and recommendations, which could be useful in developing a national DDF model for short-duration rainfall events, are given.

8.1 Results of the depth–duration–frequency analysis for short-duration rainfall events

The aim of this study was to investigate methods for extending DDF models to estimate return periods for short-duration rainfall events, which are of particular importance to small and plot-sized catchments. The smallest event duration that was considered in the report is one minute, extracted from time of tip station series. Data series for shorter event durations could potentially be built, but it is unlikely that they would be accurate.

It was initially hoped that enough (10 to 12) tipping bucket stations, with good spatial distribution, would have been available across England and Wales for very short-duration event data to be available over the whole area. The final set of tipping bucket data acquired by the CEH team did not cover the whole of England and Wales evenly since no time of tip data that could be easily processed within the timescale of the study were readily available in some areas. In order to obtain good coverage, some data records based on 15-minute rainfall accumulations were also included in the study. The final data set was composed of nine time of tip and 10 15-minute accumulation records. Of the final 19 gauges, 15 had more than 20 years of data and the longest record was 46 years.

For these 19 stations, annual and seasonal maxima were extracted for rainfall events of 15, 30, 45, 60, 90 and 120 minutes' duration. For the time of tip stations, annual and seasonal maxima were also extracted for rainfall events of one, 2, 5 and 10 minutes' duration.

A modified version of the GEV distribution is suggested for modelling the data and for estimating frequency curves which are consistent and do not cross each other at different durations. The so-called unified GEV distribution builds on standard extreme value theory, with consistency between frequency curves estimates ensured by defining some basic relationships between the distribution parameters and assuming a common skewness parameter and lower bound (per site) for all event durations. The unified GEV, with the proposed relationship between duration and location, requires six parameters to be estimated: a relatively simple model for such a complex problem.

Estimated frequency curves for the time of tip and 15-minute stations, obtained using the unified GEV distribution, are presented in Sections 5 and 6. The estimated frequency curves fit well to the observed maxima series, and the estimated rainfall depths are consistent across the different durations.

The frequency curves estimated by the unified GEV are compared to those estimated by other DDF models used in practice. No structural difference was identified between the frequency curves estimated by the unified GEV and the existing DDF models. Given that the unified GEV is fitted to the series of each station separately, the length and quality of the data at each station necessarily affect the precision of the estimated frequency curves: it is not clear if the lack of consistent differences across the methods is a spurious result of the different record lengths and qualities. If a large set of stations with long reliable series were available across the whole of England and Wales, the comparisons across methods could probably be more generalised.

The comparison of the 2-year and 5-year events as estimated by the FSR and the FEH methods against the empirical value computed from the observed data series shows that both methods give fairly reasonable results, with the FEH showing less bias.

8.2 Lessons learned and recommendations for future research

The data acquisition process revealed the challenges connected with identifying stations with sub-hourly records. The local Environment Agency and Natural Resources Wales representatives played a large part in the identification procedure by identifying reliable data. It seems unlikely that enough time of tip stations with long series could be identified to allow good coverage of England and Wales at the current time. It should be possible to identify a fairly large number of time of tip stations in the Midlands and Wales, and to retrieve larger sets of long records for 15-minute stations across the other regions of England. If enough stations are identified, it should be possible to build more sophisticated DDF models in line with the FEH and FEH13 models, in which information from surrounding stations is pooled to improve estimates at the location of interest. It is likely that the final identified set of sub-hourly stations would not be as large as the set used in the FEH and FEH13 for longer durations: any attempt at a national model for short-duration rainfalls cannot be expected to provide reliable estimates for very long return periods yet, since few large data points would be available. An additional issue, related to the length of the records available for time of tip stations, is that these stations are characterised by fairly coarse data for very short event durations (one- or 2-minute), especially in the early years of record, when the tip capacities of the buckets were generally larger. The bias present in the data recording might eventually impact the precision of frequency curve estimates, causing them to be biased as well. Methods exist to quantify measurement errors in tipping bucket gauging stations and to correct for such known errors when estimating frequency curves. To produce such a correction for a large number of stations would be laborious and it is not evident if the increased precision of the estimates would justify this effort.

If data for a small number of time of tip stations were available in specific areas, and a larger set of data for 15-minute stations were available across England and Wales, it is hoped that some rule of thumb might be developed to relate estimated rainfall depths for

durations of 15 minutes or more to estimated rainfall depths for shorter durations; this would allow credible rainfall depth estimates for shorter durations across the whole area.

For any model development, an initial study to investigate whether the analysis of peaks-over-threshold data would provide more accurate estimates than the analysis of block maxima could be envisaged. A first step towards such a study would be to define some standard procedures to extract independent peaks for the different event durations. Furthermore, a sensitivity study of the effect on the estimation of such procedures and of the average number of events per year retained in the data set should be carried out.

The study makes the following recommendations to practitioners:

- the FEH and FSR depth–duration–frequency models appear to provide reasonable estimates for frequencies of sub-hourly rainfall events down to a duration of 15 minutes, at least for the short return periods at which local data can be expected to provide suitable empirical evidence

- the FEH appears to give less biased results than the FSR and seems to be more suitable for extending to allow the model to estimate frequency curves for sub-hourly rainfall durations - however, due to the relatively small number of gauges used in the study reported here, these results should only be extrapolated to the national scale with caution

- larger uncertainties are associated with very short durations (one-minute to 15-minute durations) - the FSR and FEH were not fully calibrated on such short durations and larger errors are to be expected in the measured data, especially in the early years of the records

Further work on the extrapolation of the FEH13 model to sub-hourly durations, conducted before the release of the new FEH Web Service in 2015, found that the scaling factors between x-minute and 60-minute rainfall depth published in the FSR were acceptable to estimate FEH13 sub-hourly rainfall depths when applied to FEH13 60-minute rainfall depths (for $5 \leq x < 60$). The same scaling factors are used to estimate sub-hourly FEH22 rainfall depths.

Bibliography

BRITISH STANDARDS INSTITUTION (BSI), 2012. 'Acquisition and management of meteorological precipitation data from a raingauge network. Part 4: Code of practice for operating raingauges and managing precipitation data' BS 7843-4:2012. London: BSI.COLES, S.G., 2001. 'An introduction to statistical modelling of extreme values' London: Springer.

DEFRA, 2004. 'Floods and reservoir safety – Revised guidance for panel engineers' [online] Available at: https://britishdams.org/assets/documents/defra-reports/200403Floods%20and%20Reservoir%20Safety%20-%20Revised%20Guidance%20for%20Panel%20Engineers%20.pdf[Accessed 25 July 2014].

FAULKNER, D., 1999. 'Rainfall frequency estimation. Volume 2 of the Flood Estimation Handbook' Wallingford: Institute of Hydrology.

FAULKNER, D., KJELDSEN, T., PACKMAN, J. and STEWART, L., 2012. 'Estimating flood peaks and hydrographs for small catchments: Phase 1' Bristol: Environment Agency.

FAULKNER, D.S. and PRUDHOMME, C., 1998. 'Mapping an index of extreme rainfall across the UK' Hydrology and Earth System Sciences, 2, 183 to 194.

HOSKING, J.R.M. and WALLIS, J.R., 1997. 'Regional frequency analysis: An approach based on L-moments' Cambridge: Cambridge University Press.

HOUGHTON-CARR, H., 1999. 'Restatement and application of the Flood Studies Report rainfall–runoff method Volume 4 of the Flood Estimation Handbook' Wallingford: Institute of Hydrology.

ICE, 1996. 'Floods and reservoir safety' 3rd edn. London: Thomas Telford.

KENDON, E.J., ROBERTS, N.M., FOWLER, H.J., ROBERTS, M.J., CHAN, S.C. and SENIOR, C.A., 2014. 'Heavier summer downpours with climate change revealed by weather forecast resolution model' *Nature Climate Change*, **4,** 570 to 576. doi:10.1038/nclimate2258.

KJELDSEN, T.R., 2007. 'The revitalised FSR/FEH rainfall–runoff method' FEH Supplementary Report No. 1. Wallingford: CEH.

MAXWELL, S.E., DELANEY, H.D. and KELLEY, K., 2017. 'Designing Experiments and Analyzing Data: A Model Comparison Perspective' 3rd edn. Abingdon-on-Thames:f Routledge.

MOLINI, A., LANZA, L.G. and LA BARBERA, P., 2005. 'Improving the accuracy of tipping-bucket rain records using disaggregation techniques' Atmospheric Research, 77, 203 to 217.

NERC, 1975. 'Flood Studies Report' (five volumes). London: Natural Environment Research Council.

PAVLYUKOV, Y.B., 2007. 'Precipitation measurement with automated tipping-bucket rain gauges' Russian Meteorology and Hydrology, 32, 711 to 718.

REED, D.W., FAULKNER, D.S. and STEWART, E.J., 1999. 'The FORGEX method of rainfall growth estimation – II: Description' Hydrology and Earth System Sciences, 3, 197 to 203.

SPACKMAN, E., 1993. 'Calculation and mapping of rainfall averages for 1961–90' British Hydrology Society Meeting on Areal Rainfall. University of Salford, Manchester, 15 December 1993.

STEDINGER, J.R., VOGEL, R.M. and FOUFOULA-GIORGIOU, E., 1993. 'Frequency analysis of extreme events' In: Maidment DR. (ed.), Handbook of hydrology. London: McGraw-Hill.

STEWART, E.J., JONES, D.A., SVENSSON, C., MORRIS, D.G., DEMPSEY, P., DENT, J.E., COLLIER, C.G. and ANDERSON, C.A., 2013. 'Reservoir safety – long return period rainfall Project FD2613 WS194/2/39 *Final Report (two volumes)*' London: Defra.

SVENSSON, C. and JONES, D.A., 2010. 'Review of rainfall frequency estimation methods' Journal of Flood Risk Management, 3(4), 296 to 313.

VESUVIANO, G.. 2022. 'The FEH22 rainfall depth-duration-frequency (DDF) model: UK Centre for Ecology & Hydrology.

VESUVIANO, G. and STEWART, E., 2021. 'Recalibration of FEH13 rainfall model for Cumbria: final report' Wallingford: UK Centre for Ecology & Hydrology.

List of abbreviations

AMAX   Annual maximum or annual maxima.

CEH   Centre for Ecology & Hydrology.

DDF   Depth–duration–frequency.

FEH   Flood Estimation Handbook (mostly indicating the DDF model presented in Volume 2 of the Flood Estimation Handbook).

FEH13   Flood Estimation Handbook 2013 (indicating the DDF model as developed within the 'Reservoir safety – long return period rainfall' project).

FORGEX   Focused Rainfall Growth Extension method.

FSR   Flood Studies Report.

GEV   Generalised extreme value distribution.

NERC   Natural Environment Research Council.

POT   Peak-over-threshold.

RMED   Rainfall MEDian (median of the annual maximum rainfall depths at a given site for a given duration, equivalent to the 2-year return period rainfall depth).

SAAR   Standard-period average annual rainfall (mean value of the 30 annual rainfall depths recorded over the years 1961 to 1990 in mm).

Appendix A – Figures referenced in Sections 5, 6 and 7

A.1 Fitted model results for time of tip stations
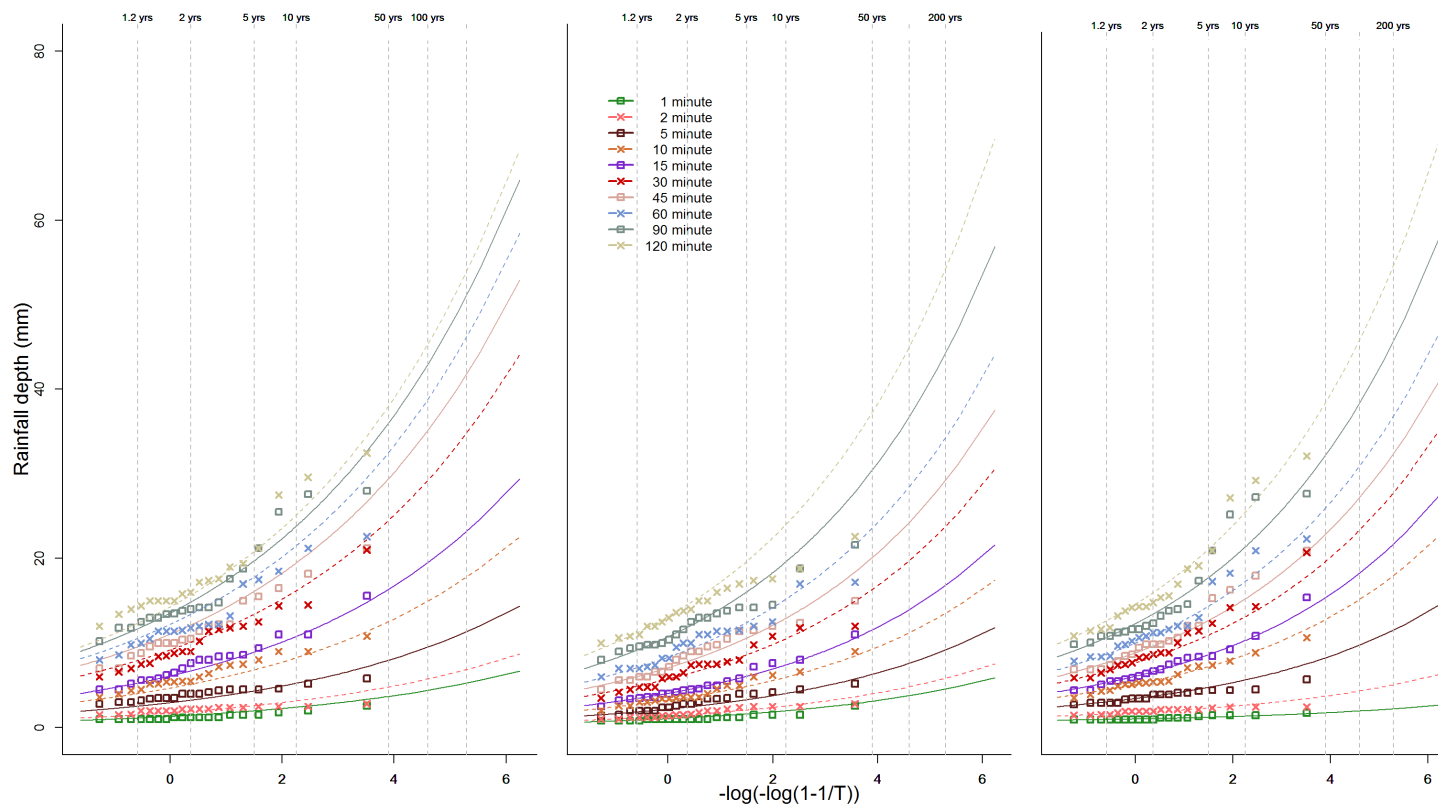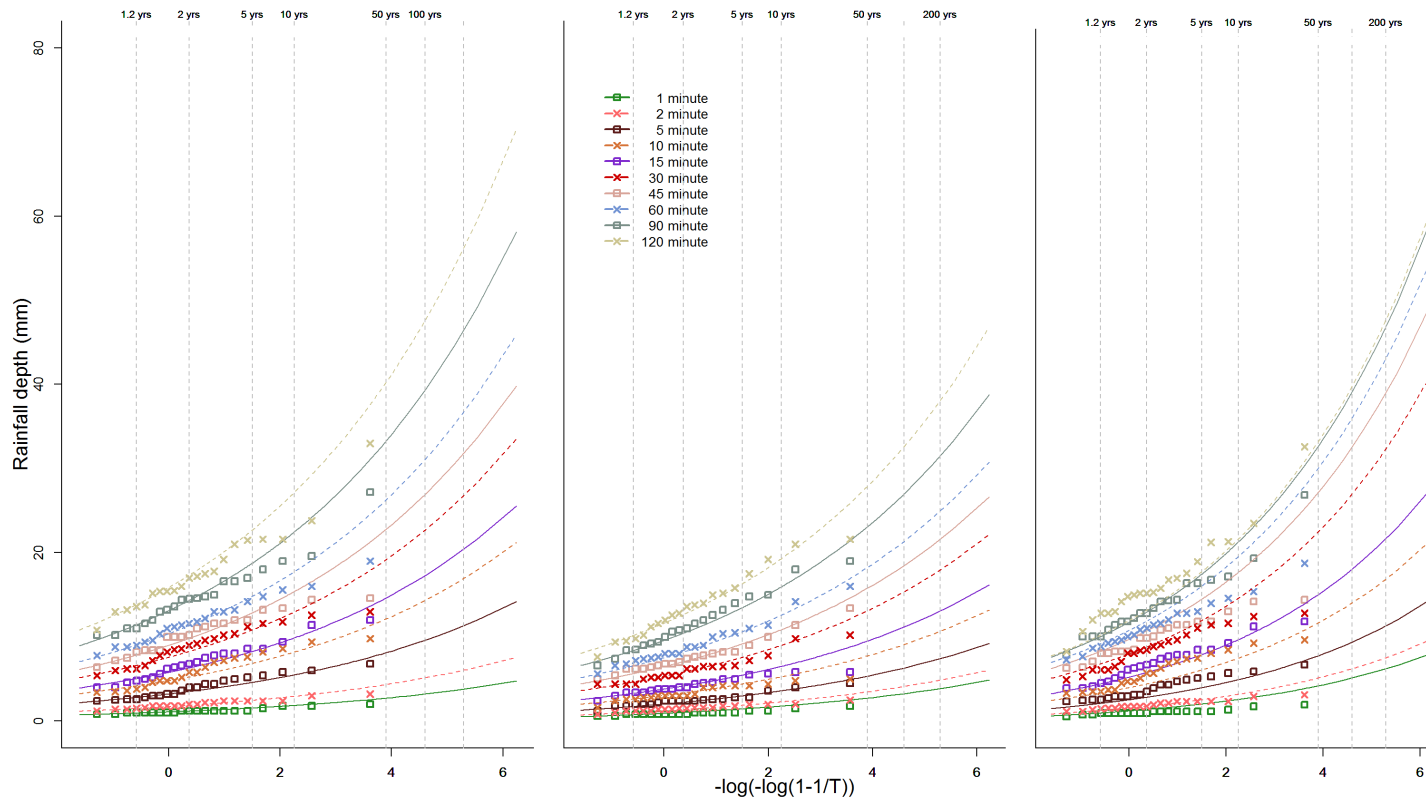
Figure 18 - Estimated frequency curves for the station at Llanychaer for the annual (left panel), winter (central panel) and summer (right panel) series, superimposed on the Gringorten plotting positions

The three graphs in Figure 18 plot the estimated frequency curves for the station at Llanychaer (shown by squares and crosses) superimposed on the Gringorten plotting positions (shown by lines) for different times periods (1, 2, 5, 10, 15, 30, 45, 60, 90 and 120 minutes) over a period of 200 years: left panel (annual series), central panel (winter series) and right panel (summer series). The x-axis on all panels shows log (natural logarithm, ln) from 0-6. The y-axis plots rainfall depth (0-80mm).

Figure 19 - Estimated frequency curves for the station at Victoria Park for the annual (left panel), winter (central panel) and summer (right panel) series, superimposed on the Gringorten plotting positions

The three graphs in Figure 19 plot the estimated frequency curves for the station at Victoria Park (shown by squares and crosses) superimposed on the Gringorten plotting positions (shown by lines) for different times periods (1, 2, 5, 10, 15, 30, 45, 60, 90 and 120 minutes) over a period of 200 years: left panel (annual series), central panel (winter series) and right panel (summer series). The x-axis on all panels shows log (natural logarithm, ln) from 0-6. The y-axis plots rainfall depth (0-80mm).
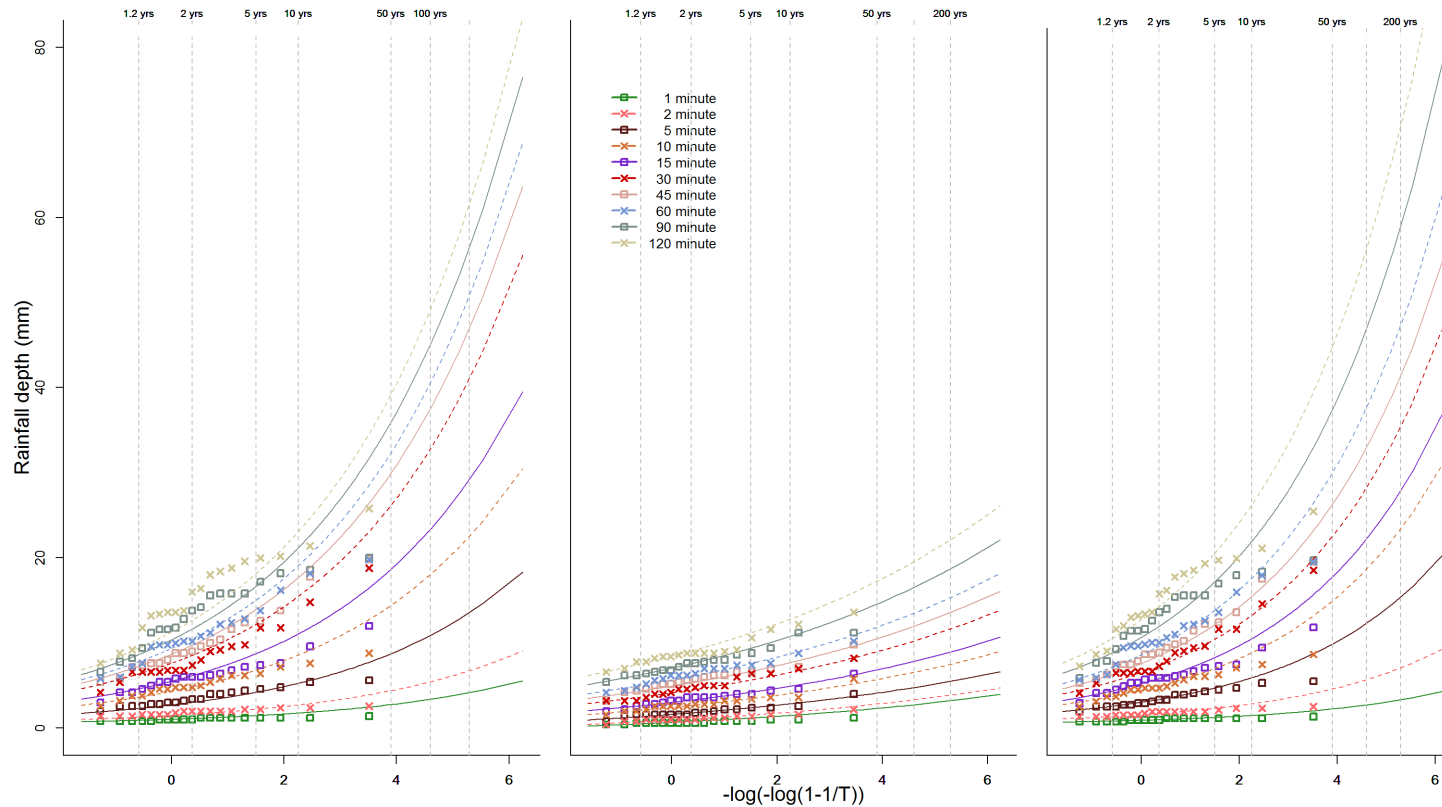
Figure 20 - Estimated frequency curves for the station at Colwyn Bay for the annual (left panel), winter (central panel) and summer (right panel) series, superimposed on the Gringorten plotting positions

The three graphs in Figure 20 plot the estimated frequency curves for the station at Colwyn Bay (shown by squares and crosses) superimposed on the Gringorten plotting positions (shown by lines) for different times periods (1, 2, 5, 10, 15, 30, 45, 60, 90 and 120 minutes) over a period of 200 years: left panel (annual series), central panel (winter series) and right panel (summer series). The x-axis on all panels shows log (natural logarithm, ln) from 0-6. The y-axis plots rainfall depth (0-80mm).
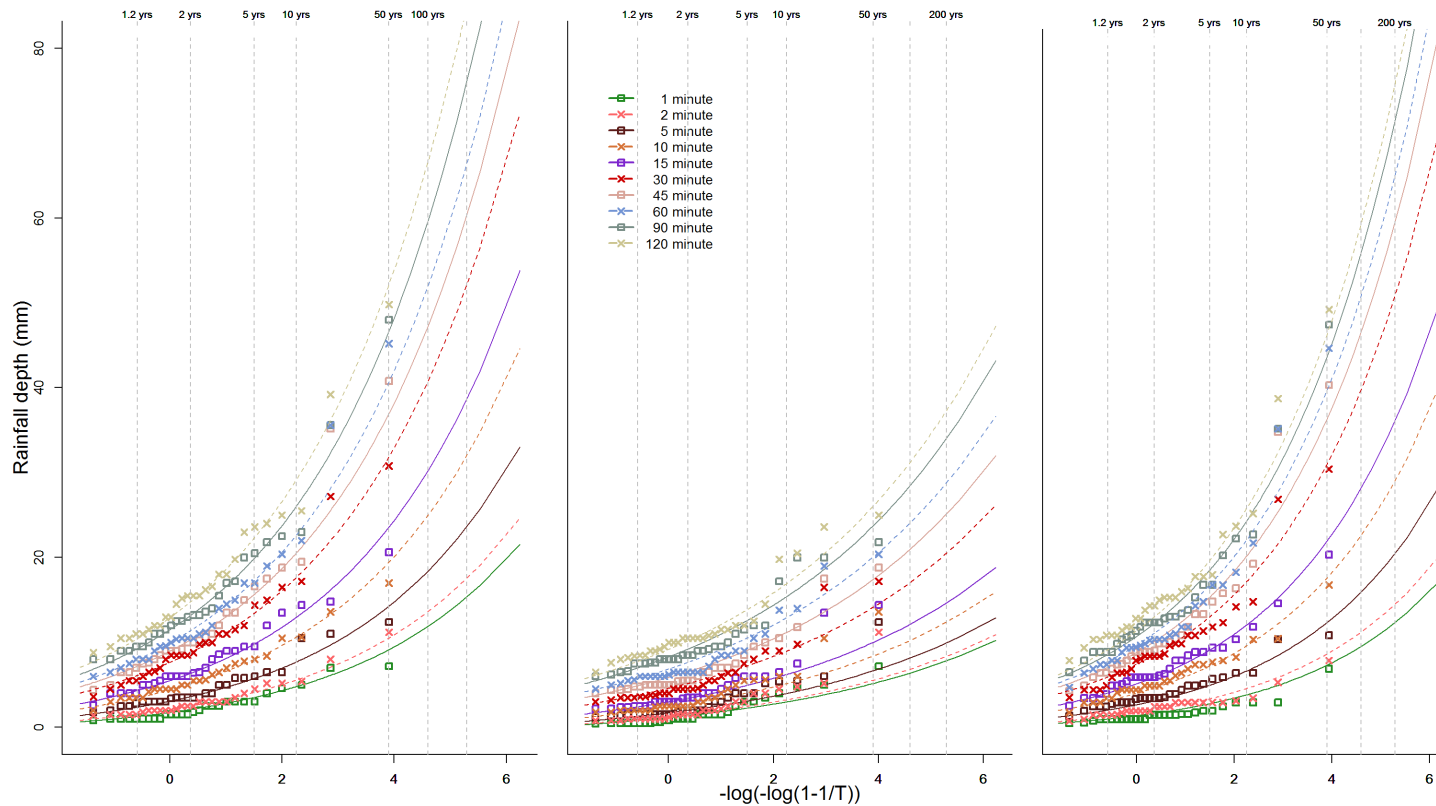
Figure 21 - Estimated frequency curves for the station at Bettws-y-Crwyn for the annual (left panel), winter (central panel) and summer (right panel) series, superimposed on the Gringorten plotting positions

The three graphs in Figure 21 plot the estimated frequency curves for the station at Bettws-y-Crwyn (shown by squares and crosses) superimposed on the Gringorten plotting positions (shown by lines) for different times periods (1, 2, 5, 10, 15, 30, 45, 60, 90 and 120 minutes) over a period of 200 years: left panel (annual series), central panel (winter series) and right panel (summer series). The x-axis on all panels shows log (natural logarithm, ln) from 0-6. The y-axis plots rainfall depth (0-80mm).
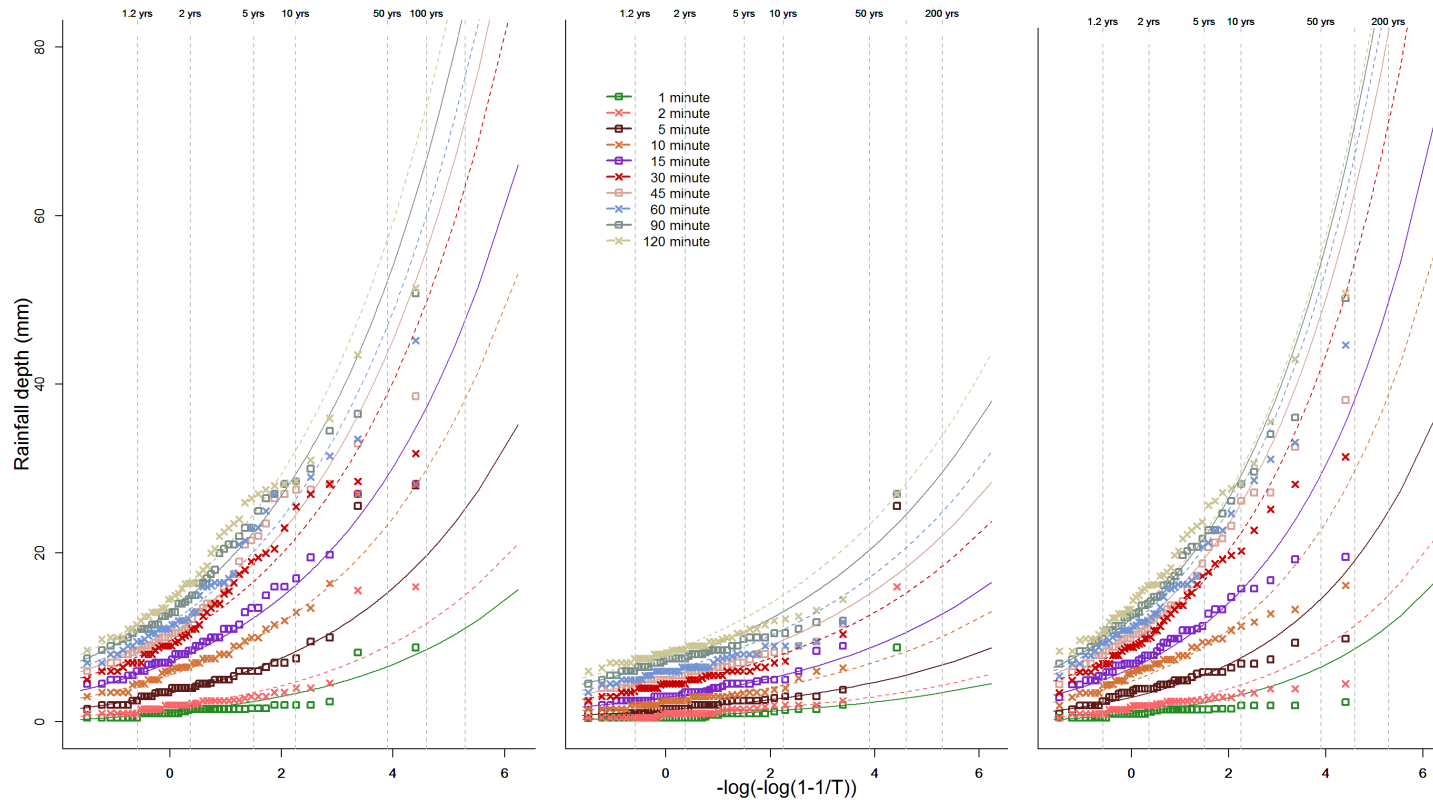
Figure 22 - Estimated frequency curves for the station at Stone for the annual (left panel), winter (central panel) and summer (right panel) series, superimposed on the Gringorten plotting positions

The three graphs in Figure 22 plot the estimated frequency curves for the station at Stone (shown by squares and crosses) superimposed on the Gringorten plotting positions (shown by lines) for different times periods (1, 2, 5, 10, 15, 30, 45, 60, 90 and 120 minutes) over a period of 200 years: left panel (annual series), central panel (winter series) and right panel (summer series). The x-axis on all panels shows log (natural logarithm, ln) from 0-6. The y-axis plots rainfall depth (0-80mm).
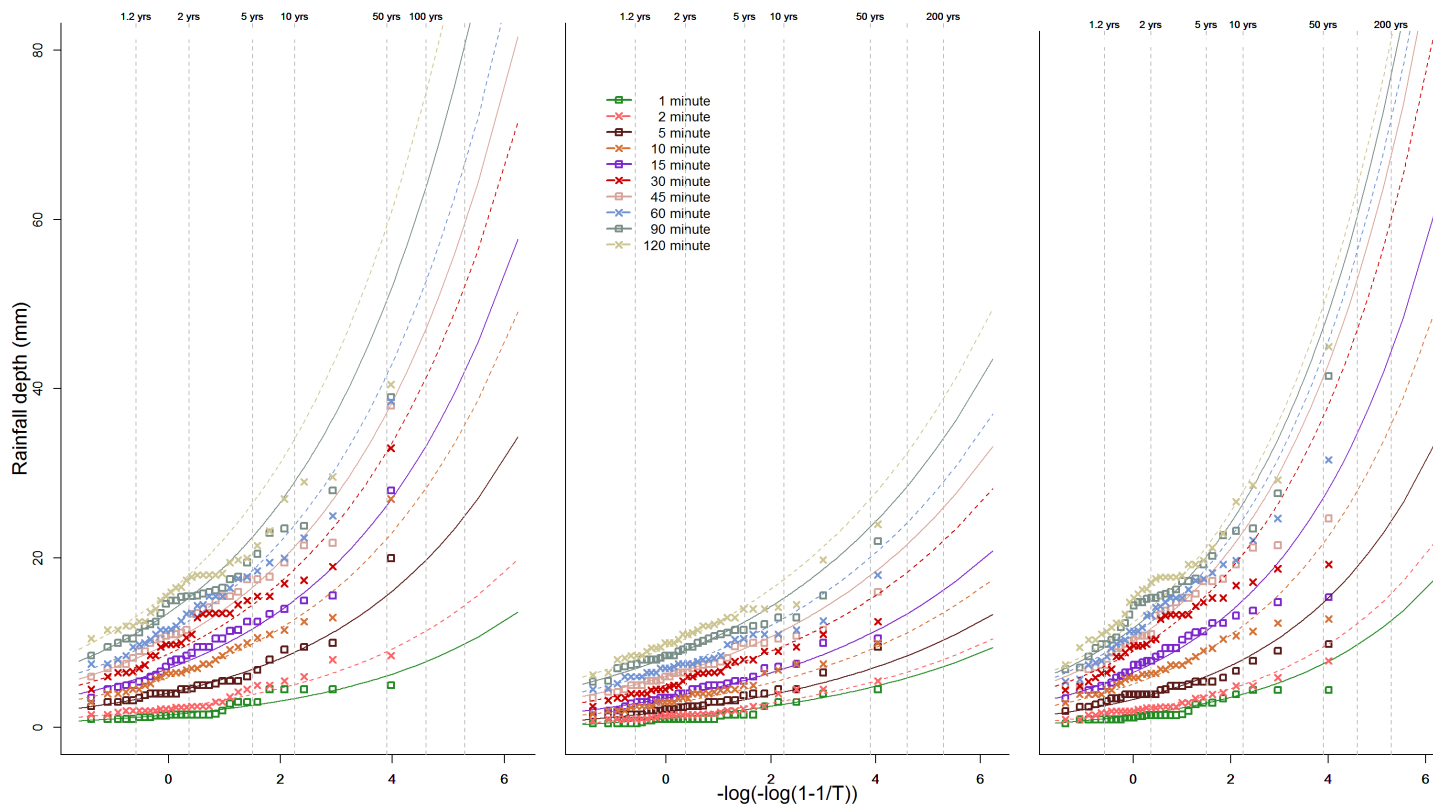
Figure 23 - Estimated frequency curves for the station at Dowdeswell for the annual (left panel), winter (central panel) and summer (right panel) series, superimposed on the Gringorten plotting positions

The three graphs in Figure 23 plot the estimated frequency curves for the station at Dowdeswell (shown by squares and crosses) superimposed on the Gringorten plotting positions (shown by lines) for different times periods (1, 2, 5, 10, 15, 30, 45, 60, 90 and 120 minutes) over a period of 200 years: left panel (annual series), central panel (winter series) and right panel (summer series). The x-axis on all panels shows log (natural logarithm, ln) from 0-6. The y-axis plots rainfall depth (0-80mm).
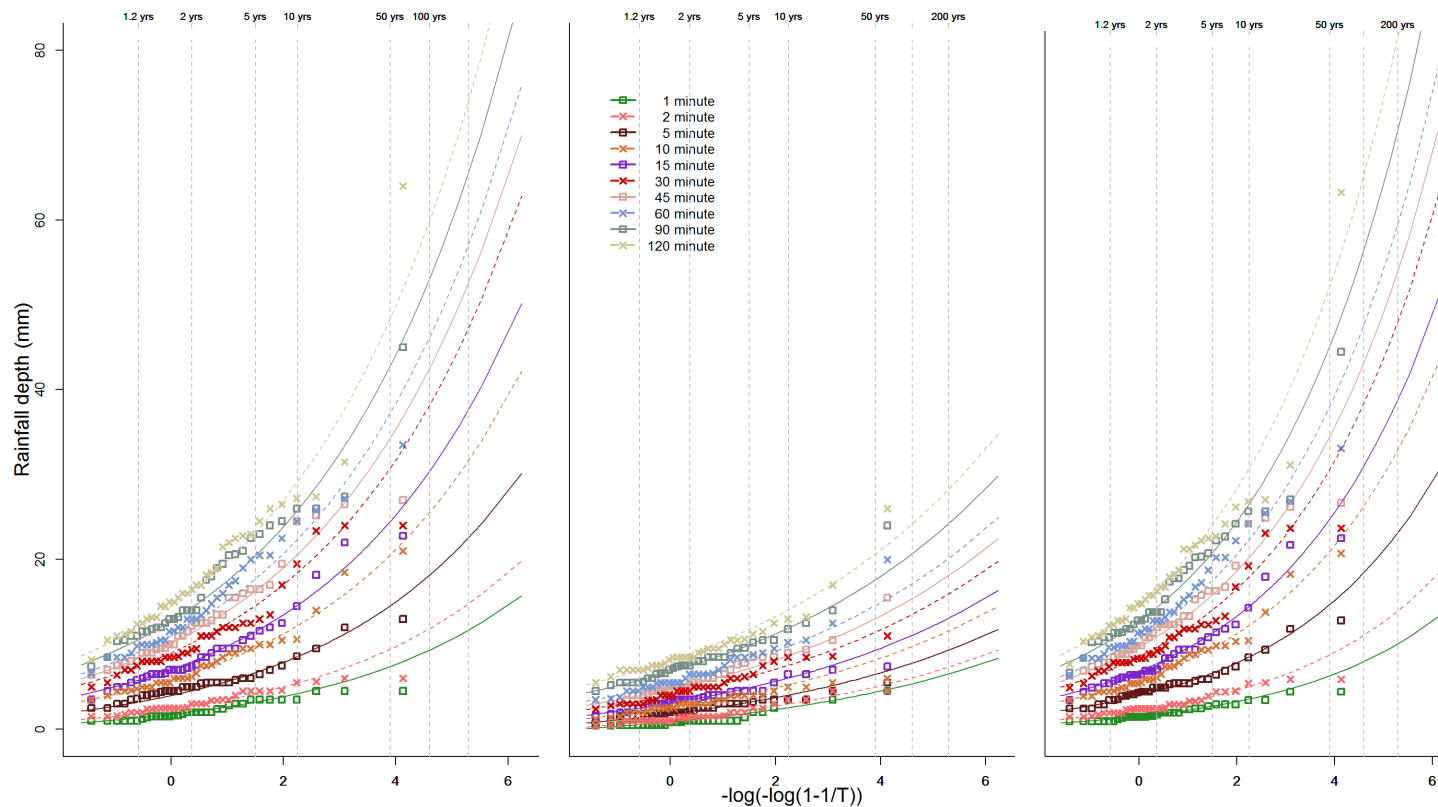
Figure 24 - Estimated frequency curves for the station at Knightcote for the annual (left panel), winter (central panel) and summer (right panel) series, superimposed on the Gringorten plotting positions

The three graphs in Figure 24 plot the estimated frequency curves for the station at Knightcote (shown by squares and crosses) superimposed on the Gringorten plotting positions (shown by lines) for different times periods (1, 2, 5, 10, 15, 30, 45, 60, 90 and 120 minutes) over a period of 200 years: left panel (annual series), central panel (winter series) and right panel (summer series). The x-axis on all panels shows log (natural logarithm, ln) from 0-6. The y-axis plots rainfall depth (0-80mm).
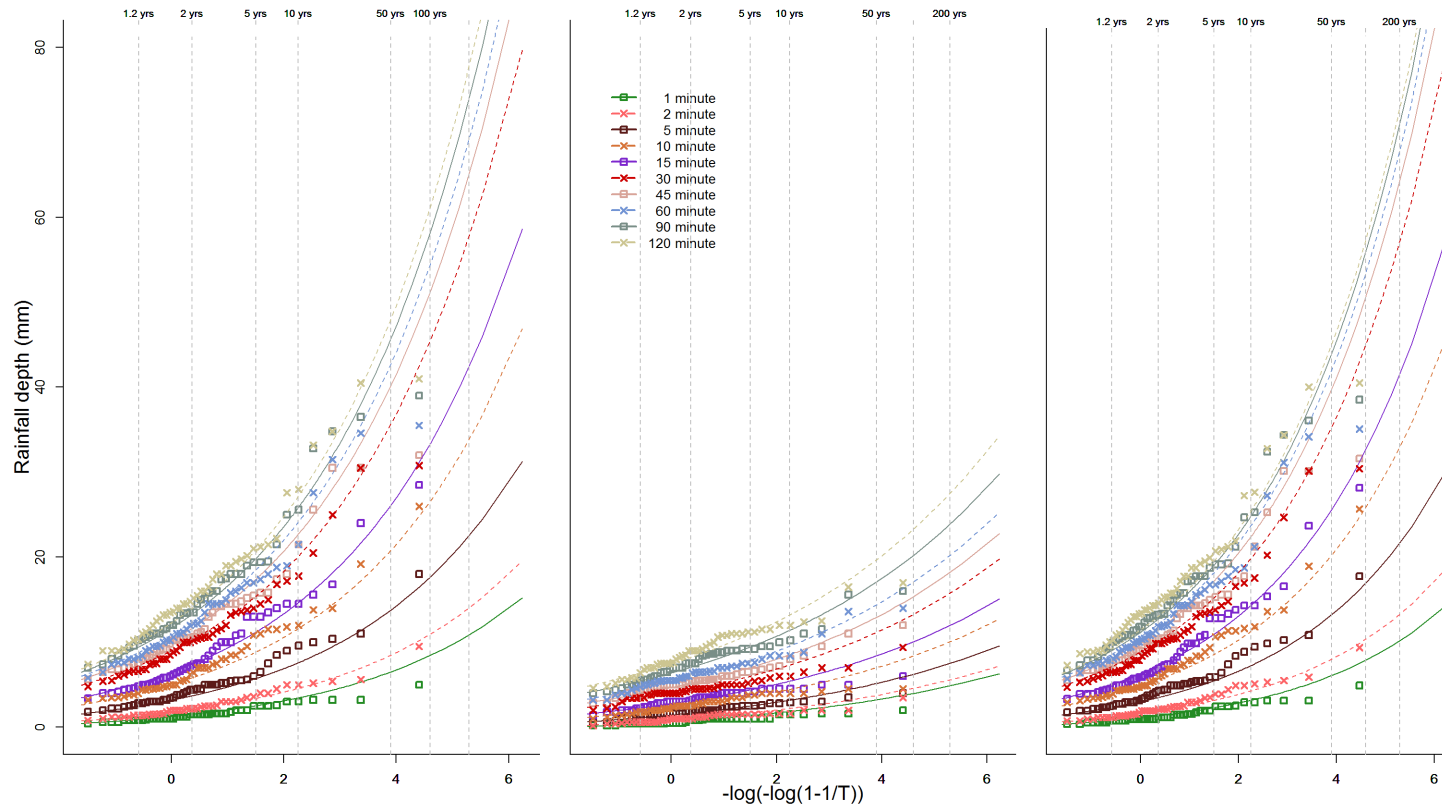
Figure 25 - Estimated frequency curves for the station at Hinckley for the annual (left panel), winter (central panel) and summer (right panel) series, superimposed on the Gringorten plotting positions

The three graphs in Figure 25 plot the estimated frequency curves for the station at Hinckley (shown by squares and crosses) superimposed on the Gringorten plotting positions (shown by lines) for different times periods (1, 2, 5, 10, 15, 30, 45, 60, 90 and 120 minutes) over a period of 200 years: left panel (annual series), central panel (winter series) and right panel (summer series). The x-axis on all panels shows log (natural logarithm, ln) from 0-6. The y-axis plots rainfall depth (0-80mm).
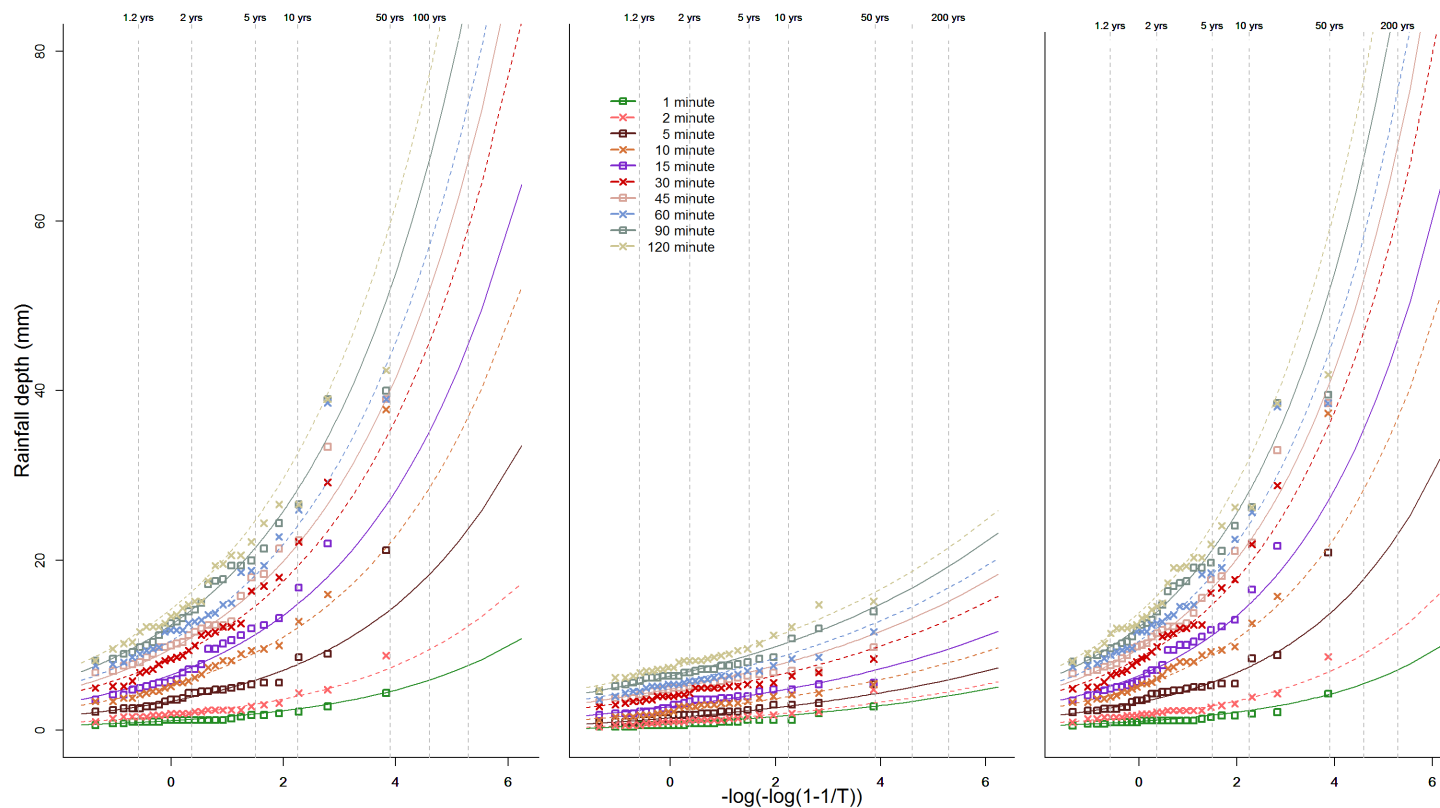
Figure 26 - Estimated frequency curves for the station at Lower Dunsforth for the annual (left panel), winter (central panel) and summer (right panel) series, superimposed on the Gringorten plotting positions

The three graphs in Figure 26 plot the estimated frequency curves for the station at Lower Dunsforth (shown by squares and crosses) superimposed on the Gringorten plotting positions (shown by lines) for different times periods (1, 2, 5, 10, 15, 30, 45, 60, 90 and 120 minutes) over a period of 200 years: left panel (annual series), central panel (winter series) and right panel (summer series). The x-axis on all panels shows log (natural logarithm, ln) from 0-6. The y-axis plots rainfall depth (0-80mm).
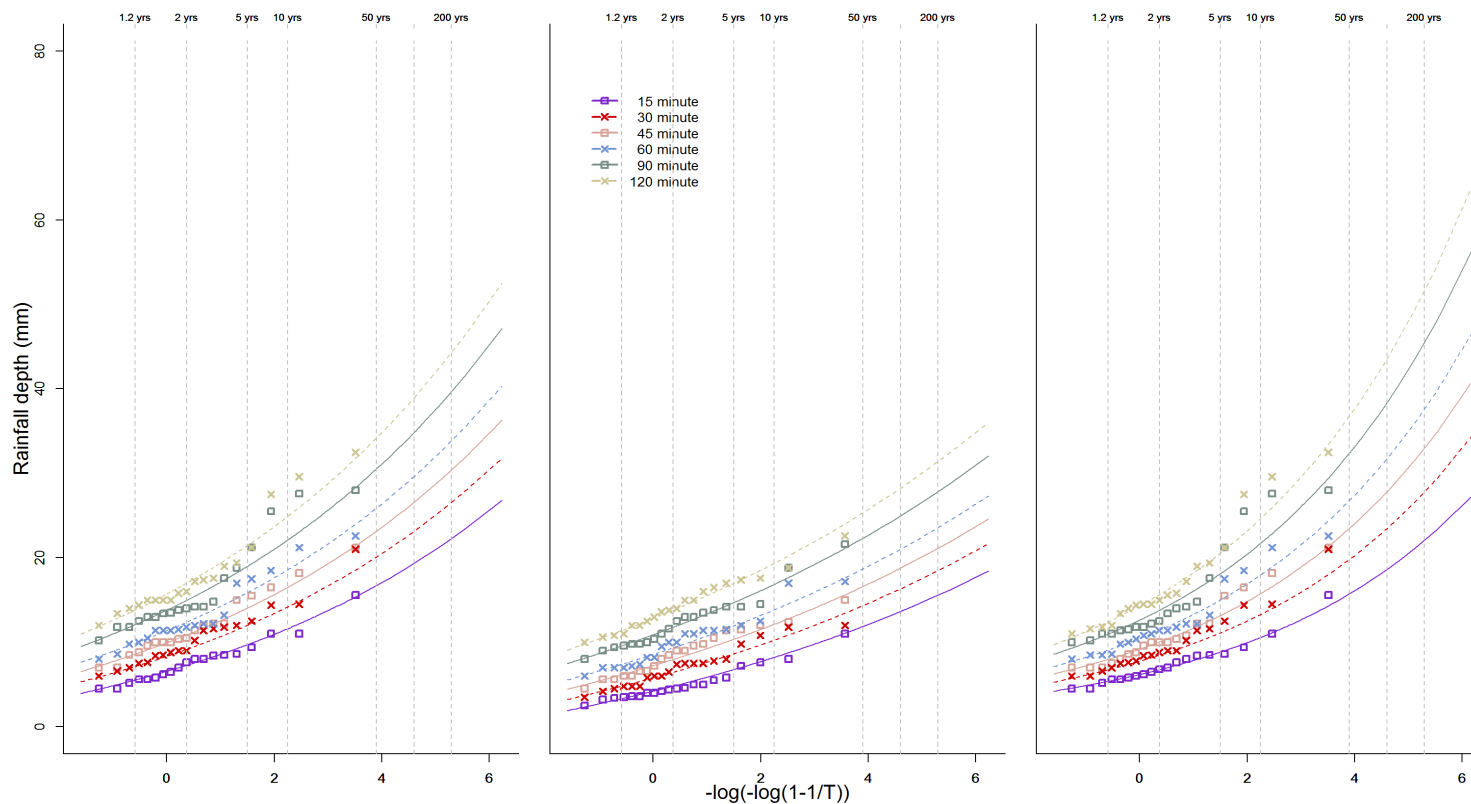
A.2 Fitted model results for 15-minute stations

Figure 27 - Estimated frequency curves for the station at Llanychaer for the annual (left panel), winter (central panel) and summer (right panel) series, superimposed on the Gringorten plotting positions

The three graphs in Figure 27 plot the estimated frequency curves for the station at Llanychaer (shown by squares and crosses) superimposed on the Gringorten plotting positions (shown by lines) for different times periods (15, 30, 45, 60, 90 and 120 minutes) over a period of 200 years: left panel (annual series), central panel (winter series) and right panel (summer series). The x-axis on all panels shows log (natural logarithm, ln) from 0-6. The y-axis plots rainfall depth (0-80mm).
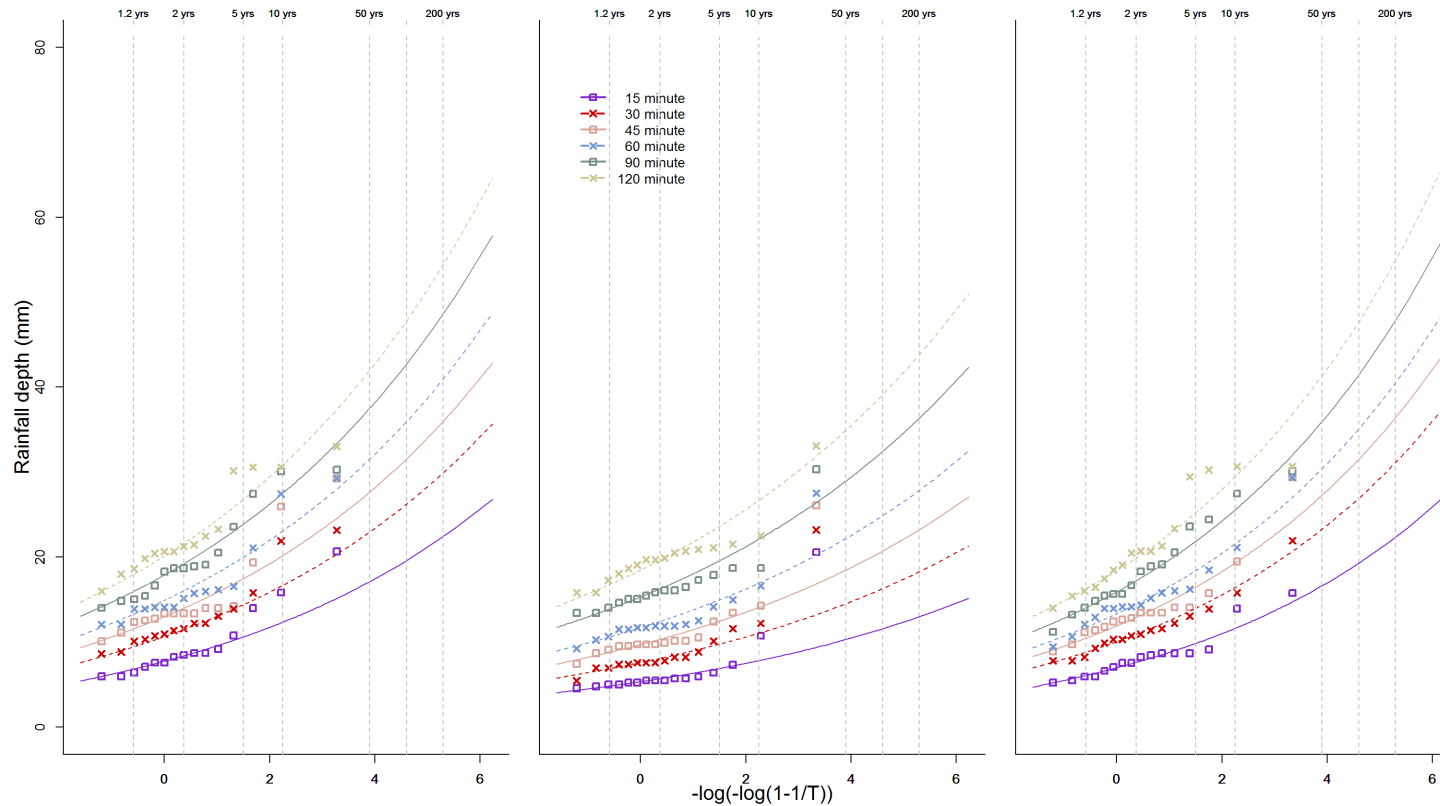
Figure 28 - Estimated frequency curves for the station at Taw Head for the annual (left panel), winter (central panel) and summer (right panel) series, superimposed on the Gringorten plotting positions

The three graphs in Figure 28 plot the estimated frequency curves for the station at Taw Head (shown by squares and crosses) superimposed on the Gringorten plotting positions (shown by lines) for different times periods (15, 30, 45, 60, 90 and 120 minutes) over a period of 200 years: left panel (annual series), central panel (winter series) and right panel (summer series). The x-axis on all panels shows log (natural logarithm, ln) from 0-6. The y-axis plots rainfall depth (0-80mm).
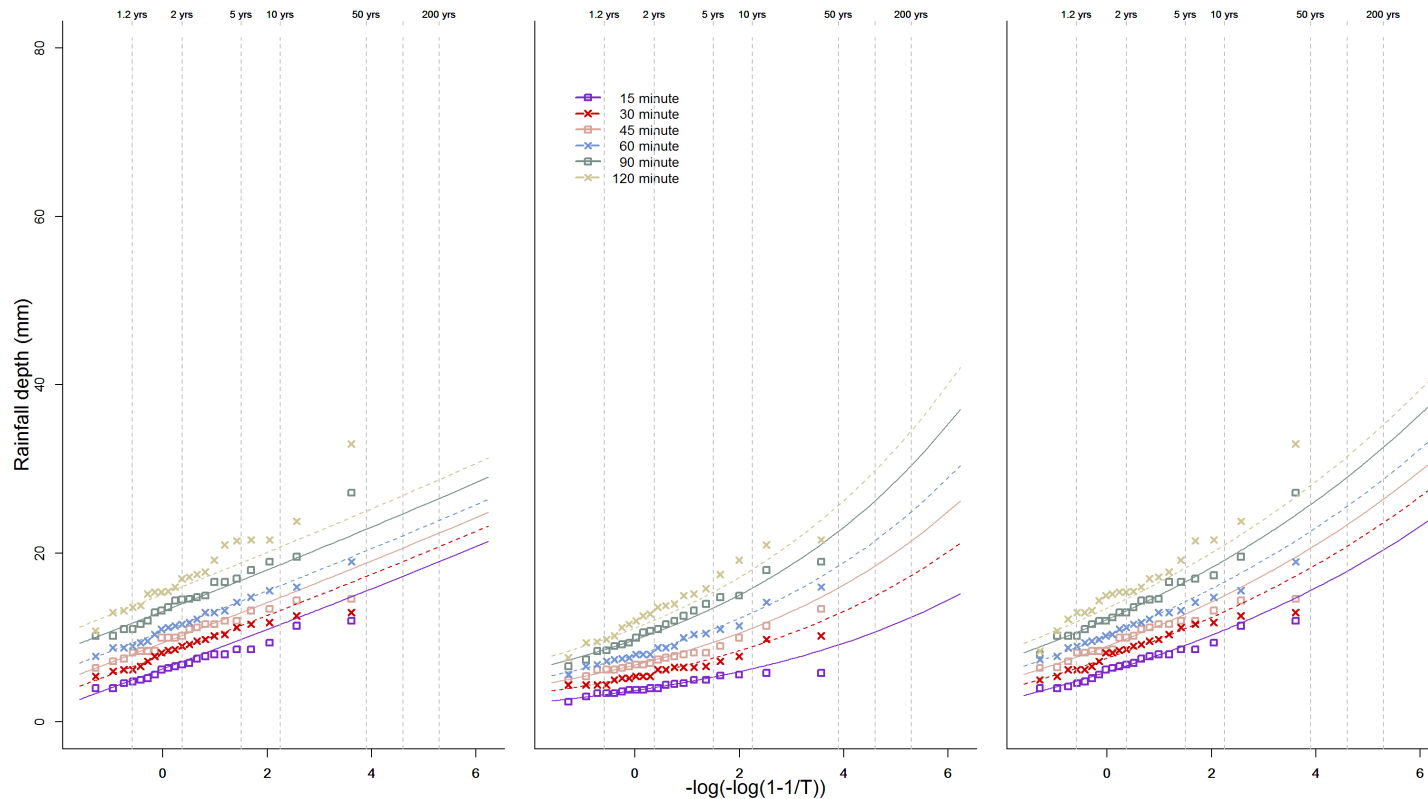
Figure 29 - Estimated frequency curves for the station at Victoria Park for the annual (left panel), winter (central panel) and summer (right panel) series, superimposed on the Gringorten plotting positions

The three graphs in Figure 29 plot the estimated frequency curves for the station at Victoria Park (shown by squares and crosses) superimposed on the Gringorten plotting positions (shown by lines) for different times periods (15, 30, 45, 60, 90 and 120 minutes) over a period of 200 years: left panel (annual series), central panel (winter series) and right panel (summer series). The x-axis on all panels shows log (natural logarithm, ln) from 0-6. The y-axis plots rainfall depth (0-80mm).

Figure 30 - Estimated frequency curves for the station at Colwyn Bay for the annual (left panel), winter (central panel) and summer (right panel) series, superimposed on the Gringorten plotting positions

The three graphs in Figure 30 plot the estimated frequency curves for the station at Colwyn Bay (shown by squares and crosses) superimposed on the Gringorten plotting positions (shown by lines) for different times periods (15, 30, 45, 60, 90 and 120 minutes) over a period of 200 years: left panel (annual series), central panel (winter series) and right panel (summer series). The x-axis on all panels shows log (natural logarithm, ln) from 0-6. The y-axis plots rainfall depth (0-80mm).
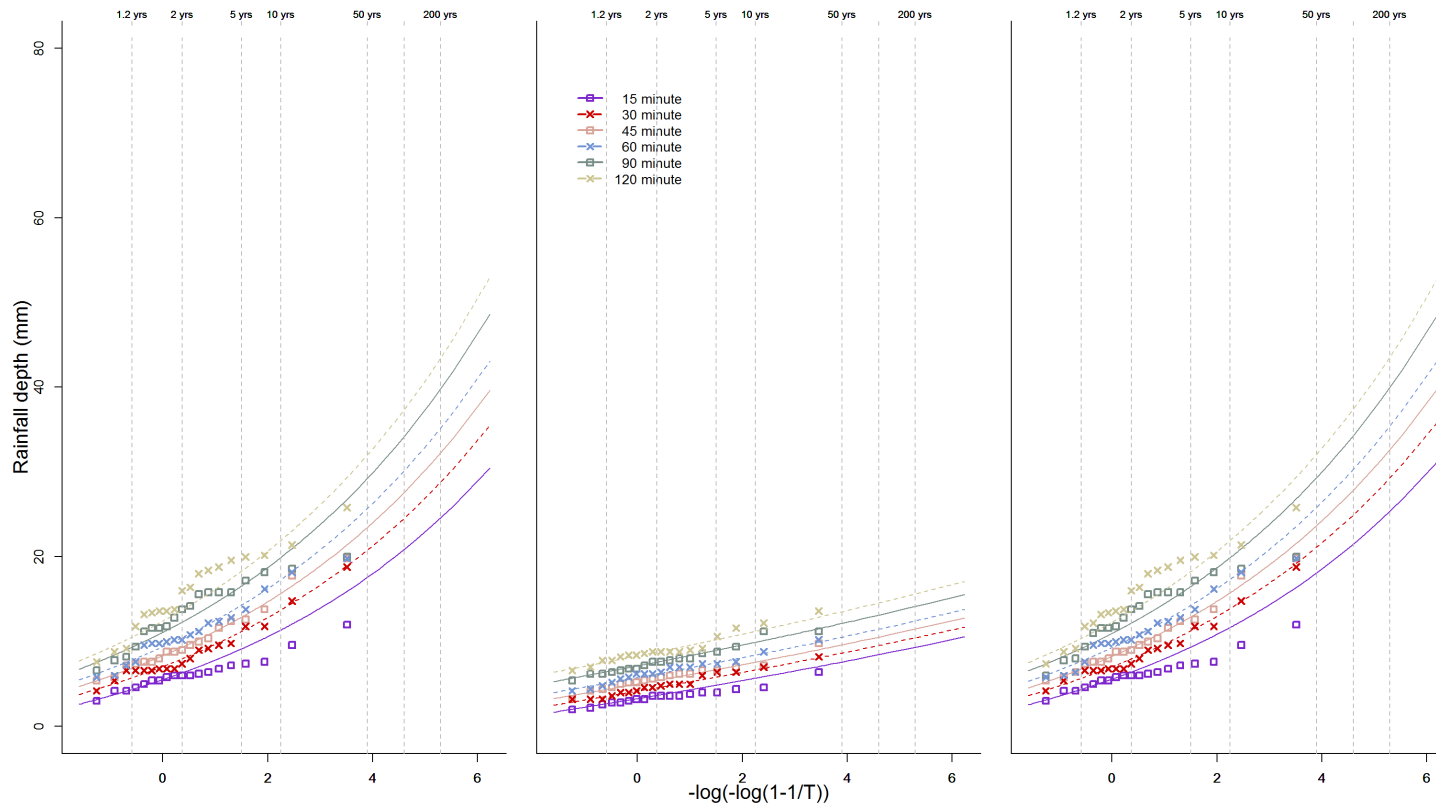
Figure 31 - Estimated frequency curves for the station at Hemyock for the annual (left panel), winter (central panel) and summer (right panel) series, superimposed on the Gringorten plotting positions

The three graphs in Figure 31 plot the estimated frequency curves for the station at Hemyock (shown by squares and crosses) superimposed on the Gringorten plotting positions (shown by lines) for different times periods (15, 30, 45, 60, 90 and 120 minutes) over a period of 200 years: left panel (annual series), central panel (winter series) and right panel (summer series). The x-axis on all panels shows log (natural logarithm, ln) from 0-6. The y-axis plots rainfall depth (0-80mm).

Figure 32 - Estimated frequency curves for the station at Bettws-y-Crwyn for the annual (left panel), winter (central panel) and summer (right panel) series, superimposed on the Gringorten plotting positions

The three graphs in Figure 32 plot the estimated frequency curves for the station at Bettws-y-Crwyn (shown by squares and crosses) superimposed on the Gringorten plotting positions (shown by lines) for different times periods (15, 30, 45, 60, 90 and 120 minutes) over a period of 200 years: left panel (annual series), central panel (winter series) and right panel (summer series). The x-axis on all panels shows log (natural logarithm, ln) from 0-6. The y-axis plots rainfall depth (0-80mm).
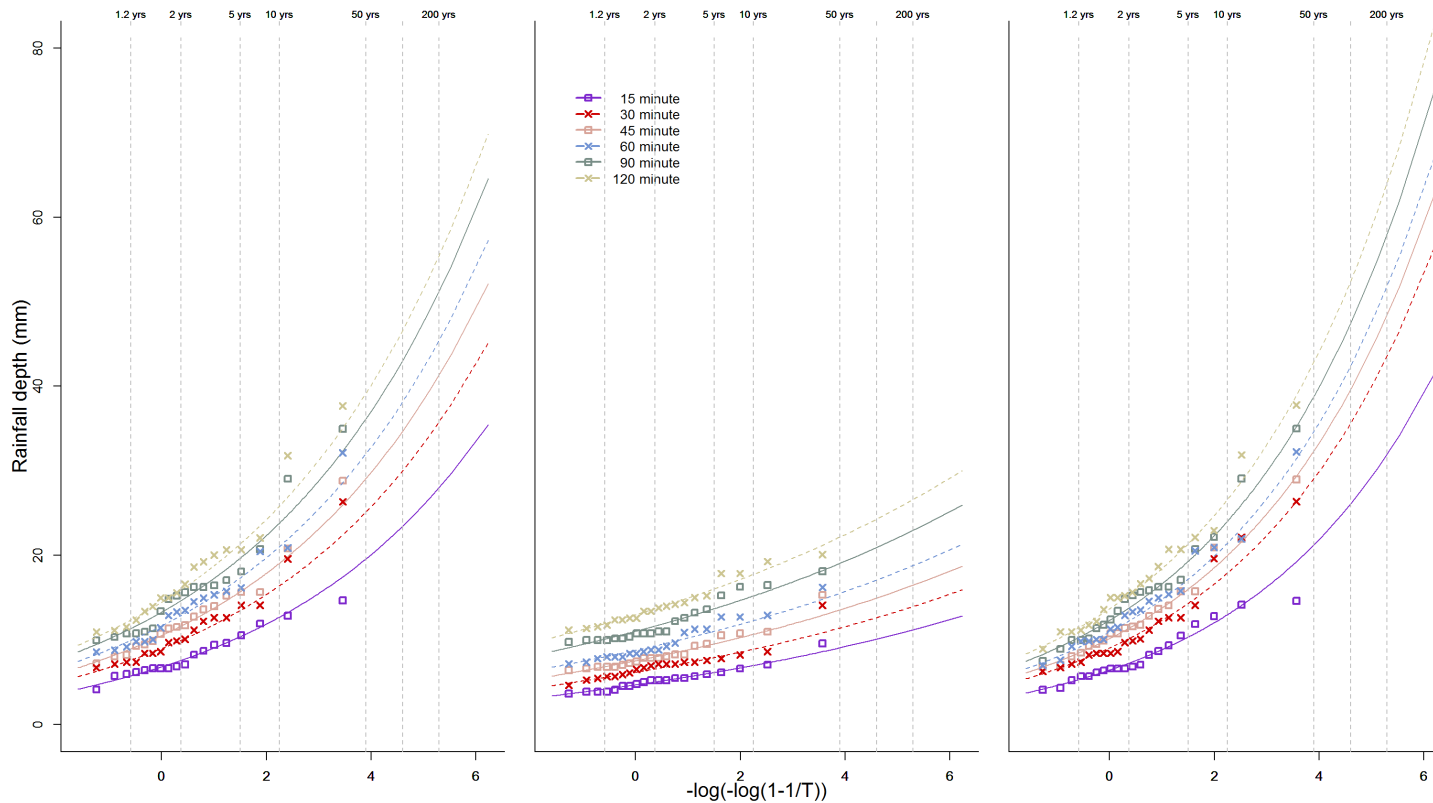
Figure 33 - Estimated frequency curves for the station at Crew Fell for the annual (left panel), winter (central panel) and summer (right panel) series, superimposed on the Gringorten plotting positions

The three graphs in Figure 33 plot the estimated frequency curves for the station at Crew Fell (shown by squares and crosses) superimposed on the Gringorten plotting positions (shown by lines) for different times periods (15, 30, 45, 60, 90 and 120 minutes) over a period of 200 years: left panel (annual series), central panel (winter series) and right panel (summer series). The x-axis on all panels shows log (natural logarithm, ln) from 0-6. The y-axis plots rainfall depth (0-80mm).
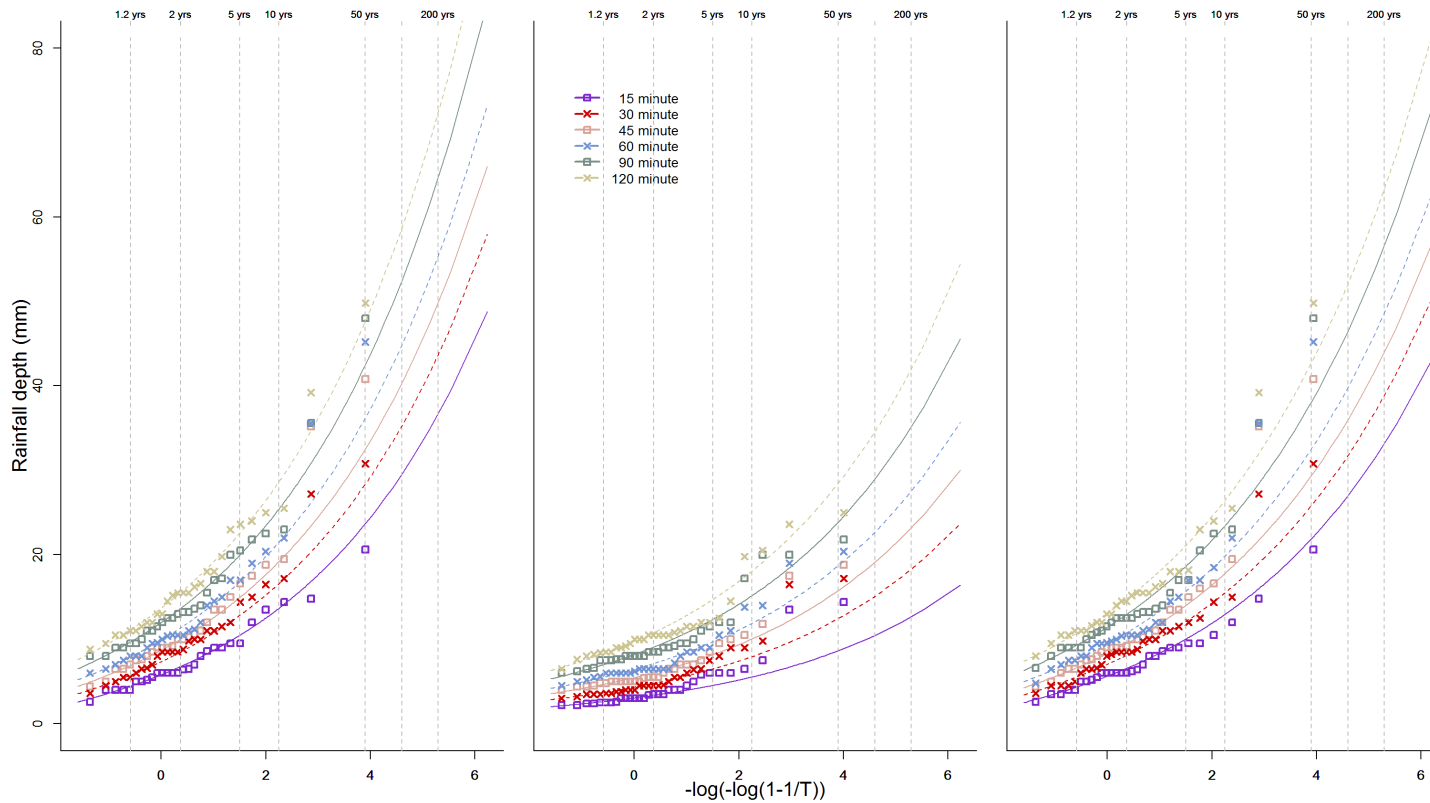
Figure 34 - Estimated frequency curves for the station at Kingswood for the annual (left panel), winter (central panel) and summer (right panel) series, superimposed on the Gringorten plotting positions

The three graphs in Figure 34 plot the estimated frequency curves for the station at Kingswood (shown by squares and crosses) superimposed on the Gringorten plotting positions (shown by lines) for different times periods (15, 30, 45, 60, 90 and 120 minutes) over a period of 200 years: left panel (annual series), central panel (winter series) and right panel (summer series). The x-axis on all panels shows log (natural logarithm, ln) from 0-6. The y-axis plots rainfall depth (0-80mm).
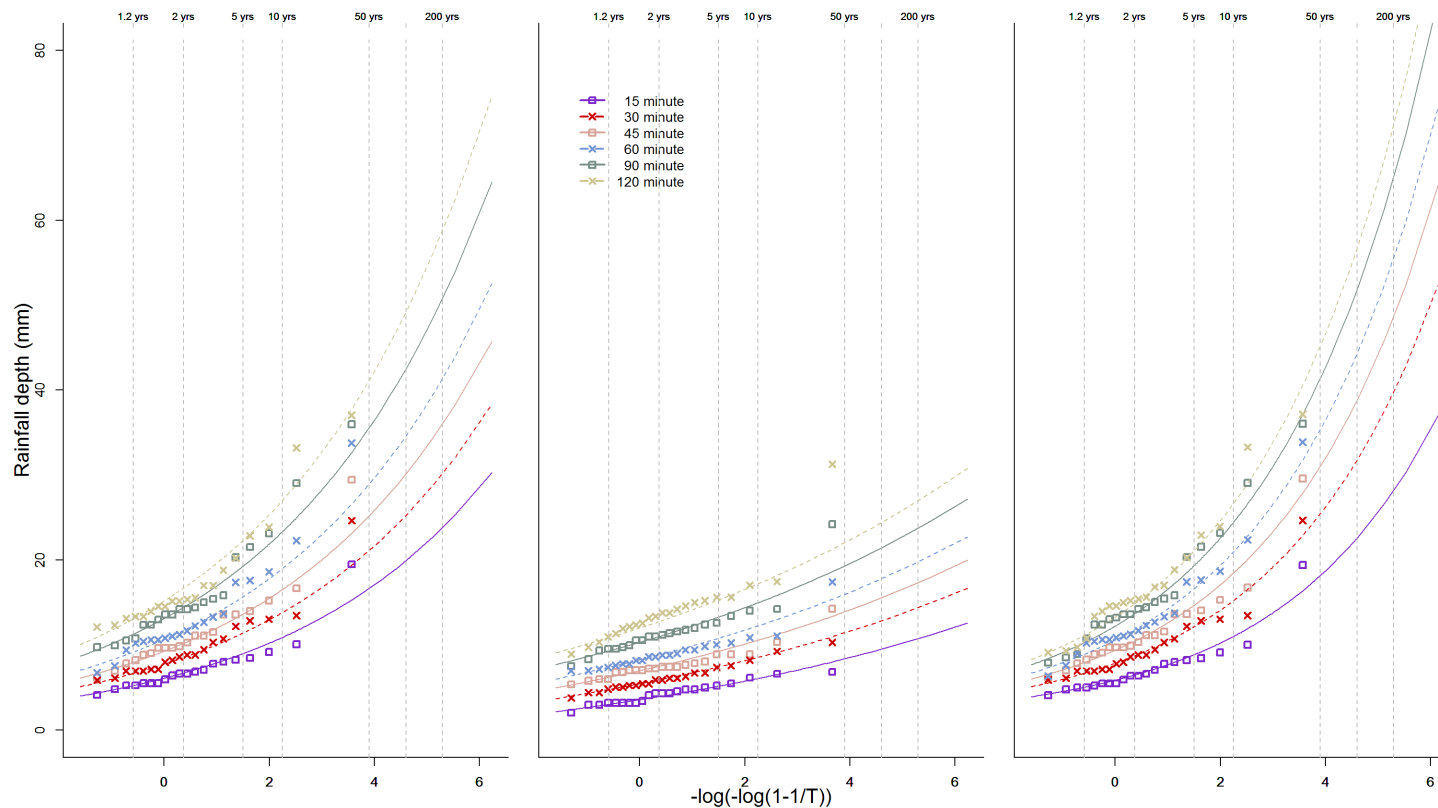
Figure 35 - Estimated frequency curves for the station at Sale Carrington for the annual (left panel), winter (central panel) and summer (right panel) series, superimposed on the Gringorten plotting positions

The three graphs in Figure 35 plot the estimated frequency curves for the station at Carrington (shown by squares and crosses) superimposed on the Gringorten plotting positions (shown by lines) for different times periods (15, 30, 45, 60, 90 and 120 minutes) over a period of 200 years: left panel (annual series), central panel (winter series) and right panel (summer series). The x-axis on all panels shows log (natural logarithm, ln) from 0-6. The y-axis plots rainfall depth (0-80mm).
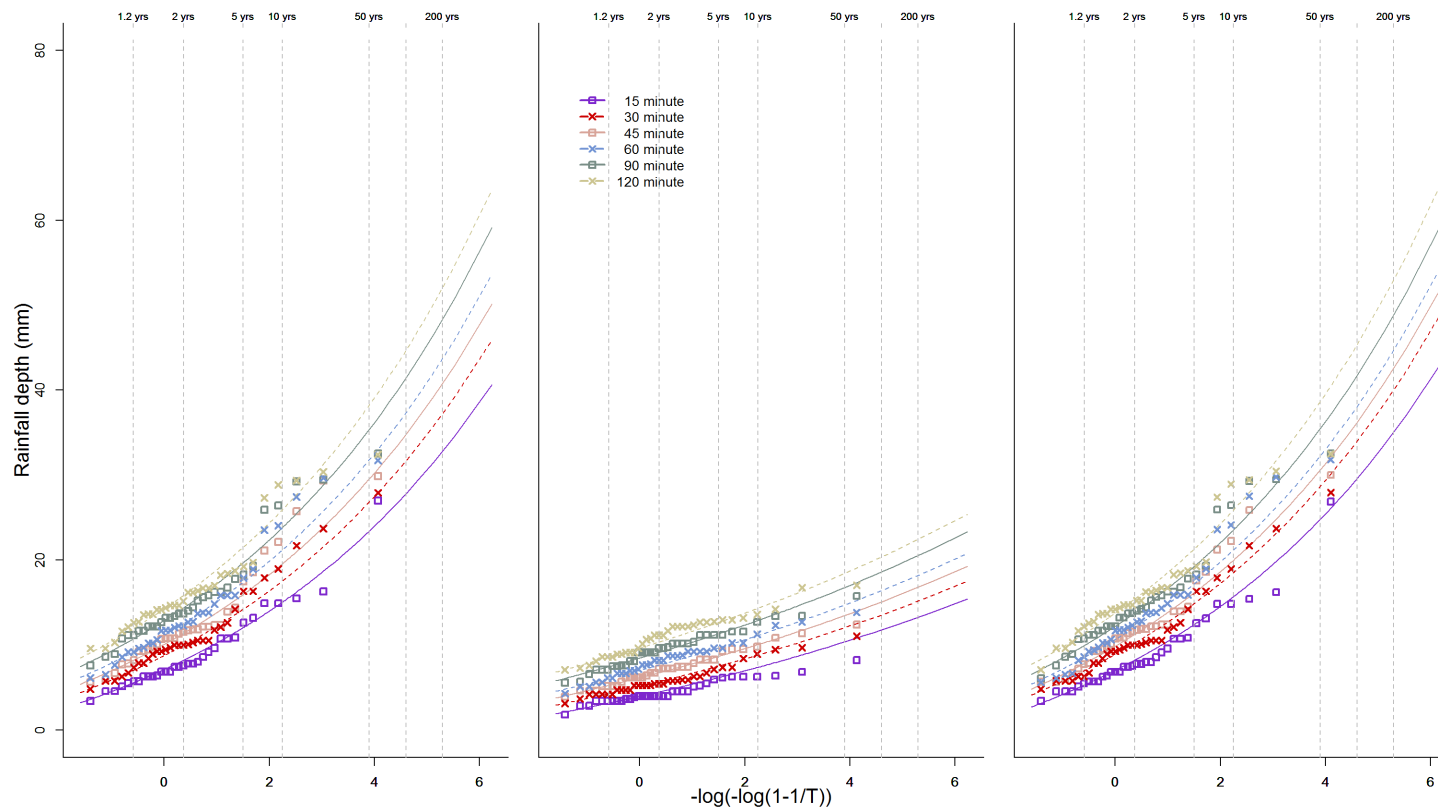
Figure 36 - Estimated frequency curves for the station at Stone for the annual (left panel), winter (central panel) and summer (right panel) series, superimposed on the Gringorten plotting positions

The three graphs in Figure 36 plot the estimated frequency curves for the station at Stone (shown by squares and crosses) superimposed on the Gringorten plotting positions (shown by lines) for different times periods (15, 30, 45, 60, 90 and 120 minutes) over a period of 200 years: left panel (annual series), central panel (winter series) and right panel (summer series). The x-axis on all panels shows log (natural logarithm, ln) from 0-6. The y-axis plots rainfall depth (0-80mm).

Figure 37 - Estimated frequency curves for the station at Dowdeswell for the annual (left panel), winter (central panel) and summer (right panel) series, superimposed on the Gringorten plotting positions

The three graphs in Figure 37 plot the estimated frequency curves for the station at Dowdeswell (shown by squares and crosses) superimposed on the Gringorten plotting positions (shown by lines) for different times periods (15, 30, 45, 60, 90 and 120 minutes) over a period of 200 years: left panel (annual series), central panel (winter series) and right panel (summer series). The x-axis on all panels shows log (natural logarithm, ln) from 0-6. The y-axis plots rainfall depth (0-80mm).

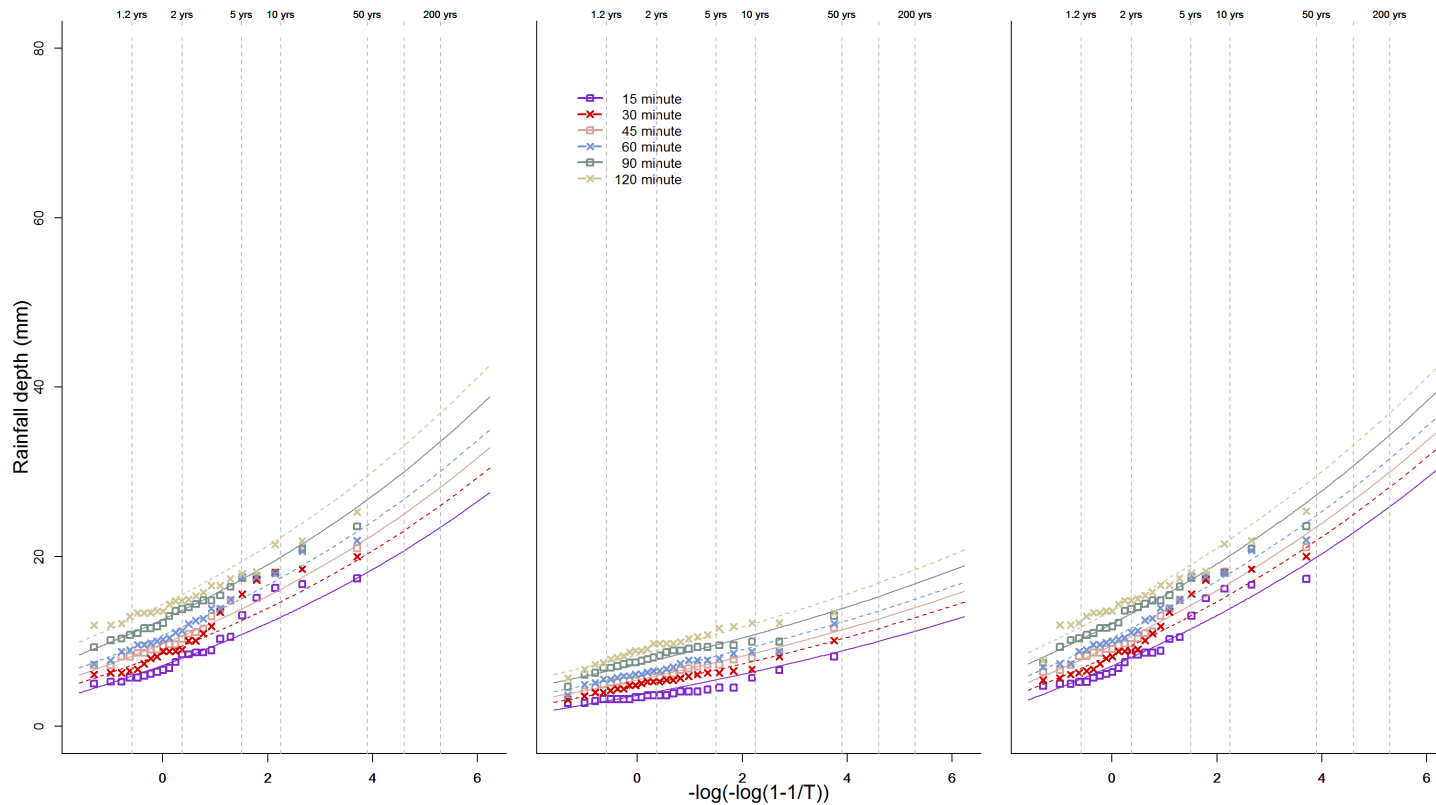**Figure 38 - Estimated frequency curves for the station at Knightcote for the annual (left panel), winter (central panel) and summer (right panel) series, superimposed on the Gringorten plotting positions**

The three graphs in Figure 38 plot the estimated frequency curves for the station at Knightcote (shown by squares and crosses) superimposed on the Gringorten plotting positions (shown by lines) for different times periods (15, 30, 45, 60, 90 and 120 minutes) over a period of 200 years: left panel (annual series), central panel (winter series) and right panel (summer series). The x-axis on all panels shows log (natural logarithm, ln) from 0-6. The y-axis plots rainfall depth (0-80mm).
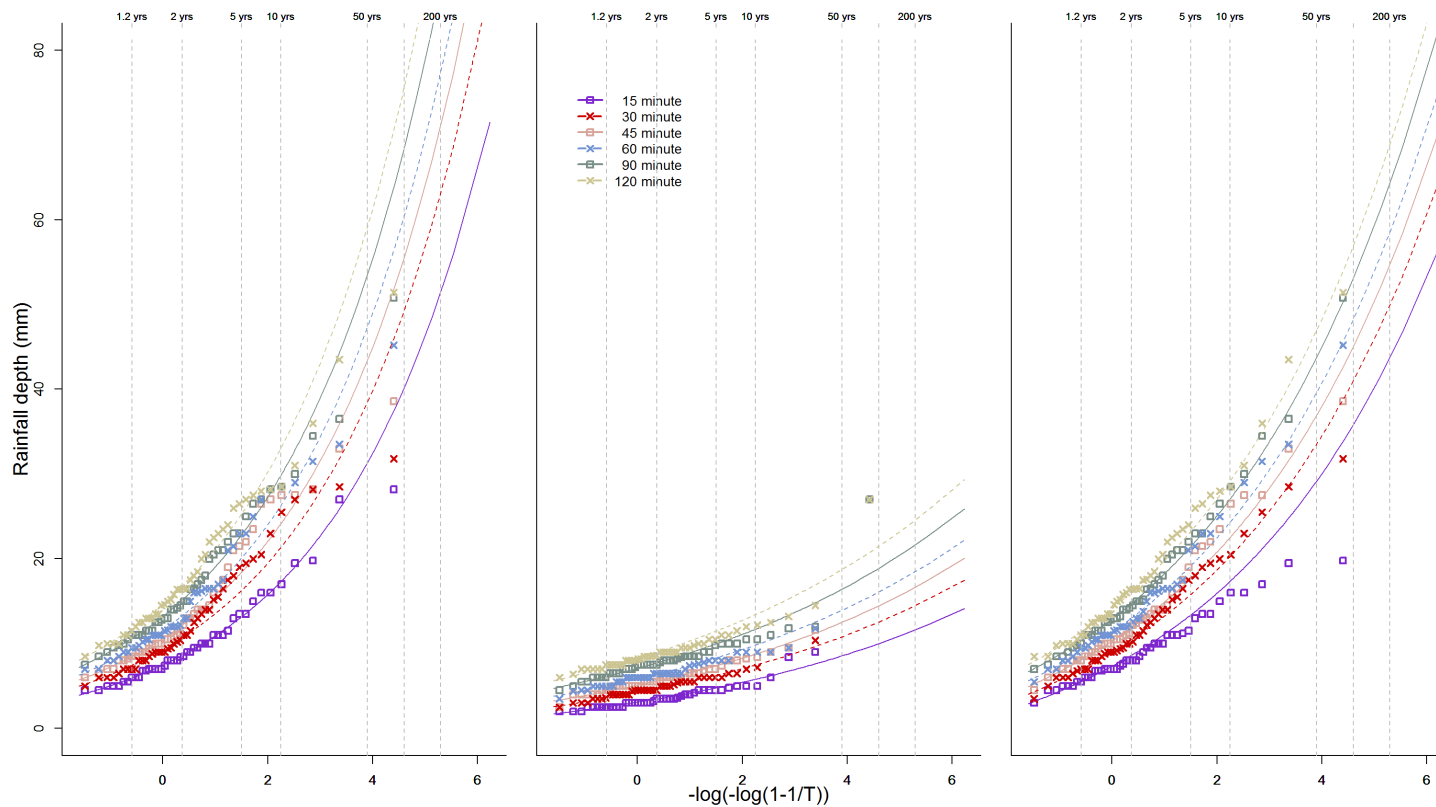
Figure 39 - Estimated frequency curves for the station at Hinckley for the annual (left panel), winter (central panel) and summer (right panel) series, superimposed on the Gringorten plotting positions

The three graphs in Figure 39 plot the estimated frequency curves for the station at Hinckley (shown by squares and crosses) superimposed on the Gringorten plotting positions (shown by lines) for different times periods (15, 30, 45, 60, 90 and 120 minutes) over a period of 200 years: left panel (annual series), central panel (winter series) and right panel (summer series). The x-axis on all panels shows log (natural logarithm, ln) from 0-6. The y-axis plots rainfall depth (0-80mm).
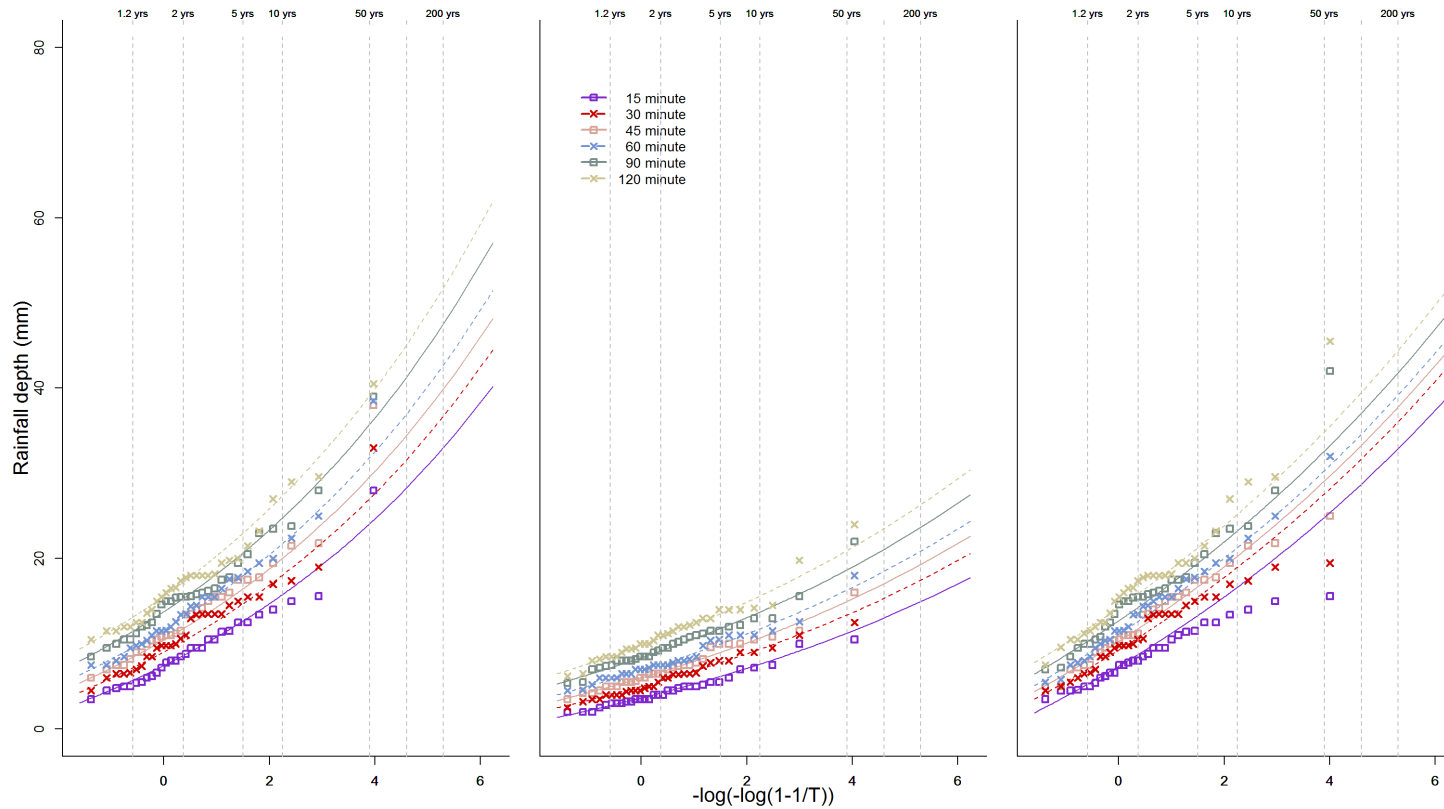
Figure 40 - Estimated frequency curves for the station at Lower Dunsforth for the annual (left panel), winter (central panel) and summer (right panel) series, superimposed on the Gringorten plotting positions

The three graphs in Figure 40 plot the estimated frequency curves for the station at Lower Dunsworth (shown by squares and crosses) superimposed on the Gringorten plotting positions (shown by lines) for different times periods (15, 30, 45, 60, 90 and 120 minutes) over a period of 200 years: left panel (annual series), central panel (winter series) and right panel (summer series). The x-axis on all panels shows log (natural logarithm, ln) from 0-6. The y-axis plots rainfall depth (0-80mm).

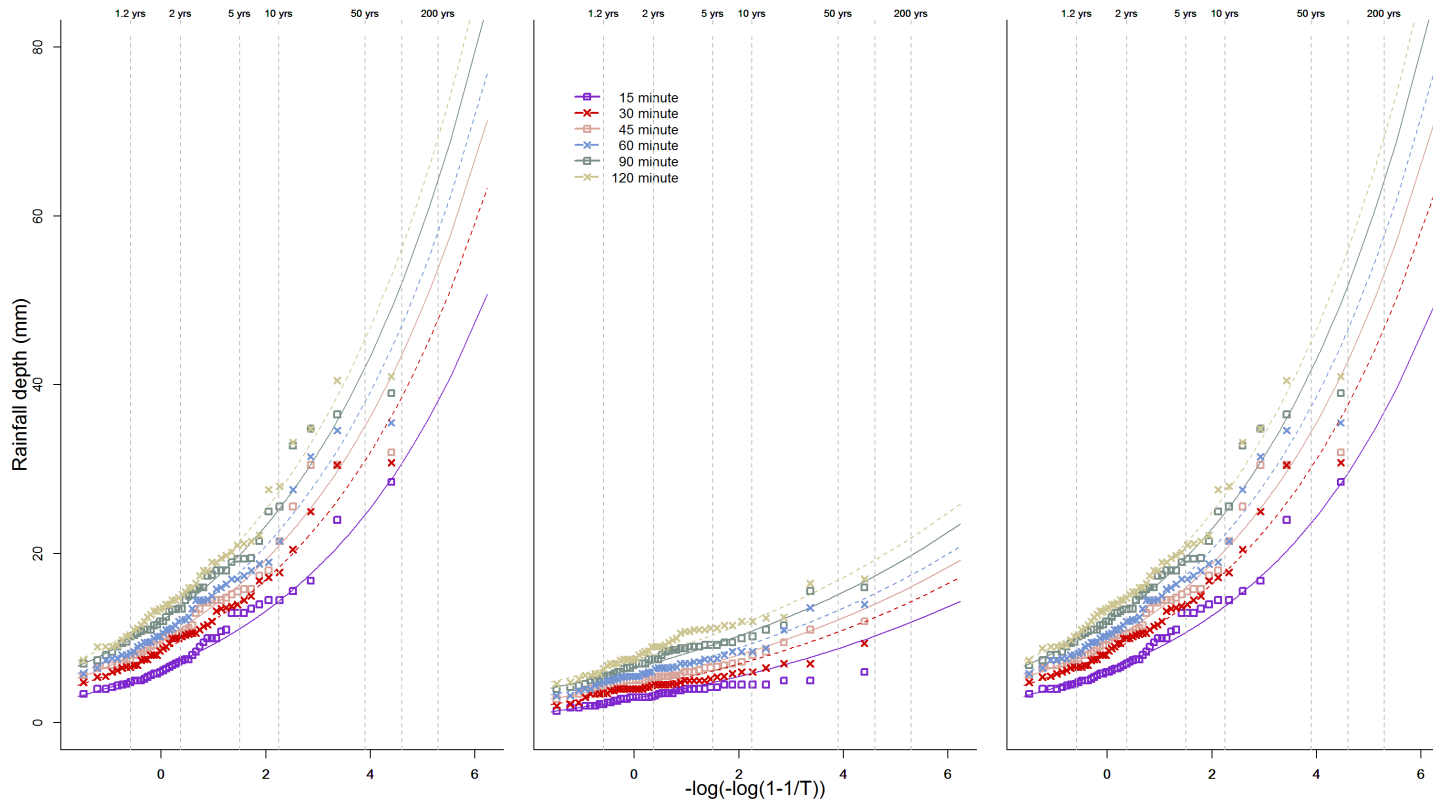**Figure 41 - Estimated frequency curves for the station at Otterbourne for the annual (left panel), winter (central panel) and summer (right panel) series, superimposed on the Gringorten plotting positions**

The three graphs in Figure 41 plot the estimated frequency curves for the station at Otterbourne (shown by squares and crosses) superimposed on the Gringorten plotting positions (shown by lines) for different times periods (15, 30, 45, 60, 90 and 120 minutes) over a period of 200 years: left panel (annual series), central panel (winter series) and right panel (summer series). The x-axis on all panels shows log (natural logarithm, ln) from 0-6. The y-axis plots rainfall depth (0-80mm).
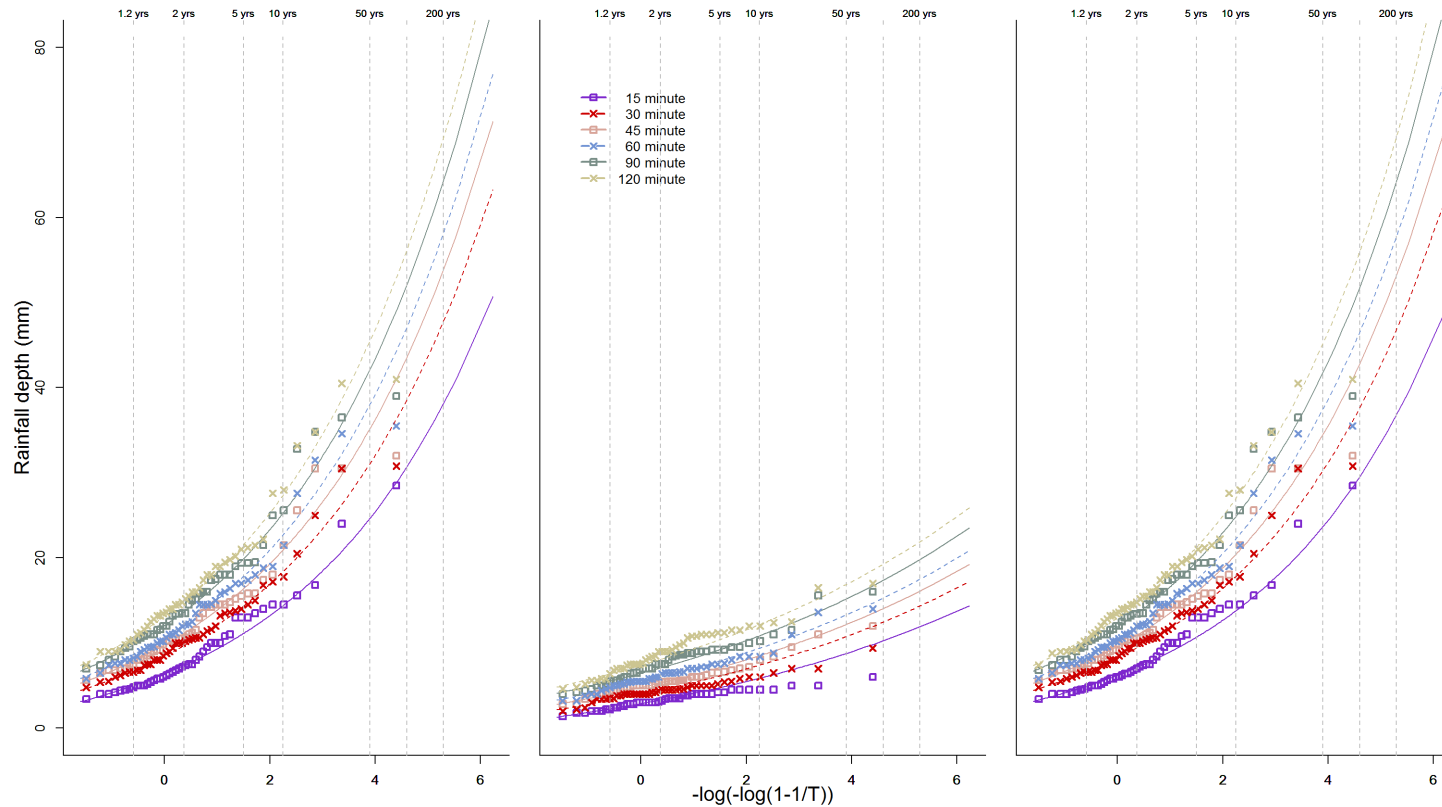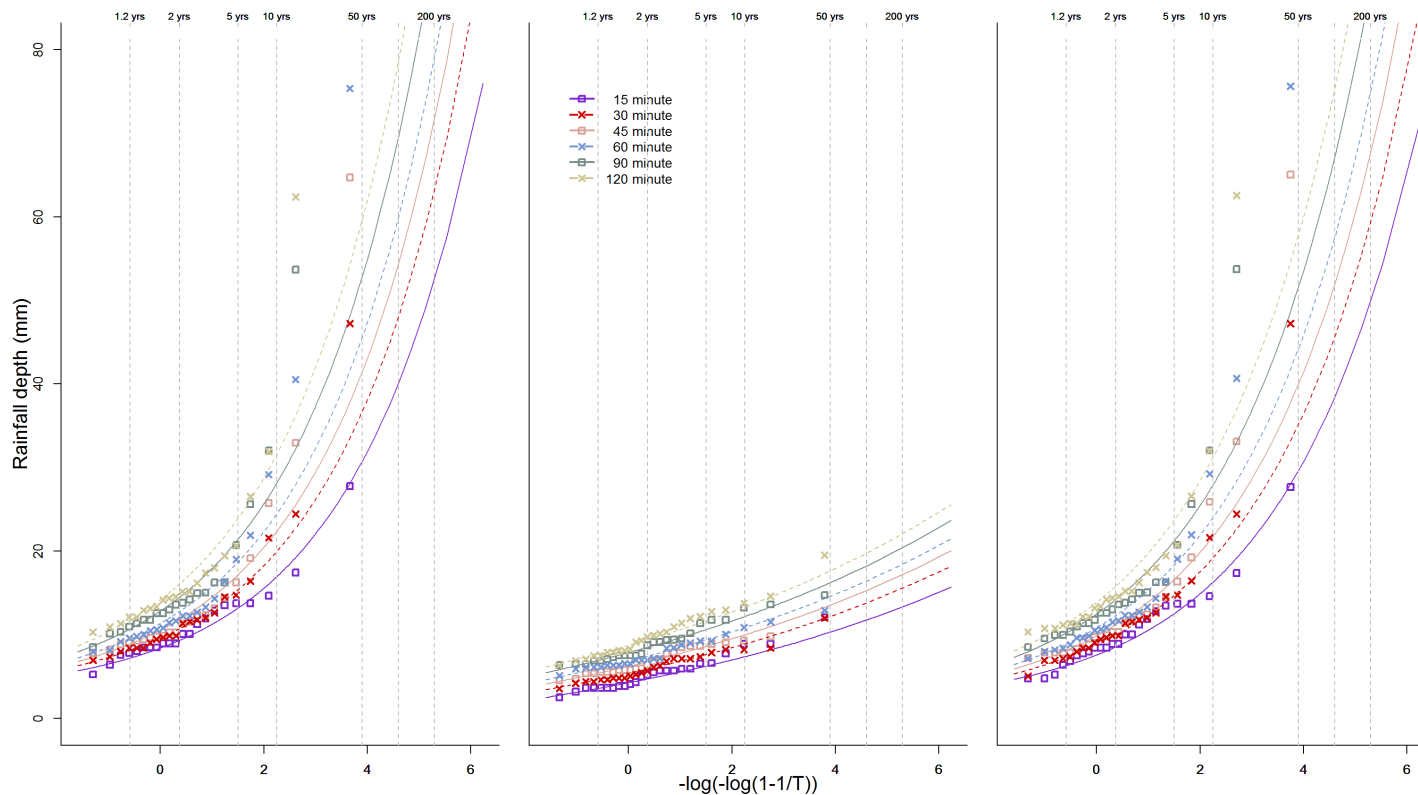
Figure 42 - Estimated frequency curves for the station at Chieveley for the annual (left panel), winter (central panel) and summer (right panel) series, superimposed on the Gringorten plotting positions

The three graphs in Figure 42 plot the estimated frequency curves for the station at Chieveley (shown by squares and crosses) superimposed on the Gringorten plotting positions (shown by lines) for different times periods (15, 30, 45, 60, 90 and 120 minutes) over a period of 200 years: left panel (annual series), central panel (winter series) and right panel (summer series). The x-axis on all panels shows log (natural logarithm, ln) from 0-6. The y-axis plots rainfall depth (0-80mm).
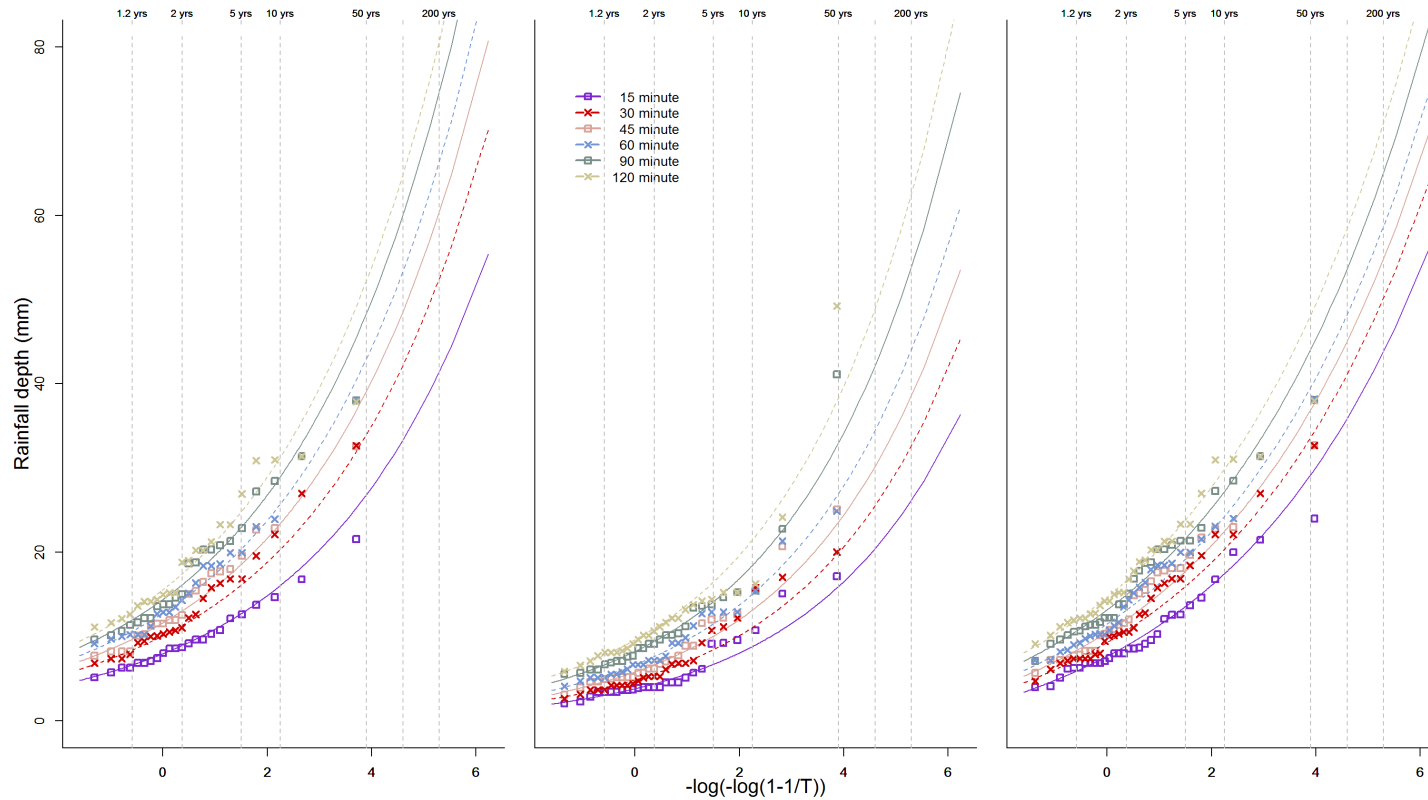
Figure 43 - Estimated frequency curves for the station at Ludford for the annual (left panel), winter (central panel) and summer (right panel) series, superimposed on the Gringorten plotting positions

The three graphs in Figure 43 plot the estimated frequency curves for the station at Ludford (shown by squares and crosses) superimposed on the Gringorten plotting positions (shown by lines) for different times periods (15, 30, 45, 60, 90 and 120 minutes) over a period of 200 years: left panel (annual series), central panel (winter series) and right panel (summer series). The x-axis on all panels shows log (natural logarithm, ln) from 0-6. The y-axis plots rainfall depth (0-80mm).
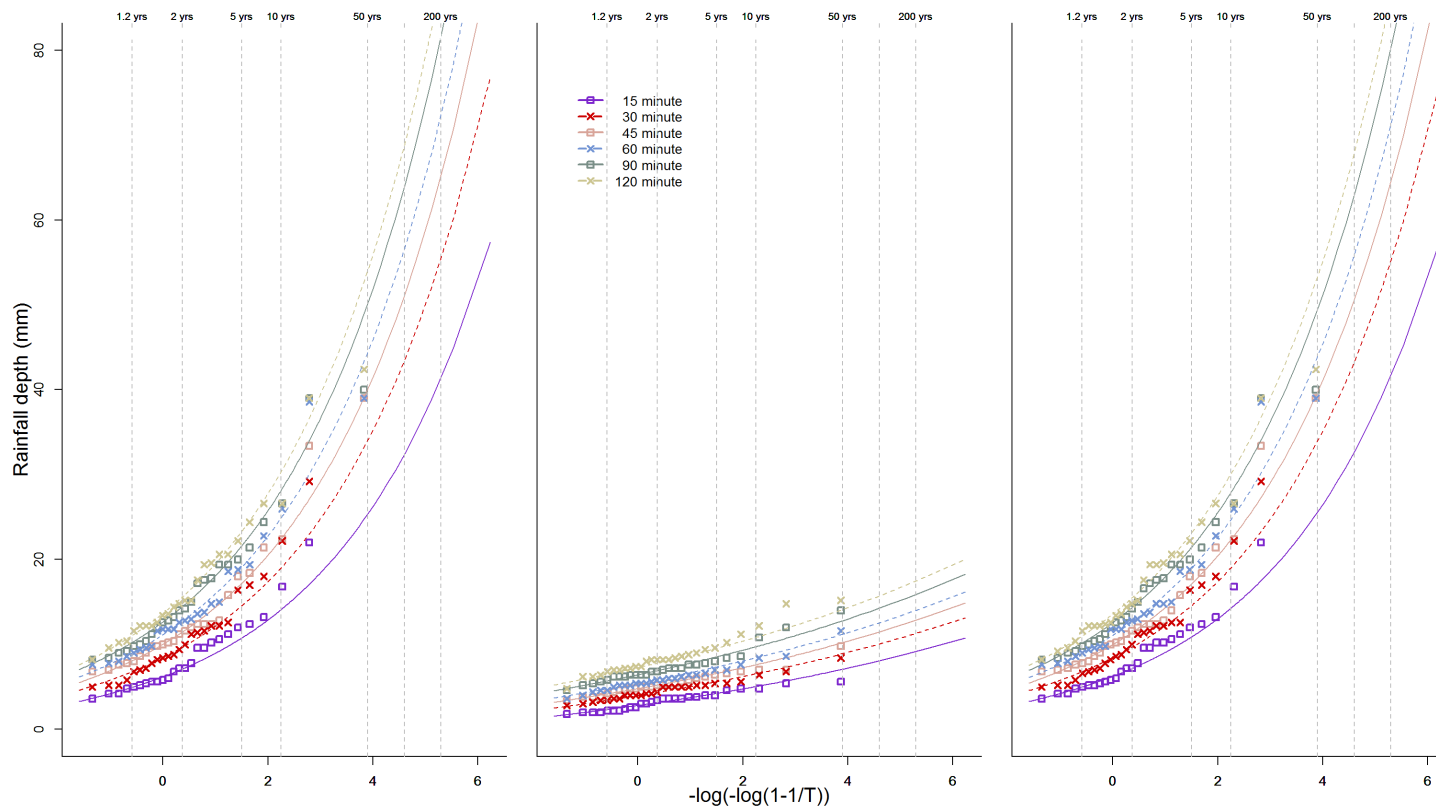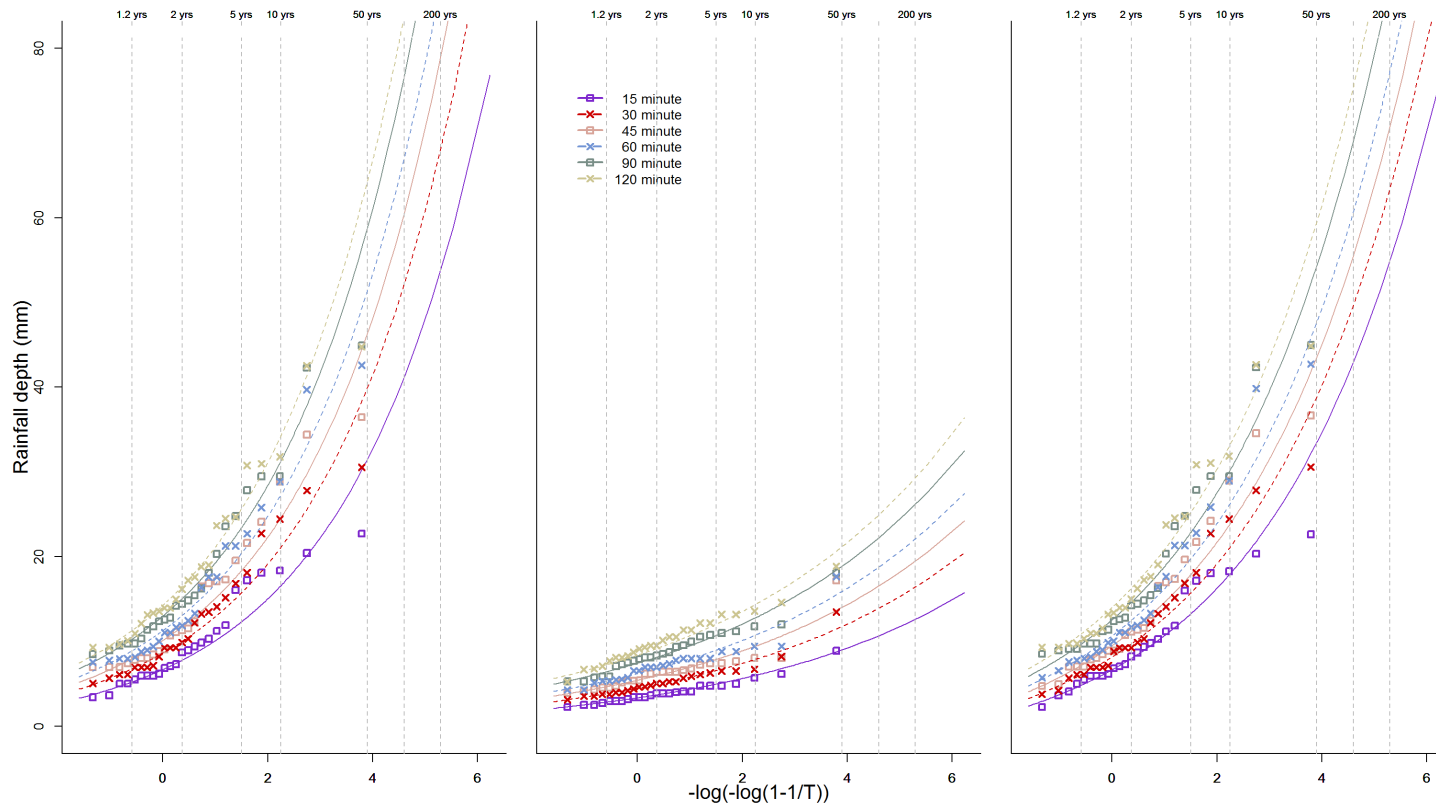
Figure 44 - Estimated frequency curves for the station at Putney Heath for the annual (left panel), winter (central panel) and summer (right panel) series, superimposed on the Gringorten plotting positions

The three graphs in Figure 44 plot the estimated frequency curves for the station at Putney Heath (shown by squares and crosses) superimposed on the Gringorten plotting positions (shown by lines) for different times periods (15, 30, 45, 60, 90 and 120 minutes) over a period of 200 years: left panel (annual series), central panel (winter series) and right panel (summer series). The x-axis on all panels shows log (natural logarithm, ln) from 0-6. The y-axis plots rainfall depth (0-80mm).
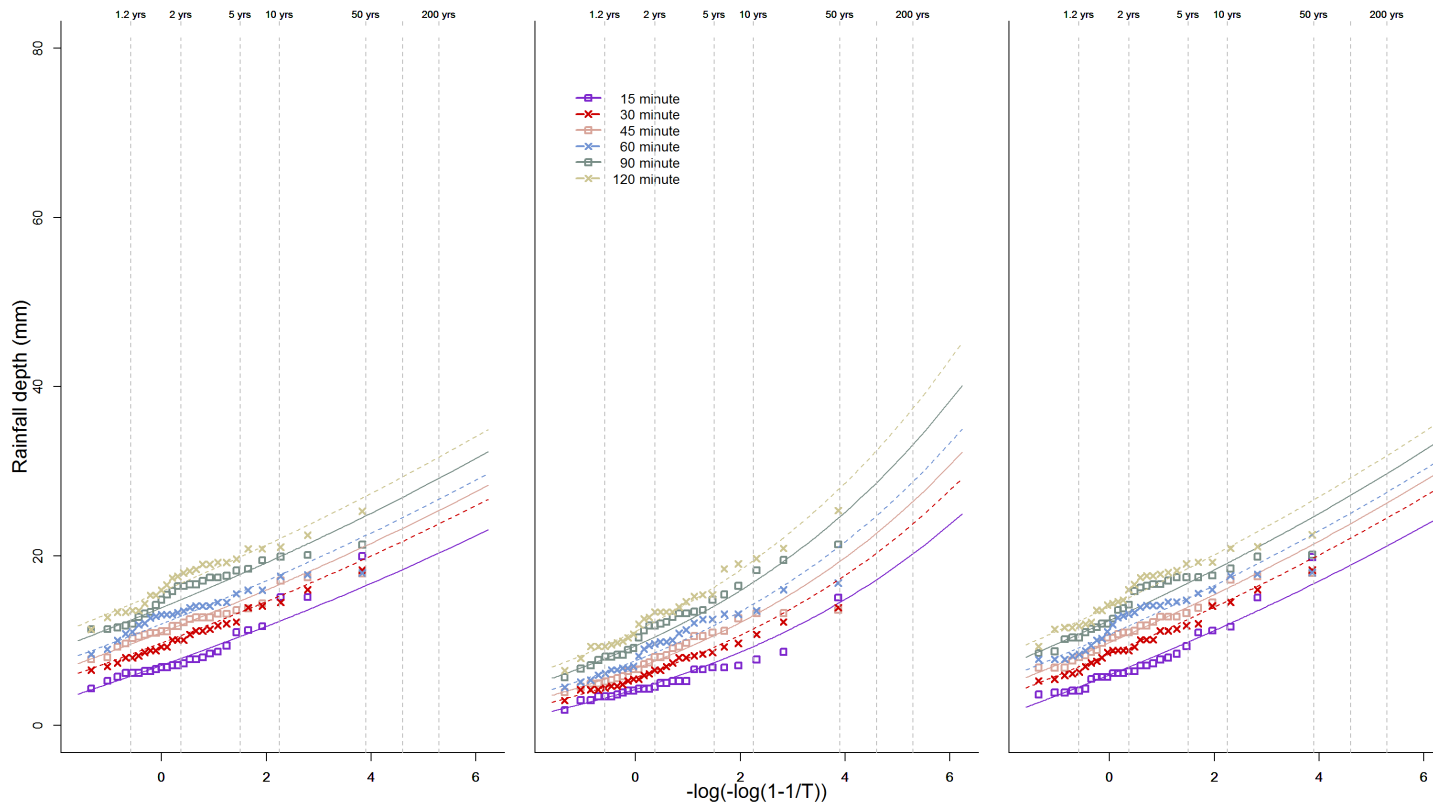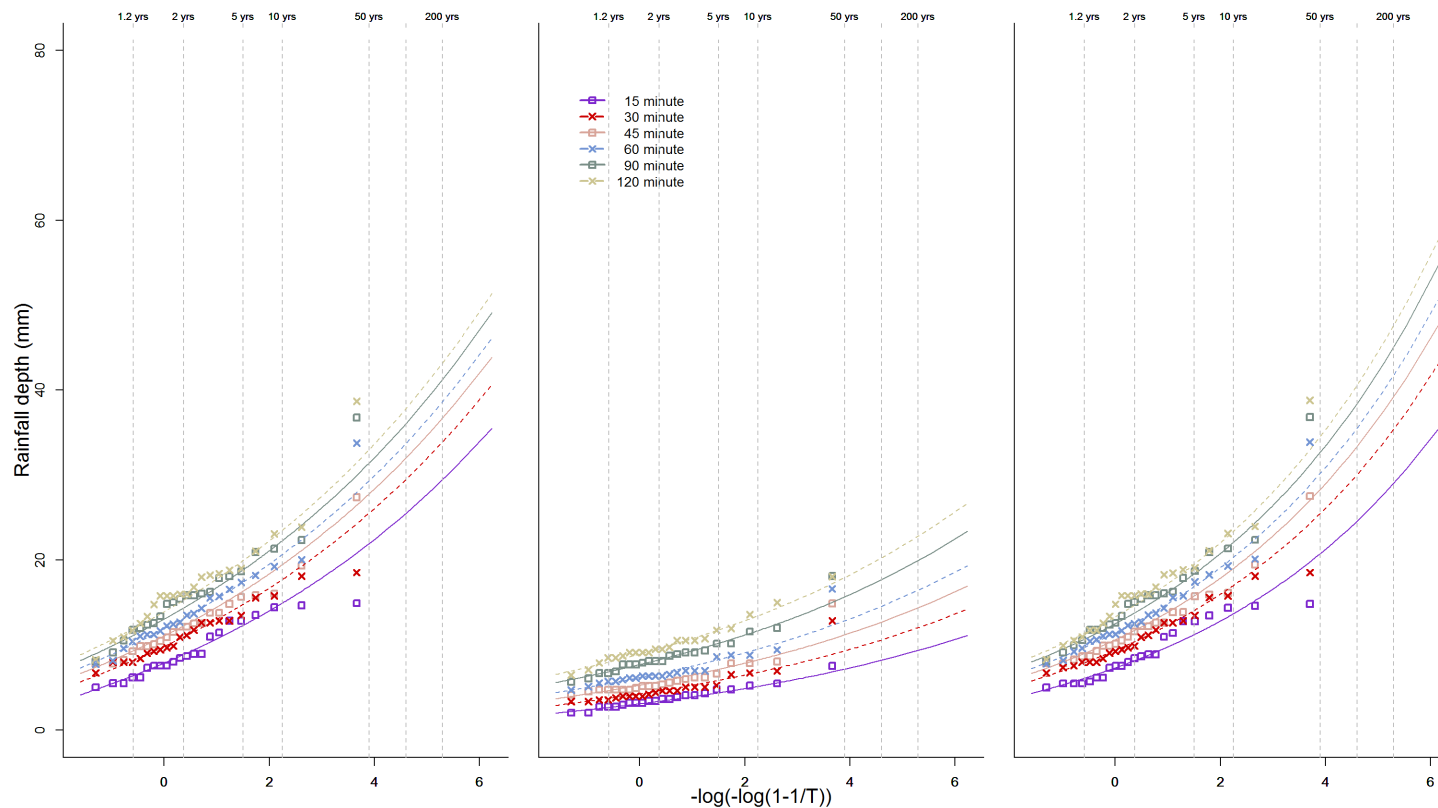
Figure 45 - Estimated frequency curves for the station at Stanford Rivers for the annual (left panel), winter (central panel) and summer (right panel) series, superimposed on the Gringorten plotting positions

The three graphs in Figure 45 plot the estimated frequency curves for the station at Standford Rivers (shown by squares and crosses) superimposed on the Gringorten plotting positions (shown by lines) for different times periods (15, 30, 45, 60, 90 and 120 minutes) over a period of 200 years: left panel (annual series), central panel (winter series) and right panel (summer series). The x-axis on all panels shows log (natural logarithm, ln) from 0-6. The y-axis plots rainfall depth (0-80mm).

A.3 Model comparisons for time of tip stations

Figure 46 - Comparison of frequency curves estimated by different methods at Llanychaer: FEH13 (left panel), FEH (central panel) and FSR (right panel)

The three graphs in Figure 46 plot the comparison of frequency curves at Llanychaer for different methods (FEH13 on the left panel, FEH on the central panel and FSR on the right panel) and time periods (1, 2, 5, 10, 15, 30, 45, 60, 90 and 120 minutes). The x-axis on all panels shows log (natural logarithm, ln) from 0-4. The y-axis plots rainfall depth (0-70mm).

**Figure 47 - Comparison of frequency curves estimated by different methods at Victoria Park: FEH13 (left panel), FEH (central panel) and FSR (right panel)**

The three graphs in Figure 47 plot the comparison of frequency curves at Victoria Park for different methods (FEH13 on the left panel, FEH on the central panel and FSR on the right panel) and time periods (1, 2, 5, 10, 15, 30, 45, 60, 90 and 120 minutes). The x-axis on all panels shows log (natural logarithm, ln) from 0-4. The y-axis plots rainfall depth (0-70mm).

Figure 48 - Comparison of frequency curves estimated by different methods at Colwyn Bay: FEH13 (left panel), FEH (central panel) and FSR (right panel)

The three graphs in Figure 48 plot the comparison of frequency curves at Colwyn Bay for different methods (FEH13 on the left panel, FEH on the central panel and FSR on the right panel) and time periods (1, 2, 5, 10, 15, 30, 45, 60, 90 and 120 minutes). The x-axis on all panels shows log (natural logarithm, ln) from 0-4. The y-axis plots rainfall depth (0-70mm).

Figure 49 - Comparison of frequency curves estimated by different methods at Bettws-y-Crwyn: FEH13 (left panel), FEH (central panel) and FSR (right panel)

The three graphs in Figure 49 plot the comparison of frequency curves at Bettws-y-Crwyn for different methods (FEH13 on the left panel, FEH on the central panel and FSR on the right panel) and time periods (1, 2, 5, 10, 15, 30, 45, 60, 90 and 120 minutes). The x-axis on all panels shows log (natural logarithm, ln) from 0-4. The y-axis plots rainfall depth (0-70mm).

Figure 50 - Comparison of frequency curves estimated by different methods at Stone: FEH13 (left panel), FEH (central panel) and FSR (right panel)

The three graphs in Figure 50 plot the comparison of frequency curves at Stone for different methods (FEH13 on the left panel, FEH on the central panel and FSR on the right panel) and time periods (1, 2, 5, 10, 15, 30, 45, 60, 90 and 120 minutes). The x-axis on all panels shows log (natural logarithm, ln) from 0-4. The y-axis plots rainfall depth (0-70mm).

**Figure 51 - Comparison of frequency curves estimated by different methods at Dowdeswell: FEH13 (left panel), FEH (central panel) and FSR (right panel)**

The three graphs in Figure 51 plot the comparison of frequency curves at Dowdeswell for different methods (FEH13 on the left panel, FEH on the central panel and FSR on the right panel) and time periods (1, 2, 5, 10, 15, 30, 45, 60, 90 and 120 minutes). The x-axis on all panels shows log (natural logarithm, ln) from 0-4. The y-axis plots rainfall depth (0-70mm).
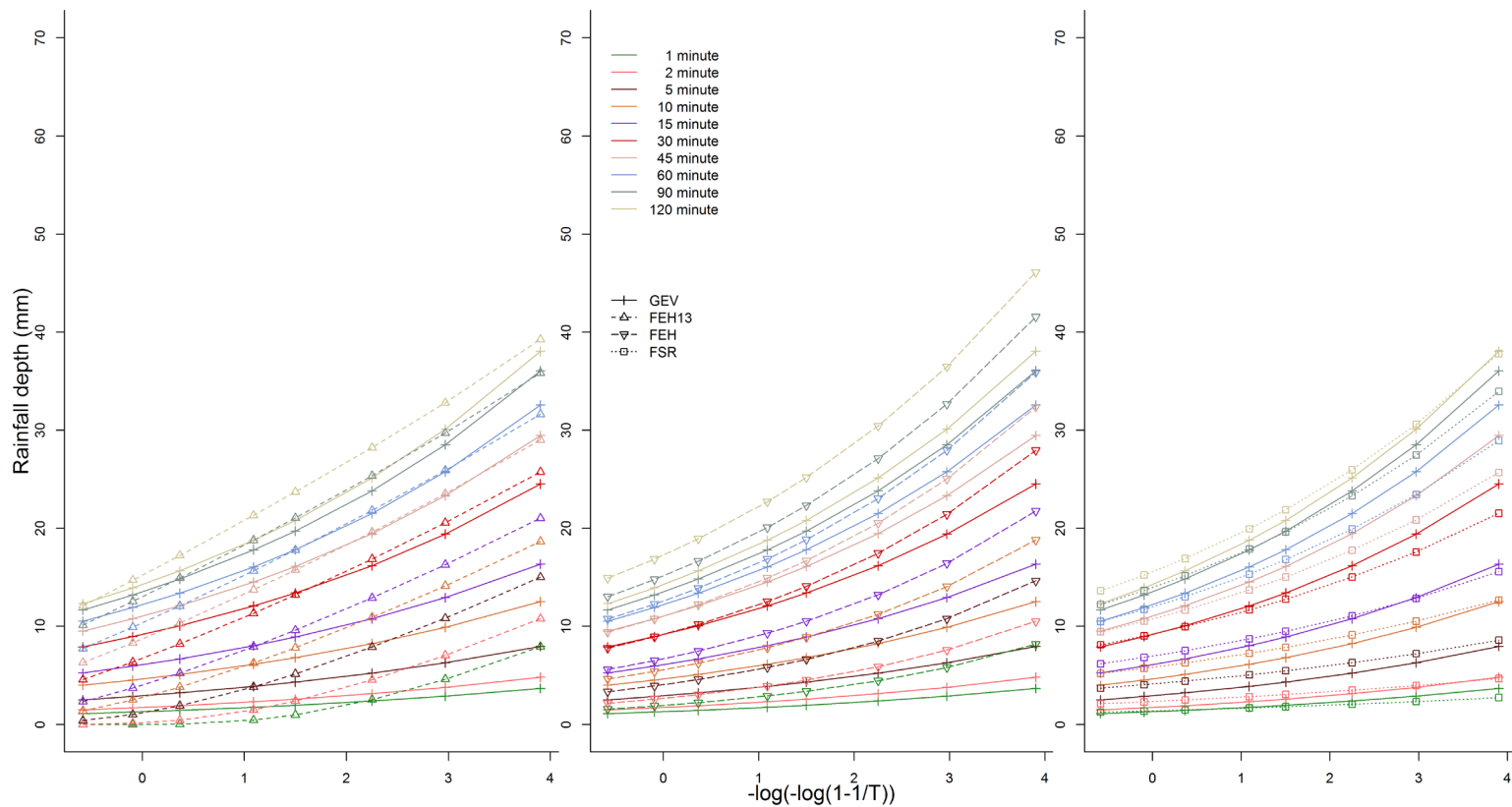
Figure 52 - Comparison of frequency curves estimated by different methods at Knightcote: FEH13 (left panel), FEH (central panel) and FSR (right panel)

The three graphs in Figure 52 plot the comparison of frequency curves at Knightcote for different methods (FEH13 on the left panel, FEH on the central panel and FSR on the right panel) and time periods (1, 2, 5, 10, 15, 30, 45, 60, 90 and 120 minutes). The x-axis on all panels shows log (natural logarithm, ln) from 0-4. The y-axis plots rainfall depth (0-70mm).
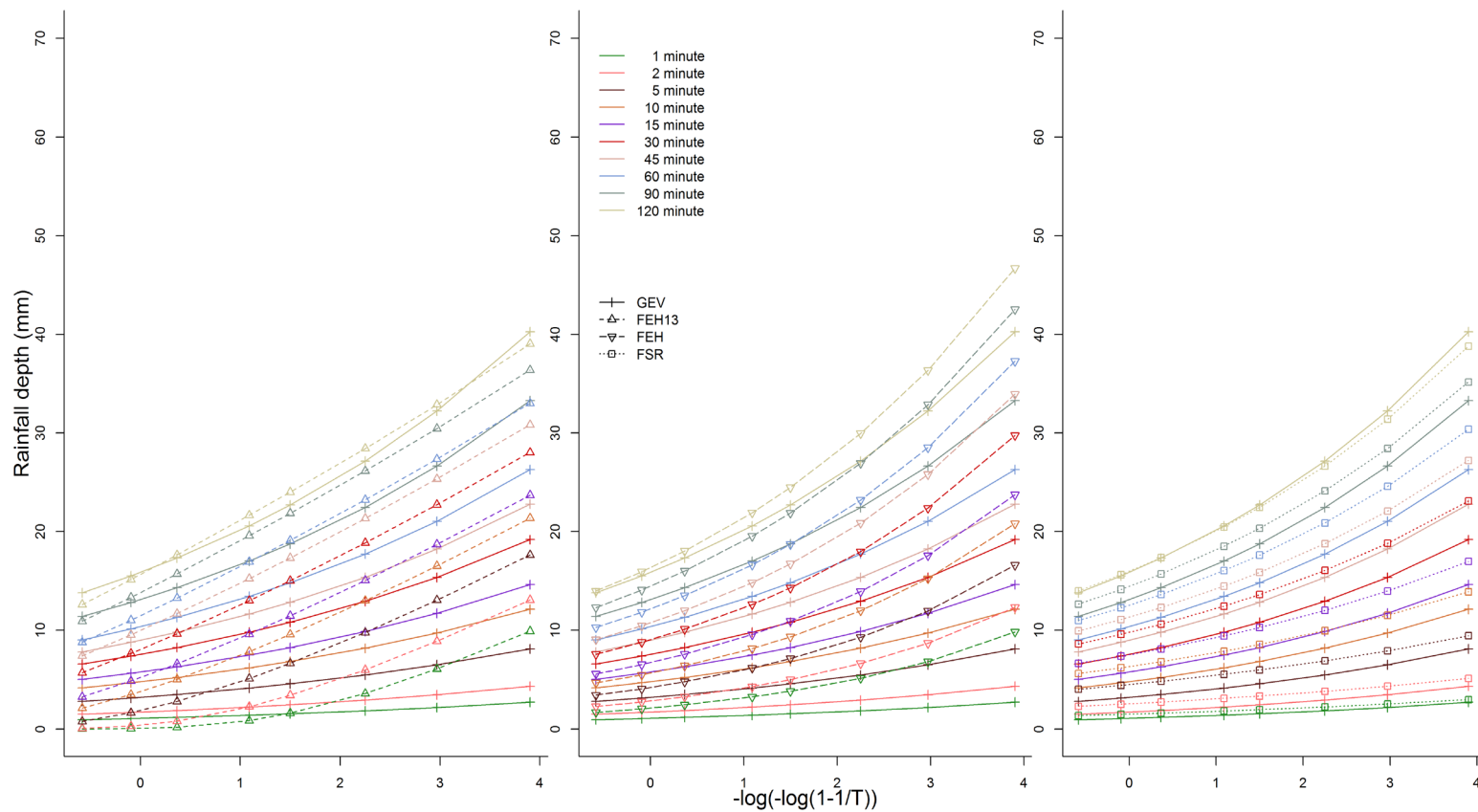
Figure 53 - Comparison of frequency curves estimated by different methods at Hinckley: FEH13 (left panel), FEH (central panel) and FSR (right panel)

The three graphs in Figure 53 plot the comparison of frequency curves at Hinckley for different methods (FEH13 on the left panel, FEH on the central panel and FSR on the right panel) and time periods (1, 2, 5, 10, 15, 30, 45, 60, 90 and 120 minutes). The x-axis on all panels shows log (natural logarithm, ln) from 0-4. The y-axis plots rainfall depth (0-70mm).

Figure 54 - Comparison of frequency curves estimated by different methods at Lower Dunsforth: FEH13 (left panel), FEH (central panel) and FSR (right panel)

The three graphs in Figure 54 plot the comparison of frequency curves at Lower Dunsforth for different methods (FEH13 on the left panel, FEH on the central panel and FSR on the right panel) and time periods (1, 2, 5, 10, 15, 30, 45, 60, 90 and 120 minutes). The x-axis on all panels shows log (natural logarithm, ln) from 0-4. The y-axis plots rainfall depth (0-70mm).
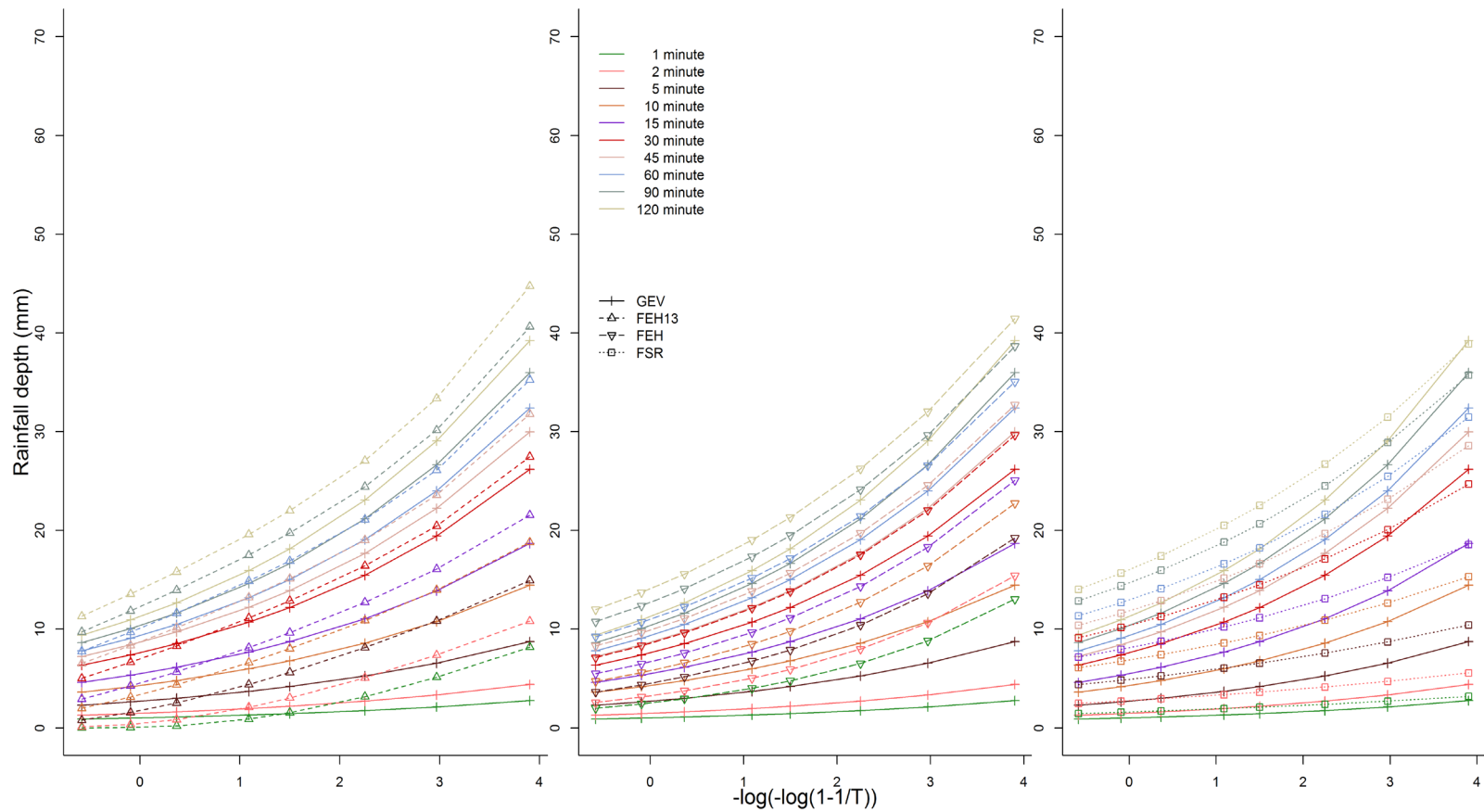
A.4 Model comparisons for 15-minute stations

Figure 55 - Comparison of frequency curves estimated by different methods at Taw Head: FEH13 (left panel), FEH (central panel) and FSR (right panel)

The three graphs in Figure 55 plot the comparison of frequency curves at Taw Head for different methods (FEH13 on the left panel, FEH on the central panel and FSR on the right panel) and time periods (15, 30, 45, 60, 90 and 120 minutes). The x-axis on all panels shows log (natural logarithm, ln) from 0-4. The y-axis plots rainfall depth (0-70mm).
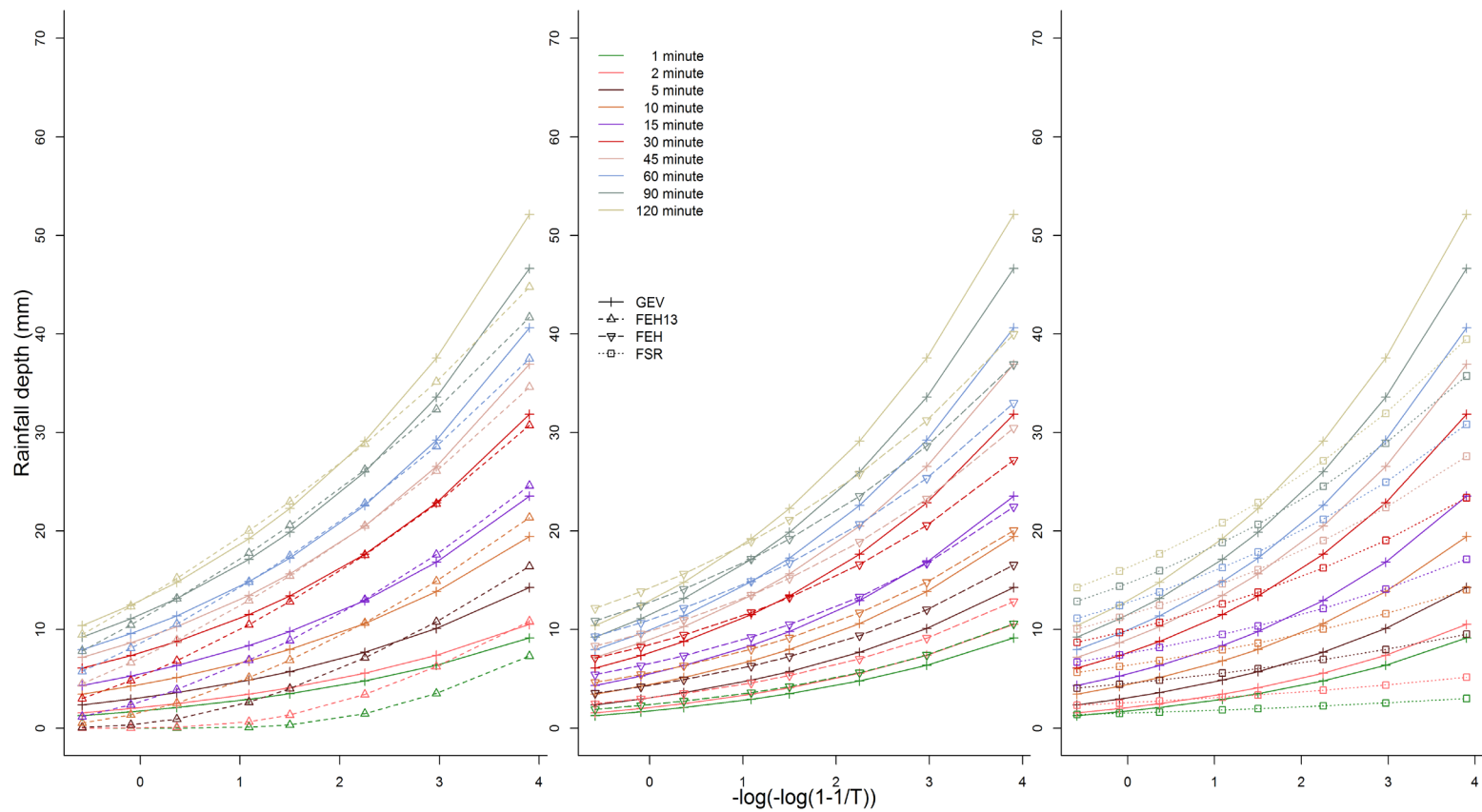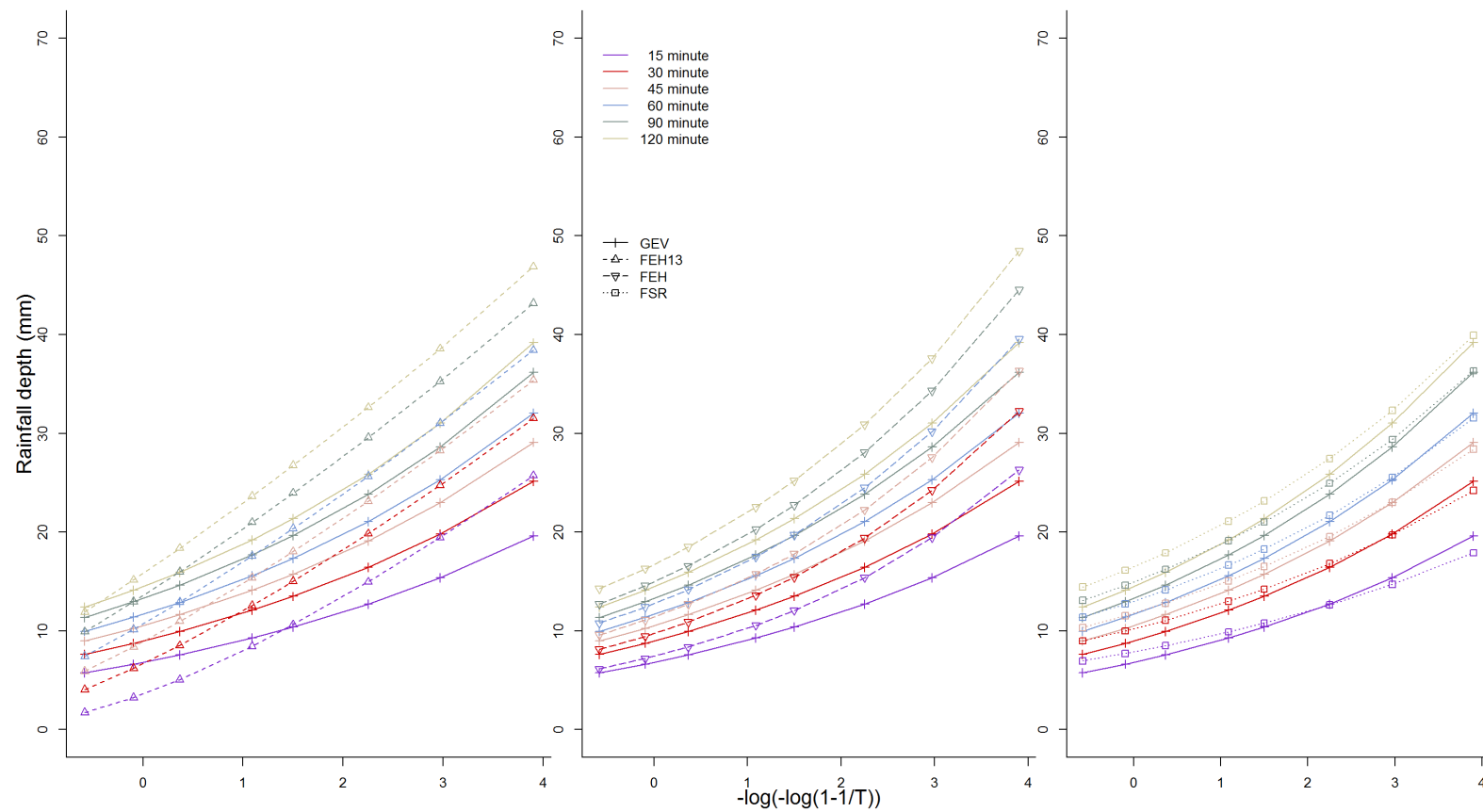
Figure 56 - Comparison of frequency curves estimated by different methods at Hemyock: FEH13 (left panel), FEH (central panel) and FSR (right panel)

The three graphs in Figure 56 plot the comparison of frequency curves at Hemyock for different methods (FEH13 on the left panel, FEH on the central panel and FSR on the right panel) and time periods (15, 30, 45, 60, 90 and 120 minutes). The x-axis on all panels shows log (natural logarithm, ln) from 0-4. The y-axis plots rainfall depth (0-70mm).
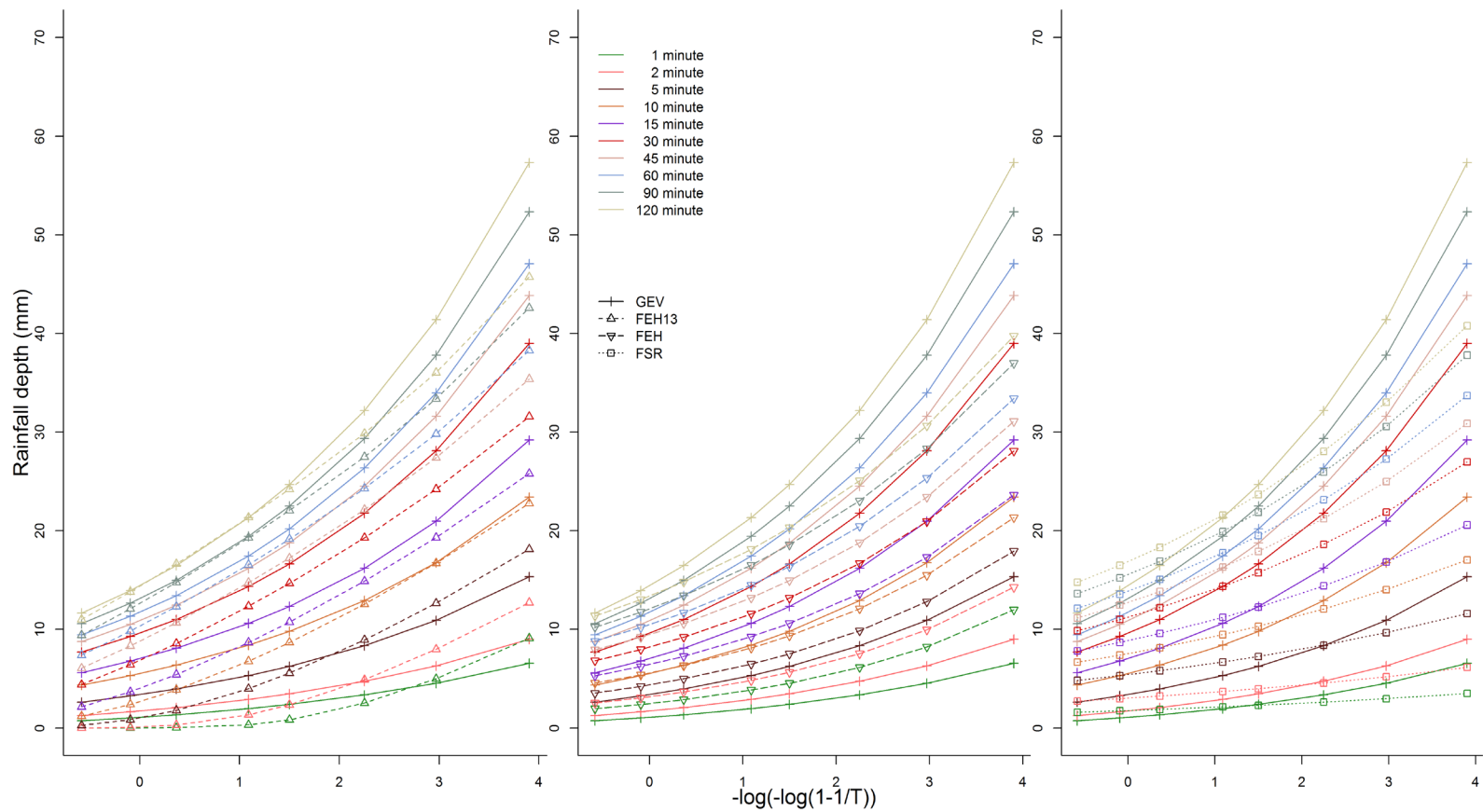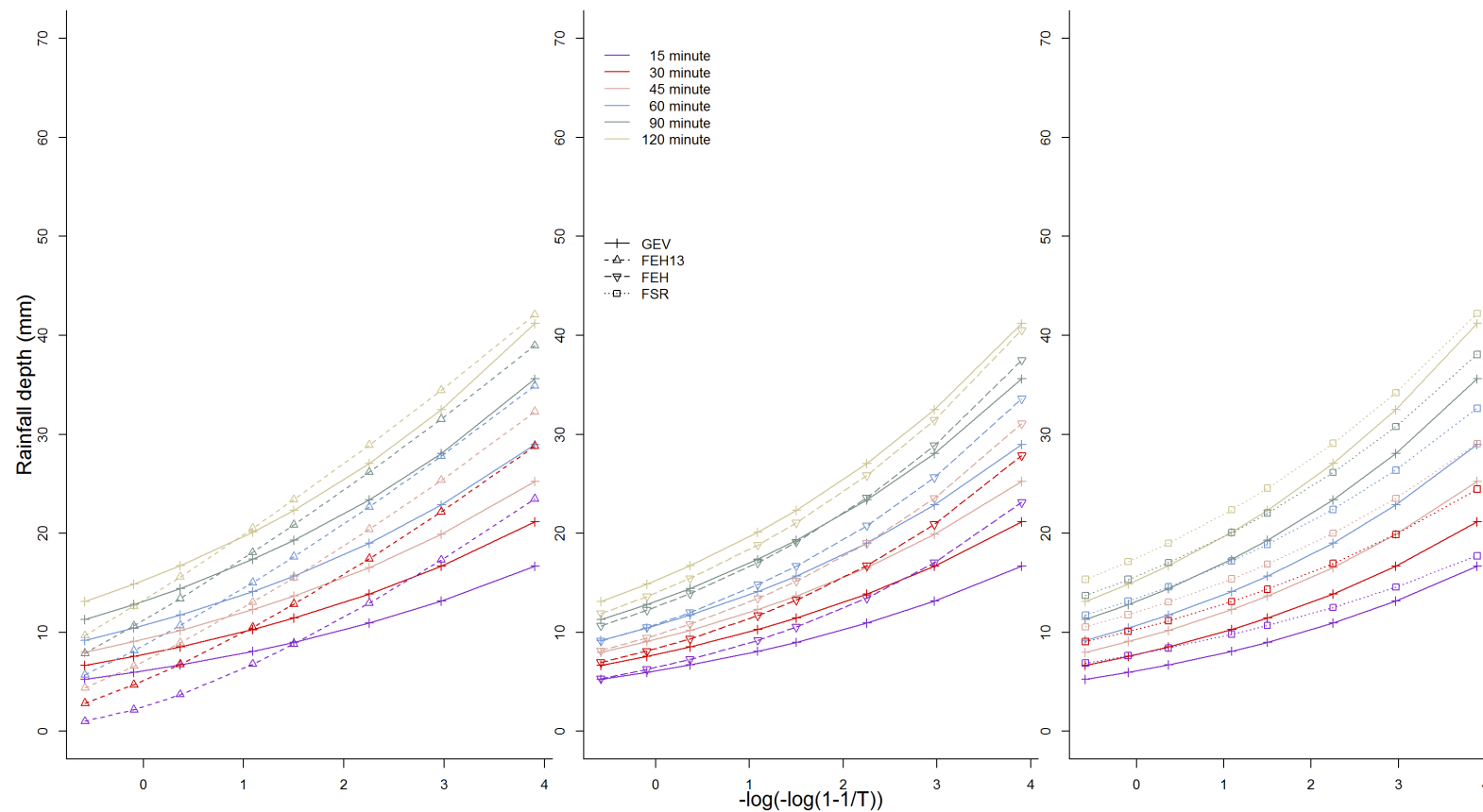
Figure 57 - Comparison of frequency curves estimated by different methods at Crew Fell: FEH13 (left panel), FEH (central panel) and FSR (right panel)

The three graphs in Figure 57 plot the comparison of frequency curves at Crew Fell for different methods (FEH13 on the left panel, FEH on the central panel and FSR on the right panel) and time periods (15, 30, 45, 60, 90 and 120 minutes). The x-axis on all panels shows log (natural logarithm, ln) from 0-4. The y-axis plots rainfall depth (0-70mm).
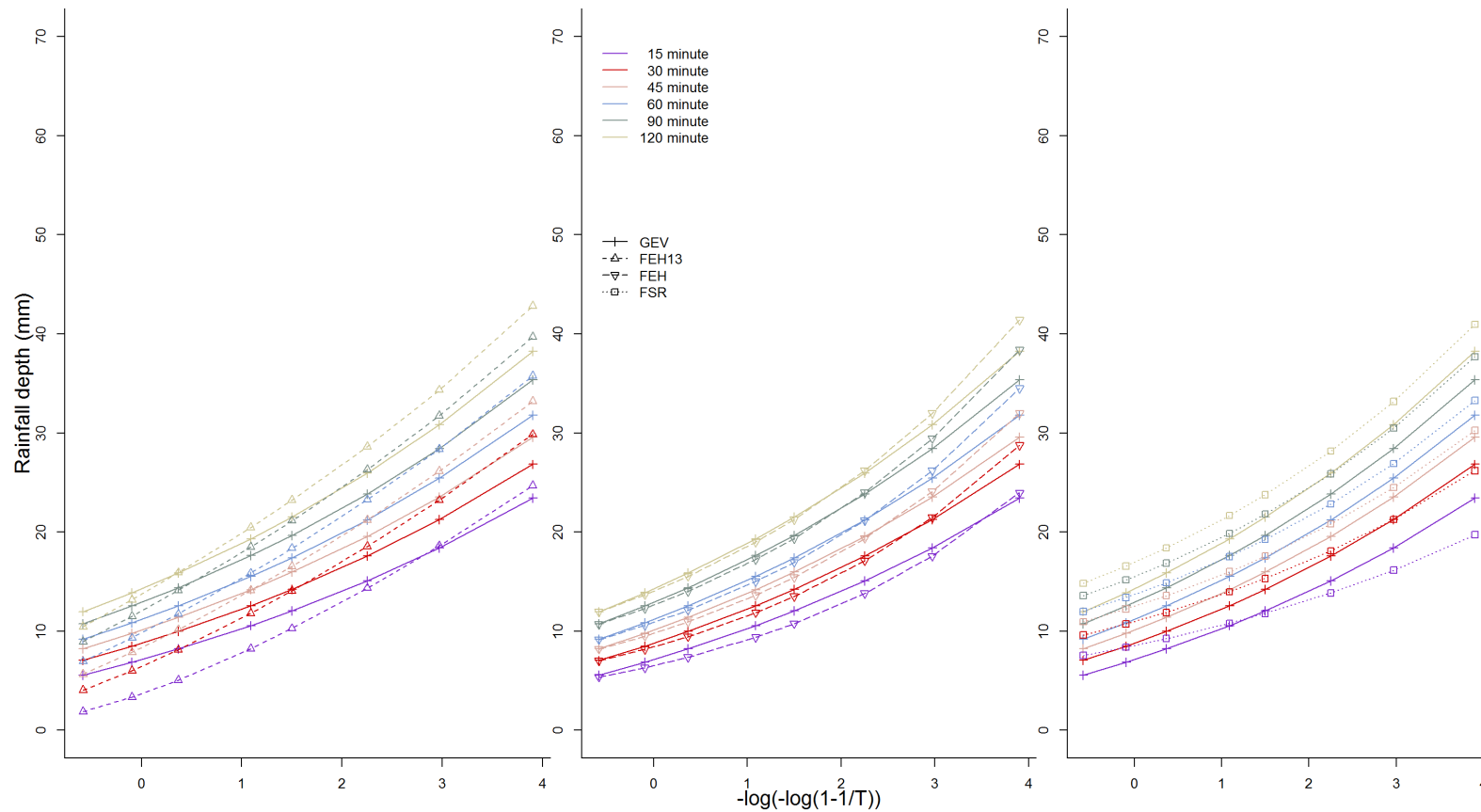
Figure 58 - Comparison of frequency curves estimated by different methods at Kingswood: FEH13 (left panel), FEH (central panel) and FSR (right panel)

The three graphs in Figure 58 plot the comparison of frequency curves at Kingswood for different methods (FEH13 on the left panel, FEH on the central panel and FSR on the right panel) and time periods (15, 30, 45, 60, 90 and 120 minutes). The x-axis on all panels shows log (natural logarithm, ln) from 0-4. The y-axis plots rainfall depth (0-70mm).
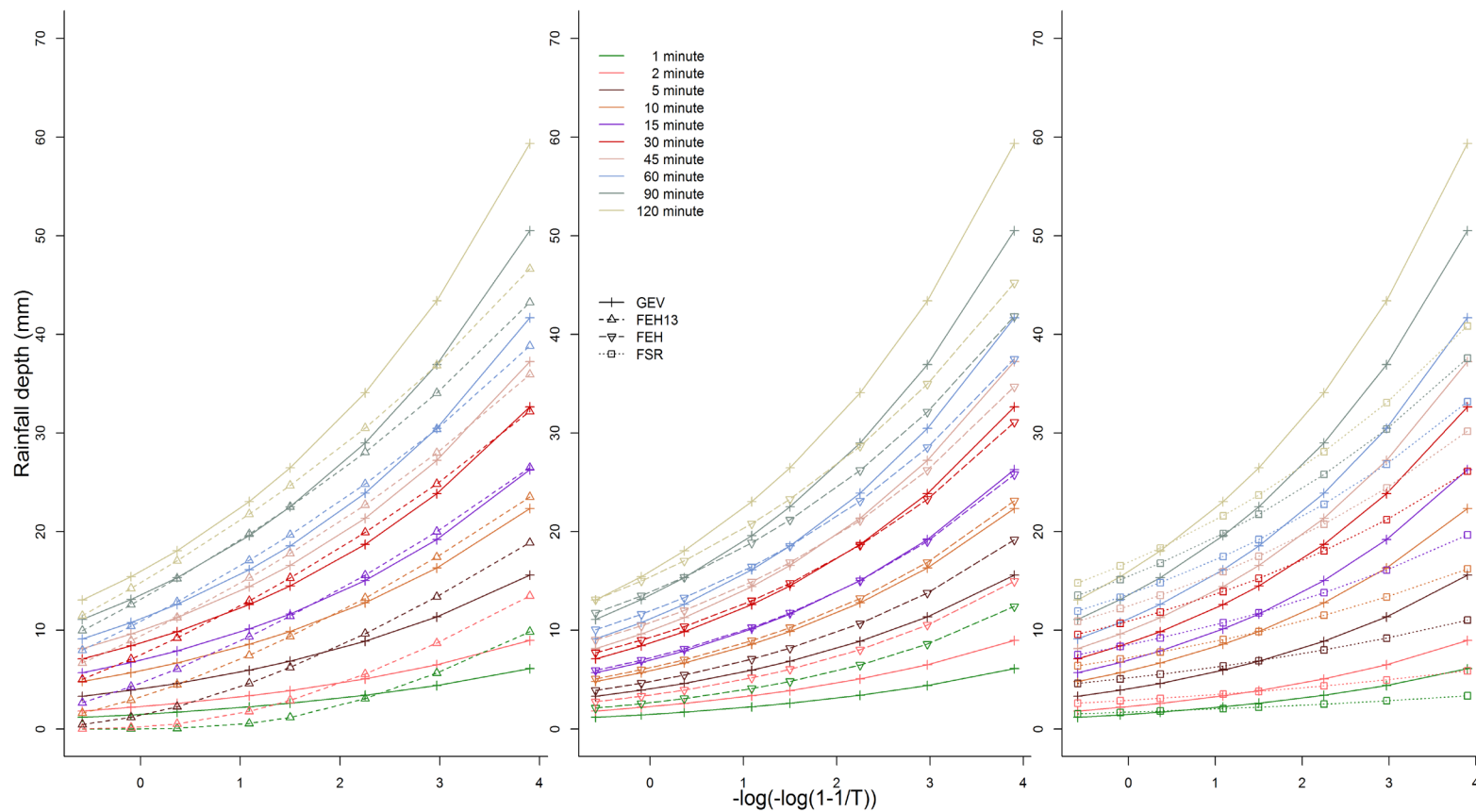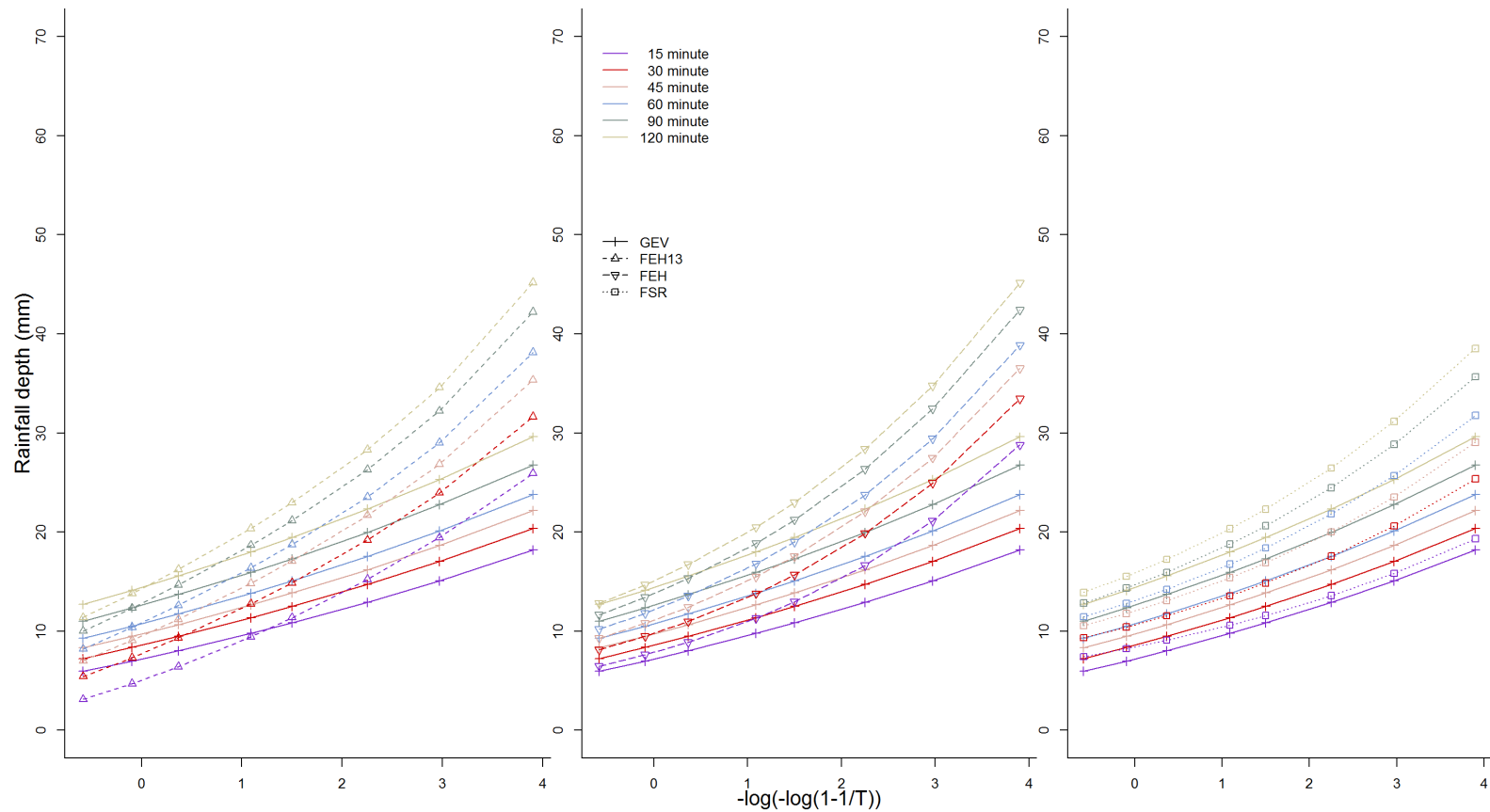
Figure 59 - Comparison of frequency curves estimated by different methods at Sale Carrington: FEH13 (left panel), FEH (central panel) and FSR (right panel)

The three graphs in Figure 59 plot the comparison of frequency curves at Sale Carrington for different methods (FEH13 on the left panel, FEH on the central panel and FSR on the right panel) and time periods (15, 30, 45, 60, 90 and 120 minutes). The x-axis on all panels shows log (natural logarithm, ln) from 0-4. The y-axis plots rainfall depth (0-70mm).
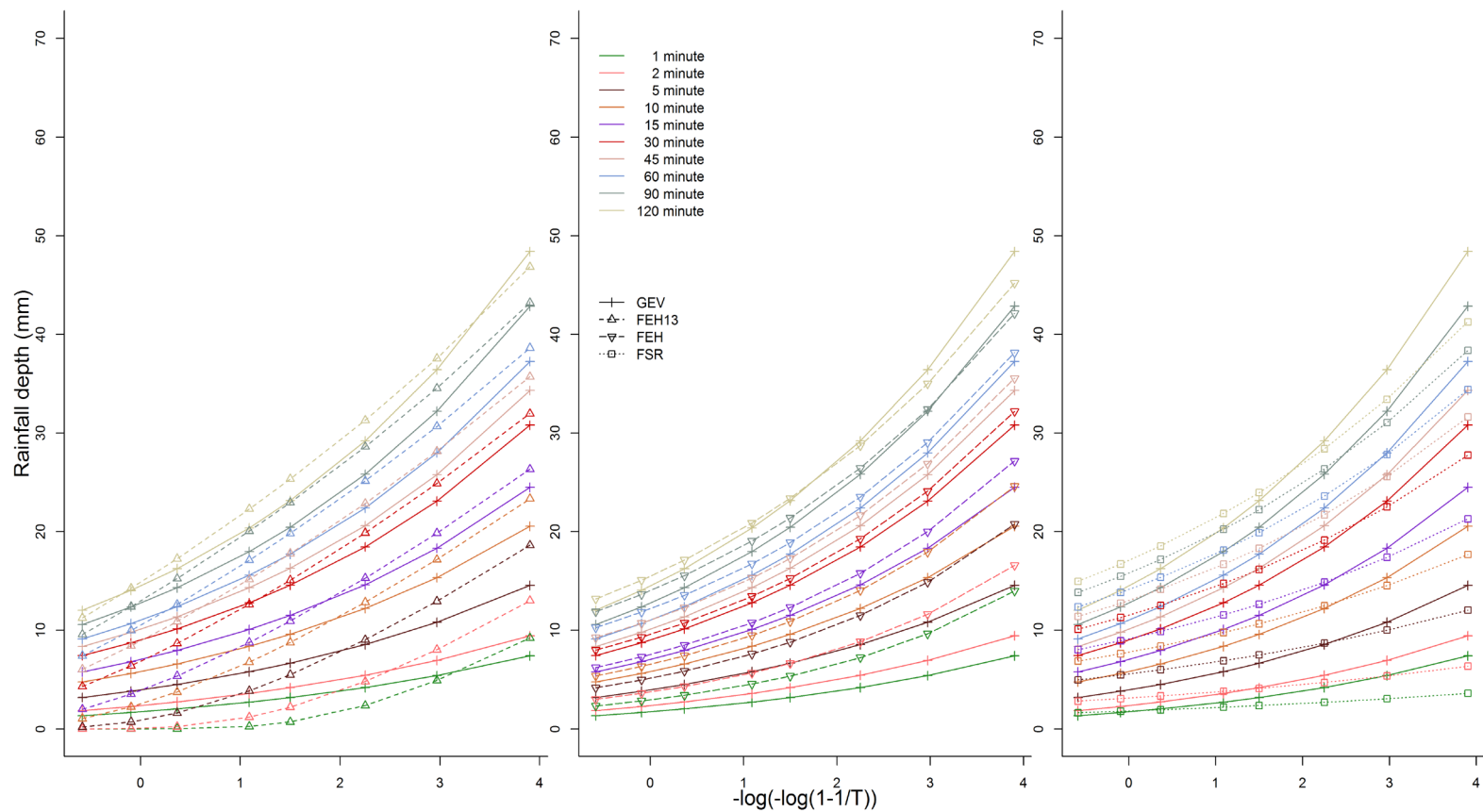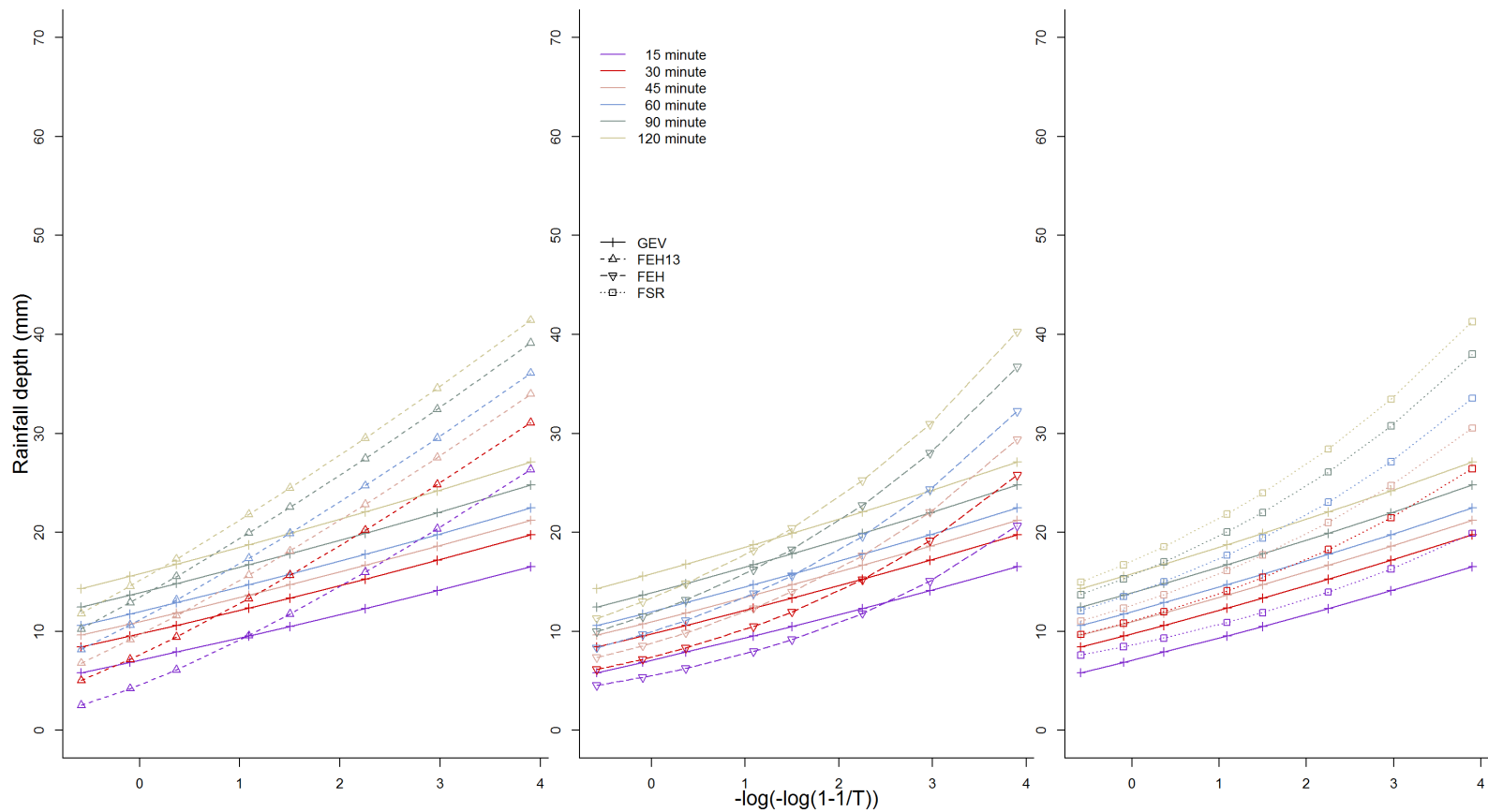
Figure 60 - Comparison of frequency curves estimated by different methods at Otterbourne: FEH13 (left panel), FEH (central panel) and FSR (right panel)

The three graphs in Figure 60 plot the comparison of frequency curves at Otterbourne for different methods (FEH13 on the left panel, FEH on the central panel and FSR on the right panel) and time periods (15, 30, 45, 60, 90 and 120 minutes). The x-axis on all panels shows log (natural logarithm, ln) from 0-4. The y-axis plots rainfall depth (0-70mm).
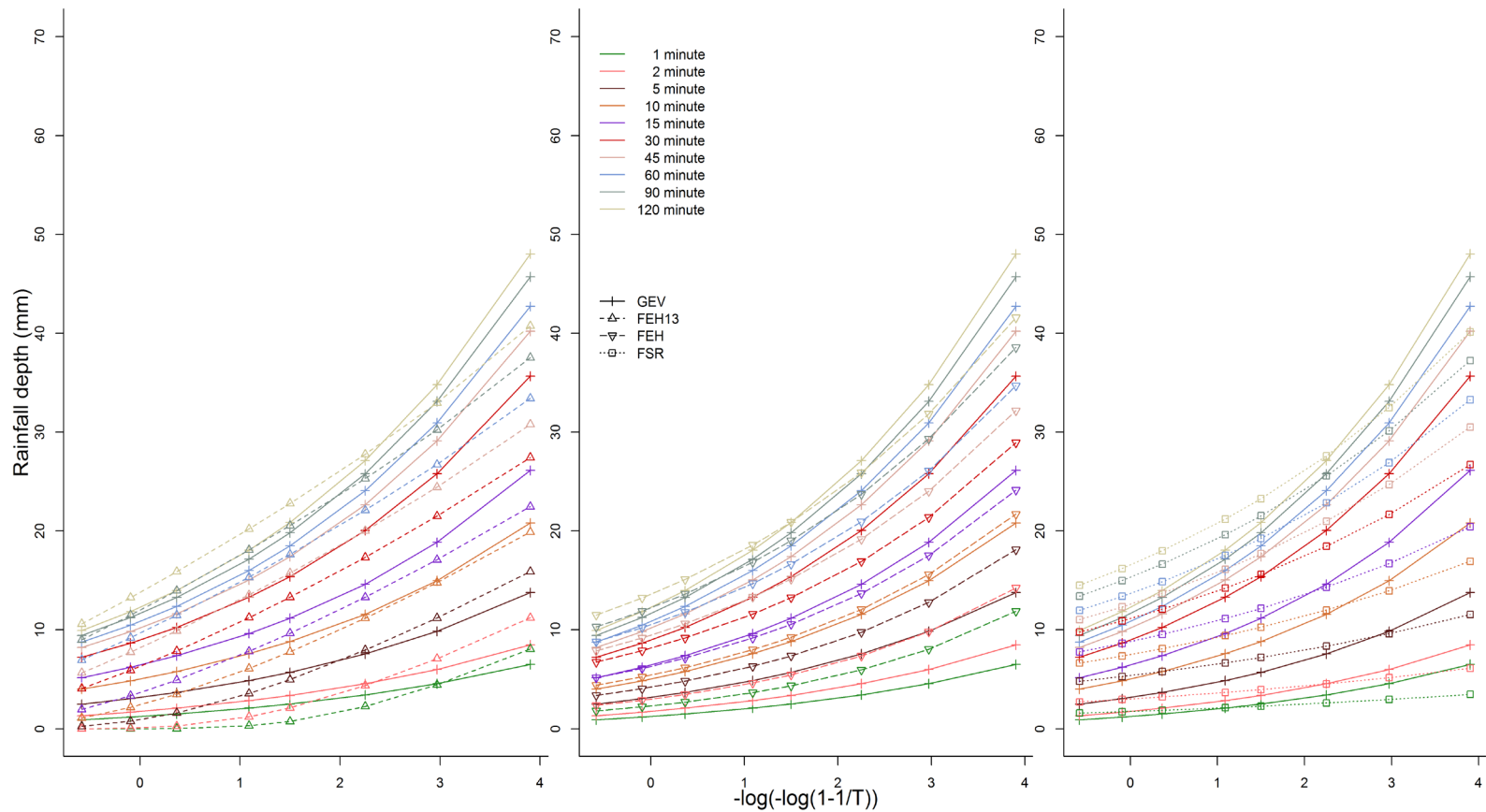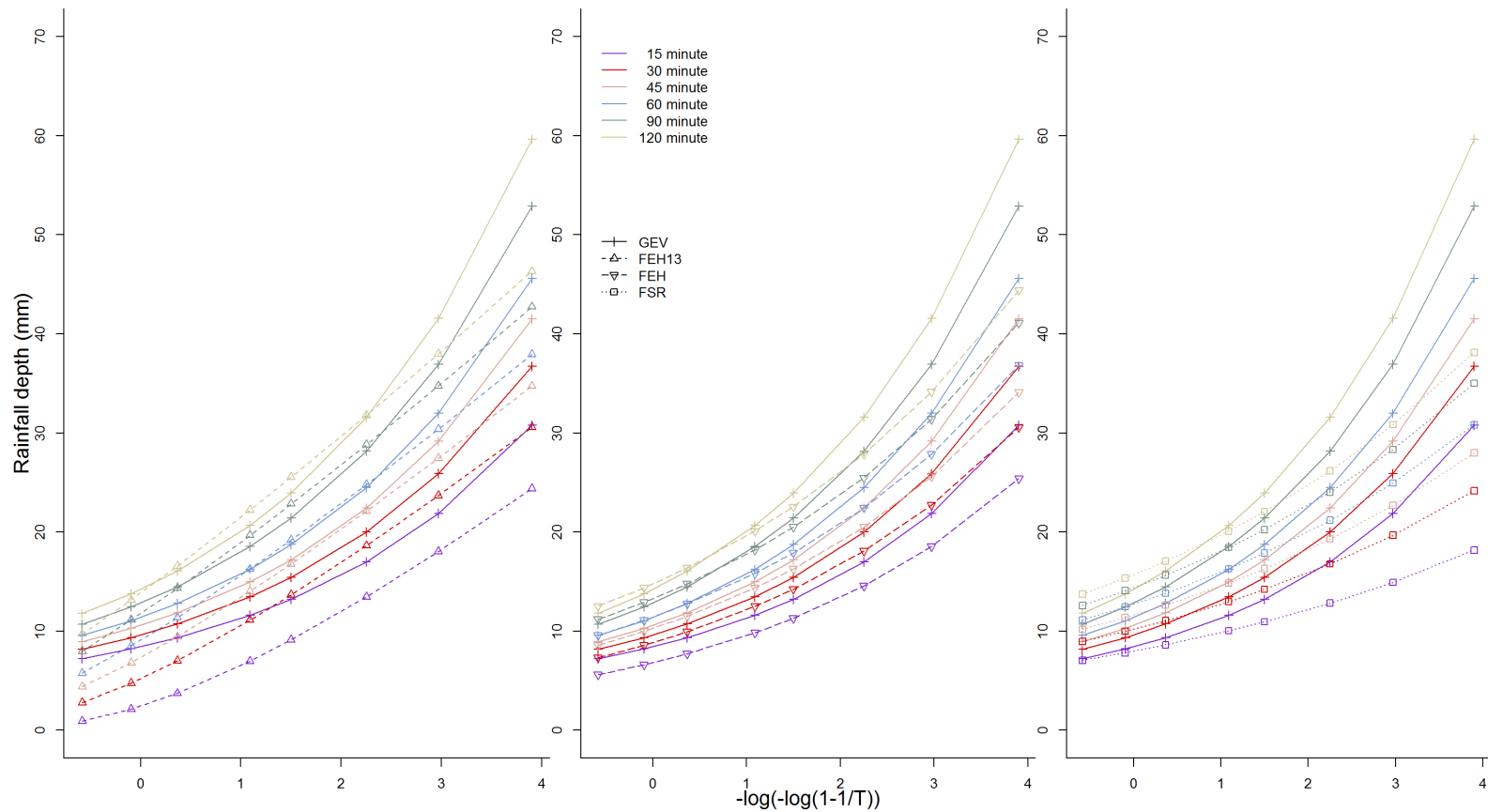
Figure 61 - Comparison of frequency curves estimated by different methods at Chieveley: FEH13 (left panel), FEH (central panel) and FSR (right panel)

The three graphs in Figure 61 plot the comparison of frequency curves at Chieveley for different methods (FEH13 on the left panel, FEH on the central panel and FSR on the right panel) and time periods (15, 30, 45, 60, 90 and 120 minutes). The x-axis on all panels shows log (natural logarithm, ln) from 0-4. The y-axis plots rainfall depth (0-70mm).
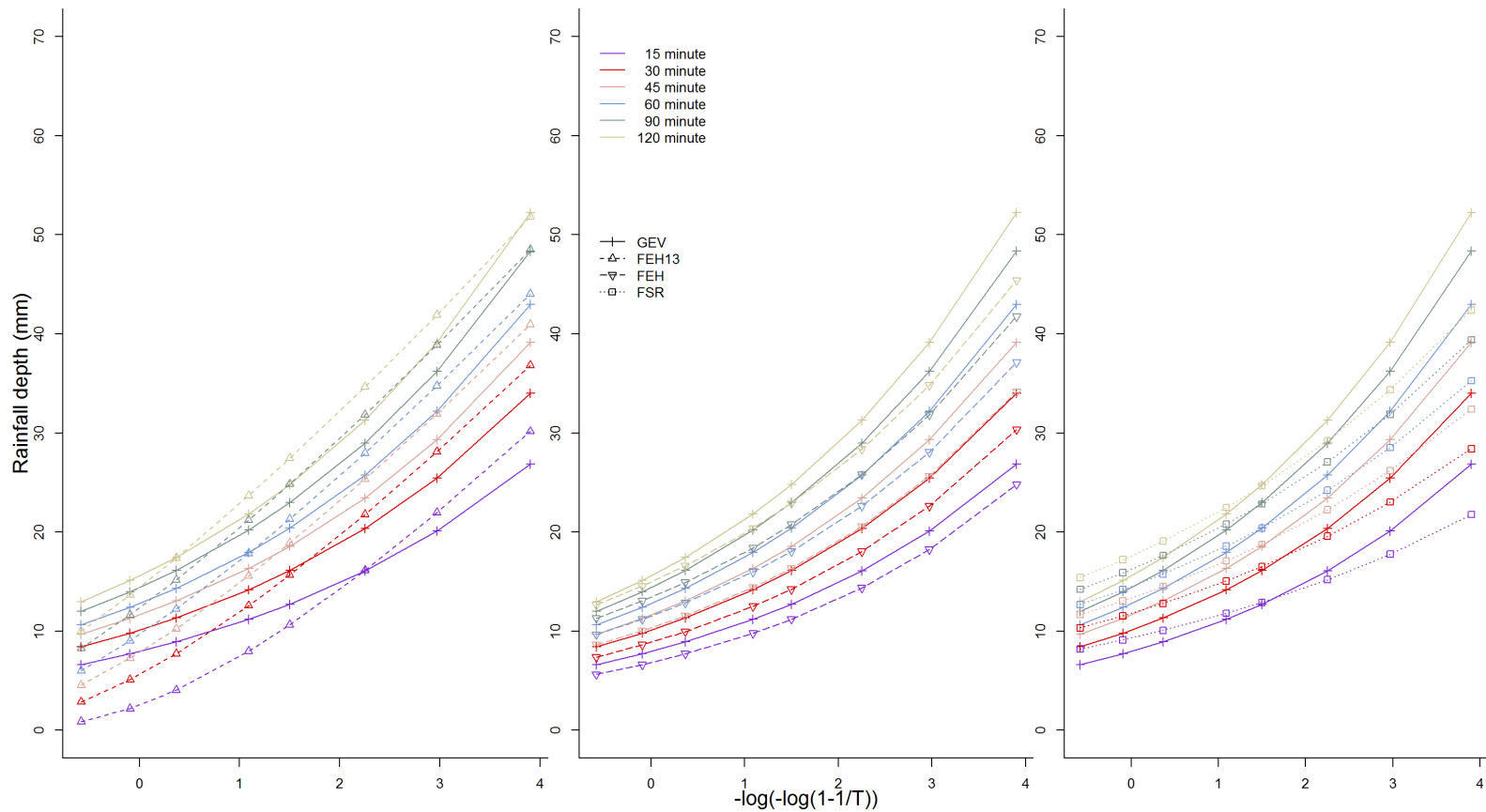
Figure 62 - Comparison of frequency curves estimated by different methods at Ludford: FEH13 (left panel), FEH (central panel) and FSR (right panel)

The three graphs in Figure 62 plot the comparison of frequency curves at Ludford for different methods (FEH13 on the left panel, FEH on the central panel and FSR on the right panel) and time periods (15, 30, 45, 60, 90 and 120 minutes). The x-axis on all panels shows log (natural logarithm, ln) from 0-4. The y-axis plots rainfall depth (0-70mm).
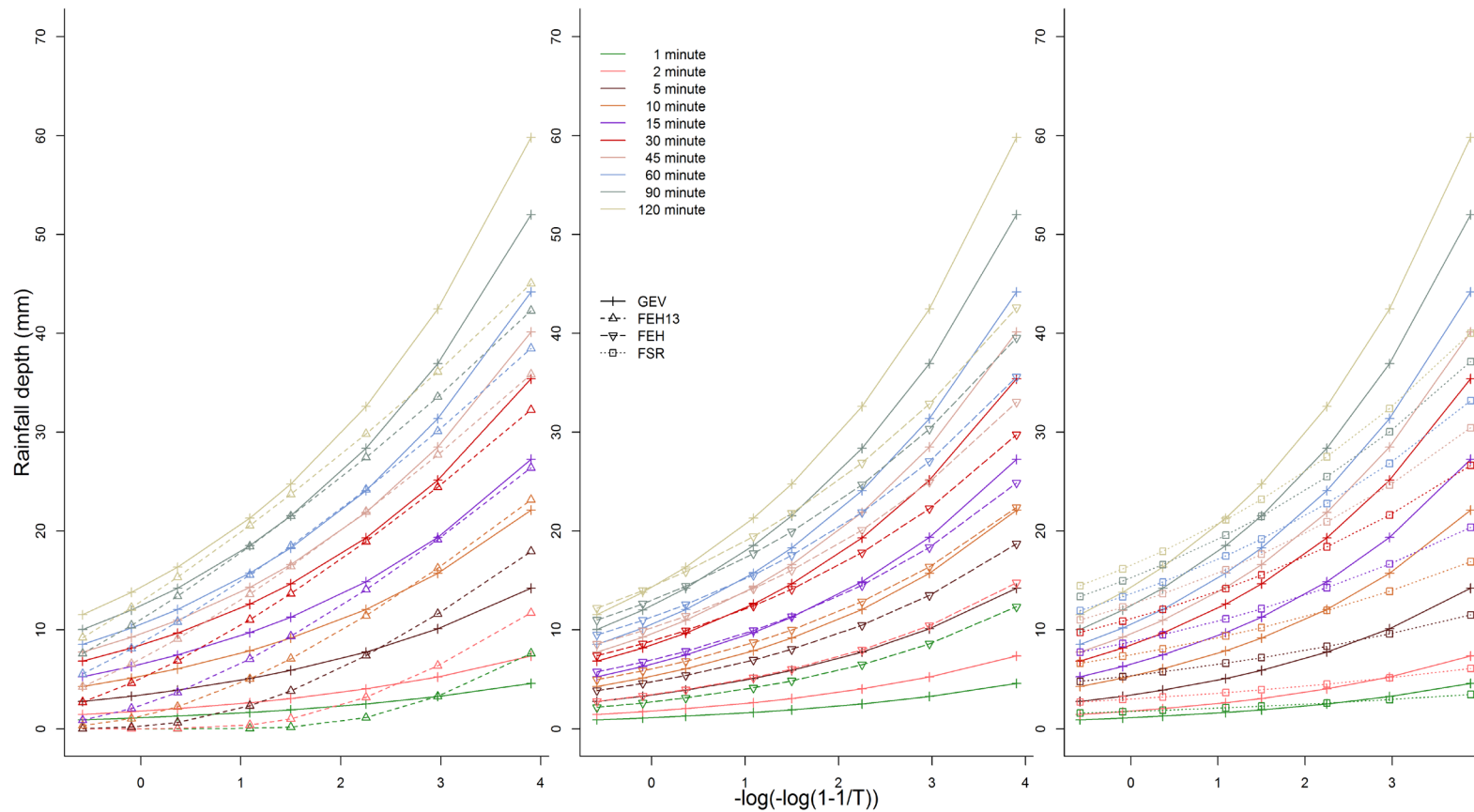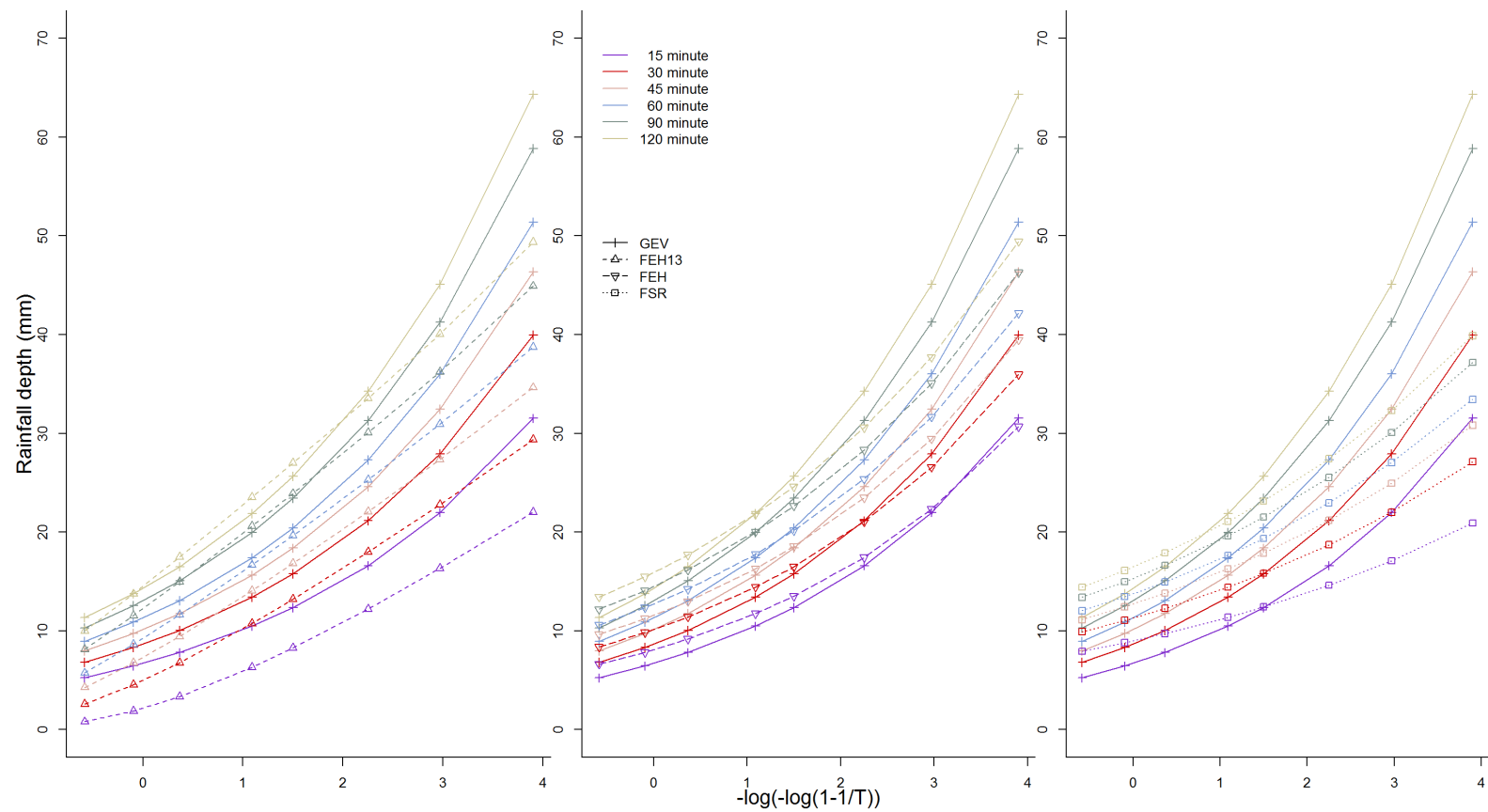
Figure 63 - Comparison of frequency curves estimated by different methods at Putney Heath: FEH13 (left panel), FEH (central panel) and FSR (right panel)

The three graphs in Figure 63 plot the comparison of frequency curves at Putney Heath for different methods (FEH13 on the left panel, FEH on the central panel and FSR on the right panel) and time periods (15, 30, 45, 60, 90 and 120 minutes). The x-axis on all panels shows log (natural logarithm, ln) from 0-4. The y-axis plots rainfall depth (0-70mm).
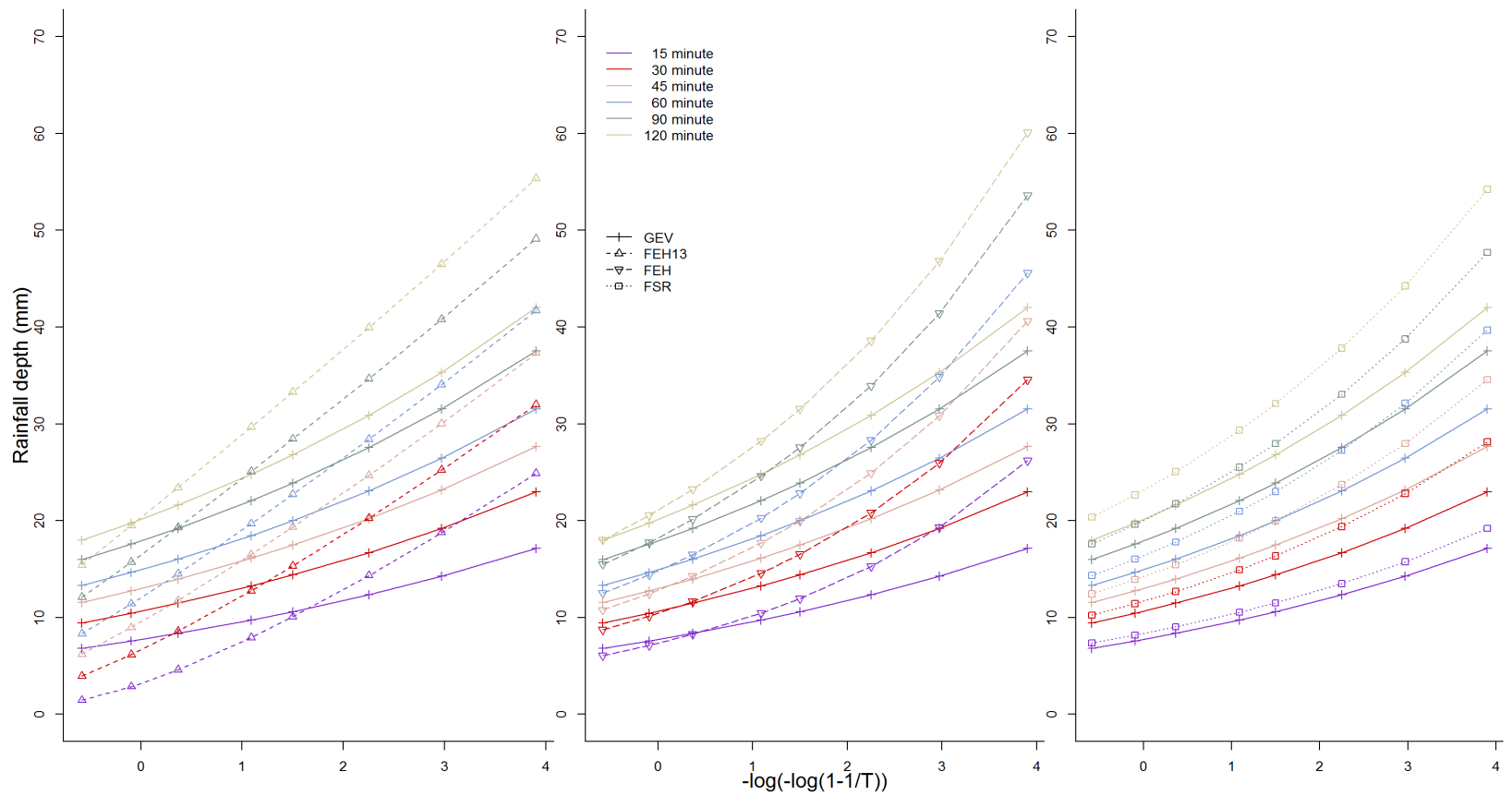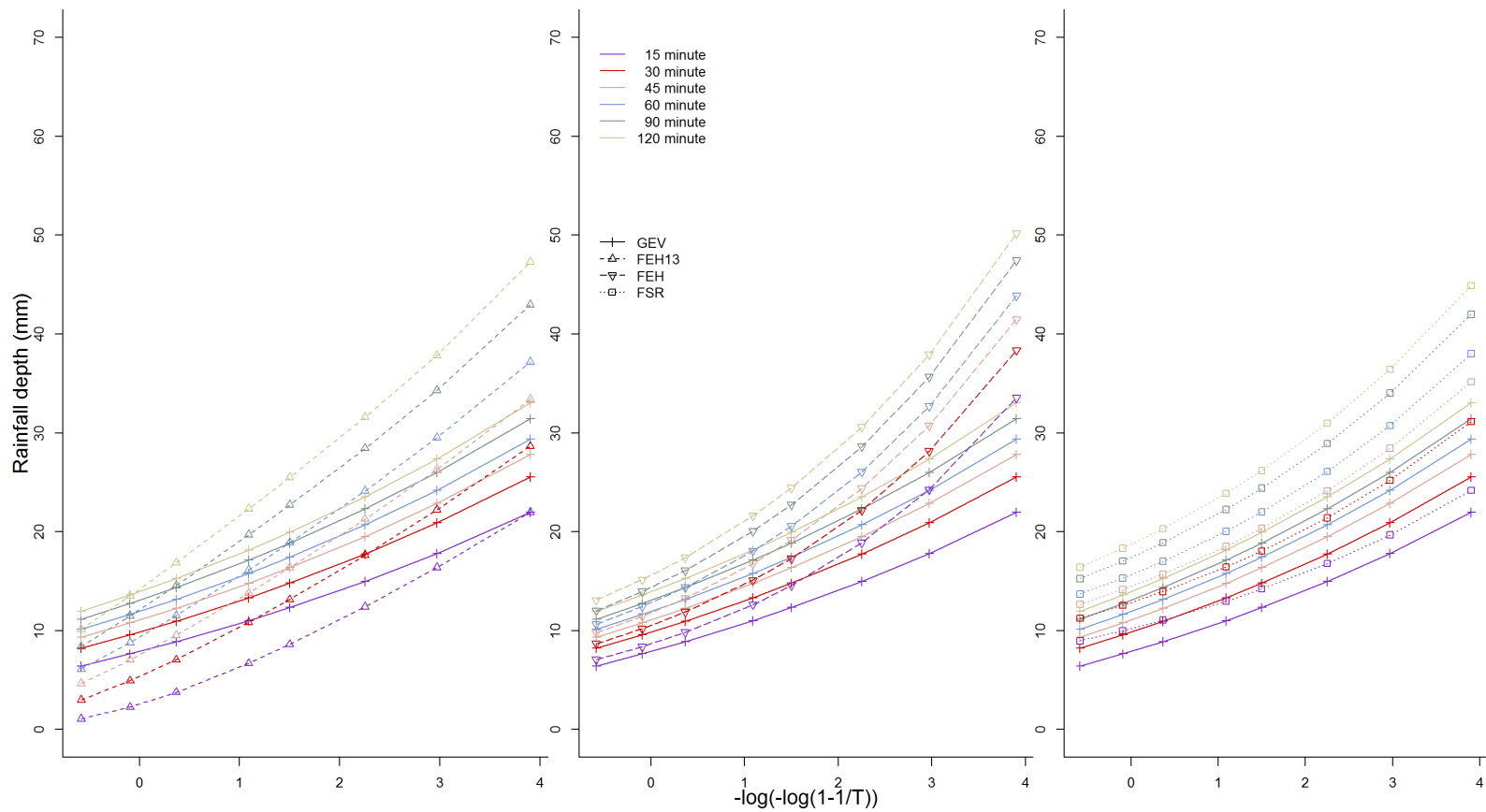
Figure 64 - Comparison of frequency curves estimated by different methods at Stanford Rivers: FEH13 (left panel), FEH (central panel) and FSR (right panel)

The three graphs in Figure 64 plot the comparison of frequency curves at Stanford Rivers for different methods (FEH13 on the left panel, FEH on the central panel and FSR on the right panel) and time periods (15, 30, 45, 60, 90 and 120 minutes). The x-axis on all panels shows log (natural logarithm, ln) from 0-4. The y-axis plots rainfall depth (0-70mm).

Appendix B – Comparison between estimated and empirical values for the 2-year, 5-year and 10-year events

Table 13 - Rainfall depths estimated by each modelling method and found as the empirical $(1 – 1/T)^{th}$ percentile of the rainfall data record at Bettws-y-Crwyn

Modelling method	T = 2 years 15 min	T = 2 years 30 min	T = 2 years 45 min	T = 2 years 60 min	T = 5 years 15 min	T = 5 years 30 min	T = 5 years 45 min	T = 5 years 60 min	T = 10 years 15 min	T = 10 years 30 min	T = 10 years 45 min	T = 10 years 60 min
Empirical	6.20	8.65	10.00	10.50	9.50	13.44	15.96	17.00	13.77	16.71	19.01	20.88
GEV	6.76	8.47	9.99	11.34	10.47	12.84	14.93	16.79	13.67	16.60	19.20	21.5
FEH	7.34	9.45	10.95	12.16	10.5	13.26	15.2	16.74	13.32	16.60	18.88	20.69
FSR	8.18	10.74	12.46	13.82	10.37	13.78	16.08	17.87	12.13	16.25	19.03	21.19

Table 14 - Rainfall depths estimated by each modelling method and found as the empirical $(1 - 1/T)^{th}$ percentile of the rainfall data record at Chieveley

Modelling method	T = 2 years 15 min	T = 2 years 30 min	T = 2 years 45 min	T = 2 years 60 min	T = 5 years 15 min	T = 5 years 30 min	T = 5 years 45 min	T = 5 years 60 min	T = 10 years 15 min	T = 10 years 30 min	T = 10 years 45 min	T = 10 years 60 min
Empirical	9.53	10.65	10.82	11.98	13.73	14.72	15.91	18.51	14.61	21.09	25.10	28.45
GEV	9.33	10.72	11.84	12.79	13.21	15.43	17.20	18.73	16.97	19.99	22.41	24.49
FEH	7.73	9.93	11.49	12.75	11.31	14.24	16.29	17.92	14.56	18.08	20.52	22.44
FSR	8.61	11.06	12.63	13.82	10.94	14.21	16.30	17.87	12.82	16.78	19.29	21.19

Table 15 - Rainfall depths estimated by each modelling method and found as the empirical $(1 - 1/T)^{th}$ percentile of the rainfall data record at Colwyn Bay

Modelling method	T = 2 years 15 min	T = 2 years 30 min	T = 2 years 45 min	T = 2 years 60 min	T = 5 years 15 min	T = 5 years 30 min	T = 5 years 45 min	T = 5 years 60 min	T = 10 years 15 min	T = 10 years 30 min	T = 10 years 45 min	T = 10 years 60 min
Empirical	6.00	7.40	9.00	10.20	7.28	10.60	12.48	13.20	8.00	12.40	14.60	16.60
GEV	6.30	7.97	9.33	10.47	9.14	11.21	12.89	14.29	11.38	13.76	15.70	17.32
FEH	7.57	9.63	11.09	12.25	11.12	13.81	15.68	17.16	14.33	17.53	19.73	21.45
FSR	8.77	11.27	12.87	14.09	11.15	14.49	16.62	18.23	13.08	17.12	19.69	21.62

Table 16 - Rainfall depths estimated by each modelling method and found as the empirical $(1 - 1/T)^{th}$ percentile of the rainfall data record at Crew Fell

Modelling method	T = 2 years 15 min	T = 2 years 30 min	T = 2 years 45 min	T = 2 years 60 min	T = 5 years 15 min	T = 5 years 30 min	T = 5 years 45 min	T = 5 years 60 min	T = 10 years 15 min	T = 10 years 30 min	T = 10 years 45 min	T = 10 years 60 min
Empirical	6.66	8.75	10.10	11.47	8.31	12.35	13.68	17.45	9.28	13.11	15.39	19.00
GEV	6.71	8.54	10.21	11.74	9.00	11.43	13.66	15.70	10.93	13.86	16.55	19.02
FEH	7.26	9.34	10.82	12.02	10.53	13.26	15.18	16.71	13.46	16.73	18.99	20.79
FSR	8.42	11.17	13.07	14.59	10.69	14.36	16.89	18.88	12.51	16.96	20.01	22.40

Table 17 - Rainfall depths estimated by each modelling method and found as the empirical $(1 - 1/T)^{th}$ percentile of the rainfall data record at Dowdeswell

Modelling method	T = 2 years 15 min	T = 2 years 30 min	T = 2 years 45 min	T = 2 years 60 min	T = 5 years 15 min	T = 5 years 30 min	T = 5 years 45 min	T = 5 years 60 min	T = 10 years 15 min	T = 10 years 30 min	T = 10 years 45 min	T = 10 years 60 min
Empirical	8.65	10.8	12.45	13.45	12.5	15.10	17.50	17.94	14.10	17.04	19.70	20.24
GEV	8.61	10.31	11.77	13.07	12.67	14.70	16.45	18.00	15.79	18.07	20.04	21.78
FEH	8.11	10.38	12.00	13.3	11.75	14.76	16.87	18.54	15.02	18.63	21.13	23.11
FSR	9.22	11.85	13.54	14.83	11.76	15.27	17.51	19.2	13.81	18.06	20.75	22.78

Table 18 - Rainfall depths estimated by each modelling method and found as the empirical $(1 - 1/T)^{th}$ percentile of the rainfall data record at Hemyock

Modelling method	T = 2 years 15 min	T = 2 years 30 min	T = 2 years 45 min	T = 2 years 60 min	T = 5 years 15 min	T = 5 years 30 min	T = 5 years 45 min	T = 5 years 60 min	T = 10 years 15 min	T = 10 years 30 min	T = 10 years 45 min	T = 10 years 60 min
Empirical	7.00	10.01	11.64	13.41	10.20	13.54	15.50	16.01	12.22	15.77	17.21	20.60
GEV	7.58	9.94	11.63	12.88	10.39	13.49	15.71	17.35	12.72	16.44	19.09	21.06
FEH	8.36	10.89	12.71	14.19	12.07	15.42	17.80	19.70	15.39	19.42	22.24	24.49
FSR	8.49	11.07	12.79	14.13	10.78	14.23	16.51	18.28	12.63	16.80	19.56	21.68

Table 19 - Rainfall depths estimated by each modelling method and found as the empirical $(1 - 1/T)^{th}$ percentile of the rainfall data record at Hinckley

Modelling method	T = 2 years 15 min	T = 2 years 30 min	T = 2 years 45 min	T = 2 years 60 min	T = 5 years 15 min	T = 5 years 30 min	T = 5 years 45 min	T = 5 years 60 min	T = 10 years 15 min	T = 10 years 30 min	T = 10 years 45 min	T = 10 years 60 min
Empirical	7.30	10.10	10.55	12.10	13.00	14.00	15.50	17.00	14.50	17.50	19.75	20.25
GEV	7.15	10.18	11.70	12.53	10.92	15.07	17.16	18.30	14.16	19.28	21.86	23.26
FEH	7.15	9.18	10.62	11.77	10.56	13.26	15.15	16.65	13.68	16.92	19.17	20.94
FSR	9.54	12.10	13.69	14.87	12.17	15.60	17.70	19.25	14.31	18.45	20.99	22.84

Table 20 - Rainfall depths estimated by each modelling method and found as the empirical $(1 - 1/T)^{th}$ percentile of the rainfall data record at Kingswood

Modelling method	T = 2 years 15 min	T = 2 years 30 min	T = 2 years 45 min	T = 2 years 60 min	T = 5 years 15 min	T = 5 years 30 min	T = 5 years 45 min	T = 5 years 60 min	T = 10 years 15 min	T = 10 years 30 min	T = 10 years 45 min	T = 10 years 60 min
Empirical	7.58	10.01	11.54	12.29	11.94	15.50	16.28	17.10	14.93	18.76	21.95	23.96
GEV	8.22	9.97	11.38	12.54	12.05	14.22	15.96	17.40	15.08	17.57	19.58	21.23
FEH	7.38	9.46	10.94	12.12	10.76	13.51	15.43	16.95	13.82	17.10	19.38	21.17
FSR	9.25	11.88	13.58	14.87	11.79	15.31	17.55	19.25	13.84	18.10	20.81	22.84

Table 21 - Rainfall depths estimated by each modelling method and found as the empirical $(1 - 1/T)^{th}$ percentile of the rainfall data record at Knightcote

Modelling method	T = 2 years 15 min	T = 2 years 30 min	T = 2 years 45 min	T = 2 years 60 min	T = 5 years 15 min	T = 5 years 30 min	T = 5 years 45 min	T = 5 years 60 min	T = 10 years 15 min	T = 10 years 30 min	T = 10 years 45 min	T = 10 years 60 min
Empirical	7.40	9.40	12.20	13.00	11.12	12.60	16.50	20.10	13.70	18.50	22.50	23.70
GEV	7.95	10.08	11.65	12.87	11.68	14.55	16.65	18.30	14.83	18.32	20.87	22.87
FEH	8.50	10.73	12.30	13.55	12.33	15.26	17.29	18.89	15.78	19.27	21.65	23.52
FSR	9.88	12.53	14.16	15.37	12.64	16.16	18.32	19.90	14.88	19.14	21.72	23.61

Table 22 - Rainfall depths estimated by each modelling method and found as the empirical $(1 - 1/T)^{th}$ percentile of the rainfall data record at Llanychaer

Modelling method	T = 2 years 15 min	T = 2 years 30 min	T = 2 years 45 min	T = 2 years 60 min	T = 5 years 15 min	T = 5 years 30 min	T = 5 years 45 min	T = 5 years 60 min	T = 10 years 15 min	T = 10 years 30 min	T = 10 years 45 min	T = 10 years 60 min
Empirical	7.60	9.00	10.50	11.80	8.92	12.20	15.20	17.20	11.00	14.42	16.84	19.04
GEV	7.25	9.14	10.84	12.36	9.71	11.99	14.04	15.87	11.60	14.19	16.51	18.59
FEH	7.48	10.20	12.22	13.90	10.54	14.09	16.70	18.84	13.22	17.46	20.54	23.05
FSR	7.52	9.98	11.67	13.02	9.50	12.77	15.03	16.82	11.09	15.04	17.77	19.93

Table 23 - Rainfall depths estimated by each modelling method and found as the empirical $(1 - 1/T)^{th}$ percentile of the rainfall data record at Lower Dunsforth

Modelling method	T = 2 years 15 min	T = 2 years 30 min	T = 2 years 45 min	T = 2 years 60 min	T = 5 years 15 min	T = 5 years 30 min	T = 5 years 45 min	T = 5 years 60 min	T = 10 years 15 min	T = 10 years 30 min	T = 10 years 45 min	T = 10 years 60 min
Empirical	7.20	9.70	11.40	12.70	12.00	16.40	18.00	18.80	15.00	20.10	21.90	24.40
GEV	7.08	9.66	11.44	12.72	10.75	14.55	17.19	19.08	14.10	19.02	22.43	24.88
FEH	7.84	9.92	11.39	12.56	11.35	14.11	16.03	17.54	14.50	17.81	20.09	21.88
FSR	9.51	12.07	13.65	14.83	12.14	15.55	17.65	19.20	14.27	18.40	20.93	22.78

Table 24 - Rainfall depths estimated by each modelling method and found as the empirical $(1 - 1/T)^{th}$ percentile of the rainfall data record at Ludford

Modelling method	T = 2 years	T = 2 years	T = 2 years	T = 2 years	T = 5 years	T = 5 years	T = 5 years	T = 5 years	T = 10 years	T = 10 years	T = 10 years	T = 10 years
	15 min	30 min	45 min	60 min	15 min	30 min	45 min	60 min	15 min	30 min	45 min	60 min
Empirical	8.73	11.07	12.57	14.33	12.45	16.87	18.96	19.96	14.51	21.63	22.83	23.77
GEV	8.93	11.33	13.05	14.34	12.73	16.12	18.57	20.40	16.08	20.36	23.45	25.75
FEH	7.71	9.96	11.56	12.85	11.22	14.23	16.36	18.06	14.38	18.03	20.59	22.62
FSR	10.08	12.80	14.49	15.76	12.90	16.53	18.75	20.40	15.19	19.57	22.25	24.20

Table 25 - Rainfall depths estimated by each modelling method and found as the empirical $(1 - 1/T)^{th}$ percentile of the rainfall data record at Otterbourne

Modelling method	T = 2 years 15 min	T = 2 years 30 min	T = 2 years 45 min	T = 2 years 60 min	T = 5 years 15 min	T = 5 years 30 min	T = 5 years 45 min	T = 5 years 60 min	T = 10 years 15 min	T = 10 years 30 min	T = 10 years 45 min	T = 10 years 60 min
Empirical	7.23	10.12	11.95	13.41	11.02	12.23	13.60	15.56	13.44	14.34	15.76	16.79
GEV	7.91	10.61	11.87	12.89	10.51	13.37	14.70	15.78	12.32	15.28	16.66	17.78
FEH	6.25	8.33	9.86	11.11	9.17	11.97	13.99	15.63	11.82	15.22	17.65	19.60
FSR	9.32	11.98	13.70	15.00	11.89	15.44	17.71	19.42	13.97	18.27	20.99	23.04

Table 26 - Rainfall depths estimated by each modelling method and found as the empirical $(1 - 1/T)^{th}$ percentile of the rainfall data record at Putney Heath

Modelling method	T = 2 years 15 min	T = 2 years 30 min	T = 2 years 45 min	T = 2 years 60 min	T = 5 years 15 min	T = 5 years 30 min	T = 5 years 45 min	T = 5 years 60 min	T = 10 years 15 min	T = 10 years 30 min	T = 10 years 45 min	T = 10 years 60 min
Empirical	8.73	9.91	11.33	11.88	16.31	17.12	19.99	21.58	18.28	23.78	26.95	27.64
GEV	7.80	10.04	11.75	13.08	12.34	15.77	18.38	20.42	16.61	21.14	24.60	27.30
FEH	9.17	11.42	12.98	14.22	13.50	16.49	18.54	20.14	17.45	21.04	23.48	25.37
FSR	9.72	12.27	13.81	14.95	12.43	15.82	17.86	19.35	14.62	18.72	21.18	22.96

Table 27 - Rainfall depths estimated by each modelling method and found as the empirical $(1 - 1/T)^{th}$ percentile of the rainfall data record at Sale Carrington

Modelling method	T = 2 years 15 min	T = 2 years 30 min	T = 2 years 45 min	T = 2 years 60 min	T = 5 years 15 min	T = 5 years 30 min	T = 5 years 45 min	T = 5 years 60 min	T = 10 years 15 min	T = 10 years 30 min	T = 10 years 45 min	T = 10 years 60 min
Empirical	8.50	9.07	10.30	11.26	12.08	15.35	16.44	16.54	16.08	17.96	18.05	17.94
GEV	8.03	9.47	10.67	11.73	10.83	12.48	13.85	15.07	12.91	14.71	16.20	17.54
FEH	8.89	10.97	12.41	13.55	12.96	15.69	17.54	18.99	16.63	19.87	22.06	23.75
FSR	9.08	11.54	13.07	14.22	11.57	14.85	16.89	18.39	13.58	17.55	20.01	21.81

Table 28 - Rainfall depths estimated by each modelling method and found as the empirical $(1 - 1/T)^{th}$ percentile of the rainfall data record at Stanford Rivers

Modelling method	T = 2 years 15 min	T = 2 years 30 min	T = 2 years 45 min	T = 2 years 60 min	T = 5 years 15 min	T = 5 years 30 min	T = 5 years 45 min	T = 5 years 60 min	T = 10 years 15 min	T = 10 years 30 min	T = 10 years 45 min	T = 10 years 60 min
Empirical	8.61	11.07	12.16	13.10	12.86	13.37	15.50	17.24	14.38	15.79	16.05	19.14
GEV	8.88	10.96	12.27	13.16	12.33	14.80	16.36	17.43	14.97	17.74	19.50	20.69
FEH13	3.77	7.05	9.53	11.53	8.61	13.14	16.37	18.90	12.42	17.63	21.29	24.15
FEH	9.82	11.89	13.29	14.38	14.56	17.30	19.14	20.56	18.90	22.19	24.37	26.05
FSR	11.06	13.95	15.71	17.00	14.21	18.05	20.34	22.00	16.78	21.40	24.13	26.09

Table 29 - Rainfall depths estimated by each modelling method and found as the empirical $(1 - 1/T)^{th}$ percentile of the rainfall data record at Stone

Modelling method	T = 2 years 15 min	T = 2 years 30 min	T = 2 years 45 min	T = 2 years 60 min	T = 5 years 15 min	T = 5 years 30 min	T = 5 years 45 min	T = 5 years 60 min	T = 10 years 15 min	T = 10 years 30 min	T = 10 years 45 min	T = 10 years 60 min
Empirical	8.45	10.70	11.70	12.60	13.50	19.00	21.50	23.00	16.50	24.25	27.25	28.35
GEV	8.60	10.71	12.16	13.28	13.16	16.27	18.42	20.09	17.32	21.36	24.14	26.31
FEH	7.27	9.22	10.59	11.68	10.61	13.17	14.96	16.36	13.62	16.69	18.80	20.45
FSR	9.59	12.21	13.84	15.06	12.25	15.74	17.90	19.50	14.41	18.62	21.22	23.13

Table 30 - Rainfall depths estimated by each modelling method and found as the empirical $(1 - 1/T)^{th}$ percentile of the rainfall data record at Taw Head

Modelling method	T = 2 years 15 min	T = 2 years 30 min	T = 2 years 45 min	T = 2 years 60 min	T = 5 years 15 min	T = 5 years 30 min	T = 5 years 45 min	T = 5 years 60 min	T = 10 years 15 min	T = 10 years 30 min	T = 10 years 45 min	T = 10 years 60 min
Empirical	8.50	11.60	13.39	15.15	11.44	14.29	15.25	17.49	15.11	19.48	23.33	24.90
GEV	8.38	11.48	13.98	16.04	10.61	14.40	17.47	19.99	12.35	16.69	20.20	23.08
FEH	8.26	11.66	14.27	16.47	11.96	16.52	19.96	22.82	15.28	20.80	24.92	28.33
FSR	9.03	12.68	15.45	17.79	11.50	16.37	20.00	23.00	13.50	19.39	23.73	27.27

Table 31 - Rainfall depths estimated by each modelling method and found as the empirical $(1 - 1/T)^{th}$ percentile of the rainfall data record at Victoria Park

Modelling method	T = 2 years	T = 2 years	T = 2 years	T = 2 years	T = 5 years	T = 5 years	T = 5 years	T = 5 years	T = 10 years	T = 10 years	T = 10 years	T = 10 years
	15 min	30 min	45 min	60 min	15 min	30 min	45 min	60 min	15 min	30 min	45 min	60 min
Empirical	6.80	9.00	10.20	11.60	8.60	11.20	12.00	14.20	9.40	11.80	13.40	15.60
GEV	7.15	8.77	10.25	11.62	9.79	11.44	12.96	14.35	11.57	13.24	14.78	16.19
FEH	7.58	10.12	11.98	13.51	10.93	14.30	16.73	18.71	13.92	17.97	20.87	23.20
FSR	8.11	10.62	12.30	13.63	10.28	13.63	15.87	17.62	12.02	16.07	18.78	20.89

Would you like to find out more about us or your environment?

Then call us on

03708 506 506 (Monday to Friday, 8am to 6pm)

Email: enquiries@environment-agency.gov.uk

Or visit our website

www.gov.uk/environment-agency

incident hotline

0800 807060 **(24 hours)**

floodline

0345 988 1188 **(24 hours)**

Find out about call charges (https://www.gov.uk/call-charges)

Environment first

Are you viewing this onscreen? Please consider the environment and only print if absolutely necessary. If you are reading a paper copy, please don't forget to reuse and recycle.